Charles University in Prague
Faculty of Mathematics and Physics

DOCTORAL THESIS

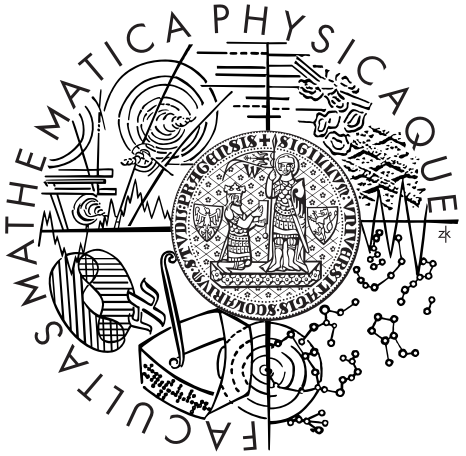

Michal Pavelka

Thermodynamic analysis of processes in Hydrogen fuel cells

Mathematical Institute

Supervisor of the doctoral thesis: František Maršík
Study programme: Physics
Specialization: Mathematical and Computer Modelling

Prague 2015

I have to express my deepest gratitude to my supervisor, František Maršík, who taught me to look at anything in the Nature as at an application of non-equilibrium thermodynamics. Moreover, he has been supporting me generously, which made it possible to write this thesis.

I would like to thank my consultant, Václav Klika, for all those interesting and productive discussions, that eventually formed the main ideas in this thesis.

I am also very grateful to Miroslav Grmela, who insipired large parts of this work and who has generously been sharing his knowledge of thermodynamics with us, and to Jay Benziger, who shared his great knowledge of fuel cells and who motivated our research of Nafion membranes.

I am also indebted to my friends Petr Vágner, whose questions and suggestions were testing and forming the generalization of exergy analysis and who helped me with numerical simulations, and Jan Kubant, who participated on development of the sorption model of Nafion membranes.

Finally, I am most thankful to my wife Zuzana, without whose support this thesis could never be written and who patiently listened to all those strange ideas in this work.

This work was developed within the CENTEM project, reg. no. CZ.1.05/2.1.00/03.0088, cofunded by the ERDF as part of the Ministry of Education, Youth and Sports OP RDI programme and, in the follow-up sustainability stage, supported through CENTEM PLUS (LO1402) by financial means from the Ministry of Education, Youth and Sports under the "National Sustainability Programme I.

This work was also supported from the POLYMEM project, reg. no CZ.1.07/2.3.00/20.0107, that is co-funded from the European Social Fund (ESF) in the Czech Republic: "Education for Competitiveness Operational Programme".

I declare that I carried out this doctoral thesis independently, and only with the cited sources, literature and other professional sources.

I understand that my work relates to the rights and obligations under the Act No. 121/2000 Coll., the Copyright Act, as amended, in particular the fact that the Charles University in Prague has the right to conclude a license agreement on the use of this work as a school work pursuant to Section 60 paragraph 1 of the Copyright Act.

In ..... date ..... signature of the author

Název práce: Termodynamická analýza procesů ve vodíkových palivových článcích

Autor: Michal Pavelka

Katedra: Matematický ústav

Vedoucí disertační práce: prof. Ing. František Maršík, DrSc., Matematický ústav UK

Abstrakt: Tato práce se zabývá nerovnovážnou termodynamikou, která slouží k odvození evolučních rovnic makroskopických a mezoskopických systémů. Je například ukázán vztah mezi teorií GENERIC (General Equation for the Nonequilibrium Reversible-Irreversible Coupling) a (ne)vratností a Onsager-Casimirovy relace reciprocity jsou pak z této teorie odvozeny. Následně jsou v rámci nerovnovážné termodynamiky odvozeny modely palivových článků a příbuzných zařízení a teoretické předpovědi jsou porovnány s výsledky experimentů. V práci je také odvozeno zobecnění analýzy exergie, které přináší novou metodu pro odhalování mapy ztrát užitečné práce v zařízeních produkujících elektřinu. Tato metoda vyžaduje, aby bylo zařízení popsáno nerovnovážně termodynamickým modelem, a obecná teorie nerovnovážné termodynamiky se tak stává nedílnou součástí popisu a optimalizace zařízení produkujících energii.

Klíčová slova: GENERIC, nerovnovážná termodynamika, exergie, palivové články, optimalizace

Title: Thermodynamic analysis of processes in Hydrogen fuel cells

Author: Michal Pavelka

Department: Mathematical Institute

Supervisor: prof. Ing. František Maršík, DrSc., Mathematical Institute of Charles University

Abstract: Non-equilibrium thermodynamics, which serves as a framework for formulating evolution equations of macroscopic and mesoscopic systems, is briefly reviewed and further developed in this work. For example, the relation between the General Equation for the Nonequilibrium Reversible-Irreversible Coupling (GENERIC) and (ir)reversibility is elucidated, and Onsager-Casimir reciprocal relations are shown to be an implication of GENERIC. Non-equilibrium thermodynamics is then applied to describe fuel cells and related devices, and theoretical conclusions are compared to experimental data. Moreover, a generalization of standard exergy analysis is developed bringing a new method for revealing a map of useful work losses in electricity producing devices. This method requires a non-equilibrium thermodynamic model, and so the general theory of non-equilibrium thermodynamics and optimization of real power generating devices stand side by side.

Keywords: GENERIC, non-equilibrium thermodynamics, exergy , fuel cells, optimization

Contents

Introduction

"Thermodynamics is a funny subject. The first time you go through it, you don't understand it at all. The second time you go through it, you think you understand it, except for one or two small points. The third time you go through it, you know you don't understand it, but by that time you are so used to it, it doesn't bother you anymore."

— A. Sommerfeld [4]

Fortunately, this still holds true for non-equilibrium thermodynamics, which makes it a fruitful land to explore. And it is the goal of this thesis to explore non-equilibrium thermodynamics and to apply it in real world problems like fuel cell modeling.

Consider a system consisting of a box filled with interacting gases. One can, in principle, see the individual molecules, motion of which is governed by Newton laws, Hamilton canonical equations or Liouville equation. Or one can regard only the one-particle distribution functions, evolution of which is described by Boltzmann equation. Or one can even see only a few moments of the one-particle distribution function, for example density, momentum density and energy (or entropy) density, evolution of which is governed by Navier-Stokes equation of classical hydrodynamics. Finally, one can regard only energy, volume and mass of the gases, which are studied within equilibrium thermodynamics. These differently detailed descriptions, each of which is defined by a different set of state variables, are referred to as particular levels of description of the system.

On each level of description evolution equations are prescribed which govern time-evolution of the state variables on the level. The evolution equations should be compatible with experimental observations made on the level. For example, one should be able to measure density, momentum density and energy density of a system when describing the system by classical hydrodynamics, and the experiments should be compatible with solutions to the Navier-Stokes equations. Therefore, none of the levels of description is better than another in general because each level is appropriate for describing experimental observations with different degree of detail. An advantage of non-equilibrium thermodynamics is that systems can be described on several levels of description consistently.

The concept of different levels of description is central in this work, and the chapters are structured accordingly. In Chap. 1 the framework of the General Equation for the Non-Equilibrium Reversible-Irreversible Coupling (GENERIC) is reviewed and further developed. Classical Irreversible Thermodynamics (CIT), which is formulated in which Chap. 2, is the highest (most detailed) level used in fuel cell modeling. However, perhaps the most practical level is the level of mechanical equilibrium, described in Chap. 3. Finally, Chap. 4 contains results on fuel cell and battery modeling on the level of description of thermodynamic equilibrium. Moreover, Appendix A contains results formulated on yet different levels of description, which are not usually considered in fuel cell modeling.

The following problems are addressed in this thesis:

- Which processes are reversible and which irreversible? And how does non-equilibrium thermodynamics describe these two kinds of processes?

- Can Onsager-Casimir reciprocal relations (OCRR) be derived from non-equilibrium thermodynamics?
- Once reversible dynamics on a more detailed level of description is known, is it possible to derive reversible dynamics on a lower level?
- How to describe processes in electrochemistry within thermodynamics efficiently?
- Absorption of water into Nafion membranes is much slower than desorption from the membranes. What is the reason?
- How does the coupling between water and proton transport in fuel cells affect the resulting I/V curve?
- Consider a device producing electricity, e.g. a fuel cell. When having a continuous thermodynamic model of the device, is it possible to show where and how much efficiency is being lost?
- What is the open circuit voltage of a vanadium redox flow battery at different states of charge?
- What is the meaning of partial pressures in a mixture of non-ideal fluids?

In Chap. 4.2.5 these problems are recalled and it is shown how this work contributes to solving them.

This work is based on our papers [80, 81, 79, 78, 82], all of which but the last one have been published in peer-reviewed journals. The last one had been submitted to the Journal of Power Sources and was under review at the time of writing. Paper [80] introduces a new concept of thermodynamic optimization. This concept is then clarified and further developed in article [79], various parts of which are included in Chap. 3. In paper [81] a new theory of mixtures is derived which takes into account the notion of multiple levels of description and (ir)reversiblity. Although this paper is not directly related to fuel cell modeling, it provides theoretical background for many results of this thesis. The main results of the paper are summarized in Sec. A.3. Paper [78], a large part of which is included in Chap. 1, brings new insight into GENERIC and into Onsager-Casimir reciprocal relations. Finally, in paper [82] the open-circuit voltage of vanadium redox flow batteries is derived from equilibrium thermodynamics, and the paper is included in Sec. 4.2 with only minor adjustments to the submitted version.

1. Non-equilibrium thermodynamics

Various forms of non-equilibrium thermodynamics have been developed, see [55] for a comprehensive review, and perhaps the most recent widely recognized theory is the General Equation for the Nonequilibrium Reversible-Irreversible Coupling (GENERIC), which represents a unifying framework for example for equilibrium thermodynamics, Classical Irreversible thermodynamics (CIT) and Extended Irreversible Thermodynamics (EIT). Besides these theories there are the Rational Thermodynamics and the Rational Extended Thermodynamics, which however, are very similar in results with EIT, [68]. Therefore, GENERIC is taken as the most general theory in this work, and EIT, CIT and other forms of thermodynamics are regarded as particular realizations of GENERIC.

GENERIC differs from the other theories because instead of starting with balance equations, one has to specify state variables (level of description) at first and, subsequently, four building blocks, namely energy, entropy, a Poisson bracket and a dissipation potential, are required. Evolution equations of the state variables then consist of a reversible part, given by the Poisson bracket and energy, and an irreversible part, given by the dissipation potential and entropy. But what is the precise meaning of reversibility and irreversibility in this theory? It is a goal of this chapter to investigate that.

Such investigation can also be seen as an investigation of the Onsager-Casimir reciprocal relations[72, 73, 20] (OCRR) in the context of far-from-equilibrium nonlinear mesoscopic dynamics possessing the structure of GENERIC (General Equation of Non-Equilibrium Reversible and Irreversible Coupling [38, 77]). In particular, it is shown that the Poisson bracket is responsible for the antisymmetric coupling (discovered originally by Casimir[20]) while the dissipation potential is responsible for the symmetric coupling. GENERIC enriched with some assumptions on its behavior with respect to time-reversal transformation (TRT) is then the far-from-equilibrium structure which yields OCRR near equilibrium.

1.1 Structure of non-equilibrium thermodynamics

1.1.1 Time-reversal transformation

Let us at first recall the notion of time-reversal transformation [72, 57]. Imagine a movie depicting motion of particles in an isolated box. Suppose that the particles behave classically, i.e. their motion is described by Newton's law

$$\dot{\mathbf{p}}_i = \mathbf{F_i}, \tag{1.1}$$

where $\mathbf{p}_i$ is momentum of the i-th particle and $\mathbf{F}_i$ is force exerted on the i-th particle by other particles and walls of the box. If the movie is played backwards, one can see that velocities of the particles are reversed[1] and that the time-stamp

[1] For quantum-mechanical interpretation our paper [78].

goes in the opposite direction. This thought experiment constitutes physical motivation for introducing time-reversal transformation (TRT), which is to be denoted by **I**.

Definition 1 (Time-reversal transformation (TRT))**.** *TRT transforms any physical quantity exactly in the same way as if velocities of all particles were reversed. Moreover, the time-stamp goes in the opposite direction.*

Let us now study properties of the transformation. Consider a state variable x_i, where i can be a discrete or a continuous index. If velocities of all particles were reversed, the state variable x_i would change to $\mathbf{I}(x_i)$. If, however, the velocities were reversed once more, the variable must return to the original value, i.e.

$$\mathbf{I}(\mathbf{I}(x_i)) = x_i. \tag{1.2}$$

Hence, operation **I** is idempotent.

If TRT does not alter the state variable or if it only changes sign of the variable, we say that the variable has even or odd parity, respectively. Parity of state variable x_i is denoted by $\mathcal{P}(x_i)$ and we say that

$$\mathcal{P}(x_i) = 1 \quad \text{for } x_i \text{ even}, \tag{1.3}$$

$$\mathcal{P}(x_i) = -1 \quad \text{for } x_i \text{ odd}. \tag{1.4}$$

For example, momenta of particles in the box are odd as $\mathbf{I}(\mathbf{p}_i) = -\mathbf{p}_i$. On the other hand, positions of the particles are even. It should be borne in mind that not all state variables have parity. For example, if we choose probability density of position and momentum (as in Boltzmann equation in Sec. A.1) as the state variable, we have

$$\mathbf{I}(f(\mathbf{r}, \mathbf{v})) = f(\mathbf{r}, -\mathbf{v}), \tag{1.5}$$

and this state variable has clearly no parity. In summary, parity can then be defined as follows

Definition 2 (Parity)**.** *A physical quantity has parity equal to 1 if TRT does not alter the quantity, i.e. the quantity is even under TRT. A physical quantity has parity equal to -1 if TRT inverts sign of the quantity, i.e. the quantity is odd under TRT.*

TRT can be also applied to time derivative of a state variable. Since time stamp of the inverted movie goes backwards, TRT acts on time derivative as follows

$$\mathbf{I}\left(\frac{\mathrm{d}x_i}{\mathrm{d}t}\right) = -\frac{\mathrm{d}}{\mathrm{d}\tau}\mathbf{I}(x_i) \tag{1.6}$$

where the backward going time step was denoted by $\mathrm{d}\tau$. Note that if the state variable is a field variable, for example momentum density $\mathbf{u}(\mathbf{r}, t)$, the time derivative in the preceding formula stands for partial time derivative.

So far we have talked about TRT acting on state variables. Let us now have a look on how TRT transforms evolution equations. Consider for example the incompressible Navier-Stokes equations [28]

$$\frac{\partial \rho}{\partial t} = -\frac{\mathbf{u}}{\rho} \cdot \nabla \rho \tag{1.7}$$

$$\frac{\partial \mathbf{u}}{\partial t} = -\mathrm{div}\left(\frac{1}{\rho}\mathbf{u} \otimes \mathbf{u}\right) - \nabla p + \mu \Delta \left(\frac{\mathbf{u}}{\rho}\right) \tag{1.8}$$

where ρ is density field and $\mathbf{u}$ is momentum density field. The former equation expresses evolution of density while the latter evolution of momentum density. Application of TRT then gives

$$-\frac{\partial \rho}{\partial \tau} = +\frac{\mathbf{u}}{\rho} \cdot \nabla \rho \tag{1.9}$$

$$\frac{\partial \mathbf{u}}{\partial \tau} = -\mathrm{div}\left(\frac{1}{\rho}\mathbf{u} \otimes \mathbf{u}\right) - \nabla p - \mu \Delta \left(\frac{\mathbf{u}}{\rho}\right). \tag{1.10}$$

Here we used that density and pressure are even variables while momentum density is odd under TRT. Obviously, evolution equation for density is not altered by TRT. On the other hand, the sign of the viscous part of the evolution equation for momentum density is changed. This means that if there were no viscosity, evolution equations (1.7) and (1.8) would describe motion of the fluid even if the movie were played backwards. With non-zero viscosity, this would not be true anymore.

Based on this motivation, let us now define the reversible and the irreversible part of an evolution equation.

Definition 3 (Reversibility based on TRT)**.** *Assume that the evolution equation is solved with respect to time derivative, i.e. is in the form where on the l.h.s. there is only time derivative of the state variable evolution of which the equation describes. Moreover, assume that there are no time derivatives on the r.h.s. of the equation. The reversible part of the evolution equation is then defined as the part of the r.h.s. which is transformed by TRT in the same way as the l.h.s. of the equation. The irreversible part is then the rest of the r.h.s. of the evolution equation.*

For example, the r.h.s. of Eq. (1.7) transforms in the same way as the l.h.s. of the equation. Indeed, equation (1.9) has the same form as equation (1.7). Gradient of pressure on the r.h.s. of Eq. (1.8) is even as well as the l.h.s. of the equation. On the other hand, the viscous part is odd. Therefore, gradient of pressure generates reversible evolution while the viscous part irreversible. The case where state variables have no parity is commented in Sec. A.1, where Boltzmann equation is analysed. This definition of reversibility can be expressed more rigorously within differential geometrically, see section 1.1.5.

1.1.2 Structure of GENERIC

Within the GENERIC[38, 77, 37] framework the evolution equation of a state variable x_i is expressed in the following form[2]

$$\frac{\mathrm{d}x_i}{\mathrm{d}t} = \sum_j L_{ij} E_{x_j} + \frac{\delta \Xi}{\delta S_{x_i}} \tag{1.11}$$

where L_{ij} represents a Poisson bivector field, Ξ is a dissipation potential, E is energy and S entropy of the system under consideration. Poisson bracket between any two functionals A and B may be constructed from the Poisson bivector as

$$\{A, B\} = \langle A, \mathbf{L} B \rangle \tag{1.12}$$

where $\langle \bullet, \bullet \rangle$ represents scalar product in an appropriate space of state variables [37]. The Poisson bracket is antisymmetric and fulfills Jacobi identity, see [32]. The dissipation potential is supposed to be a convex function of thermodynamic force S_{x_i} near S_{x_i} equal to 0, it is zero for the force equal to zero and it reaches minimum for S_{x_i} equal to 0, see [37] for more details.

Note that in general the irreversible part of the evolution equation is given by

$$\frac{\delta \Xi}{\delta x_i^\star}\Big|_{x_i^\star = \frac{\delta S}{\delta x_i}} \tag{1.13}$$

The quantity $x_i^\star$ is referred to as the conjugate variable to variable x_i, which is naturally defined within the geometric formulation of GENERIC [37]. The more explicit form (1.11) is used only for brevity.

Approximating the dissipation potential by a quadratic function in forces (here denoted by $\mathbf{X}$), i.e. exploiting convexity of the dissipation potential near equilibrium,

$$\Xi = \frac{1}{2} \langle \mathbf{X}, \mathbf{M} \mathbf{X} \rangle \tag{1.14}$$

where $\mathbf{M}$ is the positive semidefinite matrix of second derivatives of Ξ, leads to formulation of a dissipative bracket

$$[A, B] = \langle A_{\mathbf{x}}, \mathbf{M} \cdot B_{\mathbf{x}} \rangle. \tag{1.15}$$

This way evolution equation (1.11) may be approximated by evolution equation

$$\frac{\mathrm{d}x_i}{\mathrm{d}t} = \sum_j L_{ij} E_{x_j} + \sum_j M_{ij} S_{x_j} \tag{1.16}$$

[2]Subscripts often denote derivatives in this work. Moreover, derivative of a functional with respect to a field x_i is denoted by subscript, by $\frac{\partial}{\partial x_i}$ or by $\frac{\delta}{\delta x_i}$. This derivative is calculated as

$$\frac{\mathrm{d}A(x + \lambda \delta x)}{\mathrm{d}x}\bigg|_{\lambda = 0} = \left\langle \frac{\delta A}{\delta x}, \delta x \right\rangle$$

where the duality is often interpreted as an integral. This derivative is referred to as functional or Volterra derivative, see [75] for physical motivation or [60] for more precise mathematical definition. Moreover, Einstein's summation convention is often used, and positions of the summation indexes then match as usually in the convention.

where M_{ij} is the dissipative matrix, which is symmetric and positive semidefinite. Moreover, both matrices are assumed to fulfill the following degeneracy conditions

$$\sum_j L_{ij} S_{x_j} = 0 = \sum_j M_{ij} E_{x_j}, \tag{1.17}$$

that guarantee the separation of antisymmetric (reversible, see below) and symmetric (irreversible, see below) part of a given evolution equation. Similar degeneracies are usually required to hold for the dissipation potential as well, see [37].

Note that if i and j are continuous indices, e.g. position vectors $\mathbf{r}$ and $\mathbf{r}'$, respectively, matrix multiplication in (1.16) also consists of integration with respect to $\mathbf{r}'$. We also suppose that the system, which is to be described, is isolated, infinite or periodic, so that boundary terms disappear when integrating by parts.

In the whole manuscript we use the following assumption:

Assumption 1. *We assume that evolution equations of any physical system can be written in the GENERIC form. Therefore, we limit ourselves to such time evolution that, from the physical point of view, describes systems approaching a reduced description (e.g. the description used in the classical thermodynamics).*

Evolution equation (1.16) can be equivalently expressed in terms of the thermodynamic potential

$$\Phi(\mathbf{x}) \stackrel{def}{=} -S(\mathbf{x}) + \frac{1}{T^0} E(\mathbf{x}) - \frac{\mu^0}{T^0} N(\mathbf{x}) \tag{1.18}$$

where T^0 is equilibrium temperature, μ^0 is equilibrium chemical potential and N is amount of mass in the system. Note that neither the Poisson bracket nor the dissipative bracket (or dissipation potential) alter the amount of mass $N(\mathbf{x})$ (and also energy $E(\mathbf{x})$ as we have seen above). Equation (1.16) then becomes

$$\frac{\mathrm{d}x_i}{\mathrm{d}t} = (T^0 L_{ij} - M_{ij}) \Phi_{x_j}. \tag{1.19}$$

Both equations (1.16) and (1.19) are equivalent because of the degeneracies of the brackets.

From the degeneracies and the positive semidefiniteness of the matrix $\mathbf{M}$ it follows that the thermodynamic potential decreases in time, i.e.

$$\frac{\mathrm{d}\Phi}{\mathrm{d}t} \leq 0, \tag{1.20}$$

and that it decreases until equilibrium is reached [66]. We thus see that, from the physical point of view, the GENERIC equation (1.11) represents a passage from the mesoscopic level on which x plays the role of state variables to the level of equilibrium thermodynamics on which (V, E, N), where $E = E(x_{th}), N = N(x_{th})$ or alternatively (T_0, μ_0) serve as state variables.

1.1.3 On equivalence of notions of reversibility

In the GENERIC framework the notion of reversibility is such that[38, 77]

Definition 4 (Reversibility within GENERIC)**.** *The Poisson bracket generates reversible evolution while the dissipation potential (or the dissipative bracket) generates irreversible evolution.*

On the other hand, reversible processes in an isolated system are often identified [53] via entropic arguments:

Definition 5 (Entropic reversibility)**.** *Reversible evolution of an isolated system does not raise entropy, i.e.* $\dot{S} = 0$*, while irreversible evolution raises entropy.*

Are these two notions of reversibility/irreversibility compatible? And are they compatible with Definition 3 of reversibility based on TRT?

Evolution equation of an arbitrary functional A of the state variables can be formulated using a Poisson and a dissipative bracket (in the approximation of quadratic dissipation potential) as

$$\frac{\mathrm{d}A}{\mathrm{d}t} = \{A, E\} + [A, S], \tag{1.21}$$

which follows from equation (1.16) and definitions of Poisson bracket and dissipative bracket. In particular, consider A being entropy, evolution equation of which is the following (due to the degeneracy conditions (1.17))

$$\frac{\mathrm{d}S}{\mathrm{d}t} = \{S, E\} + [S, S] = [S, S] \geq 0, \tag{1.22}$$

and where

$$\frac{\mathrm{d}S}{\mathrm{d}t} = 0 \Longleftrightarrow [S, S] = 0. \tag{1.23}$$

Therefore, if the dissipative matrix/bracket is not present in the evolution equation of state variable x_i, equation (1.16), the evolution equation describes some reversible processes within the system in the sense of Definition 5 of entropic reversibility. Thus, reversible processes in the sense of Definition 4 do not raise entropy of an isolated system, and these two notions or reversibility/irreversibility are in agreement. The same conclusion holds if dissipation potential is used instead of the dissipative bracket. Thus we have just proven the following lemma

Lemma 1. *Definition 4 of reversibility/irreversibility within GENERIC and the entropic Definition 5 are equivalent.*

Are these two notions of reversibility compatible with definition 3 of TRT based reversibility/irreversibility?

Assume that all state variables have definite parities, which means that

$$\mathbf{I}(x_i) = \mathcal{P}(x_i)\, x_i = \pm x_i. \tag{1.24}$$

What is the parity of the functionals generating the evolution, E and S? In the whole manuscript we use the following assumption:

Assumption 2 (Parity of E, S, Φ and Ξ)**.** *Energy, entropy, thermodynamic potential and dissipation potential are assumed to be even under TRT.*

For energy the assumption is quite natural because if energy (or Hamiltonian) were not even, Hamilton equations would not be reversible, see e.g. [54]. For entropy, the assumption also seems to be quite natural because the author is not aware of any particular example of non-even entropy, and for example if entropy is constructed as $S = -k\sum_i p_i \ln p_i$ as is usual in statistical mechanics[98], the entropy is obviously even. Moreover, non-equilibrium statistical physics also leads to the same conclusion[57]. The statement that entropy is even should, however, be taken as an assumption. The thermodynamic potential is even because it is formed from energy and entropy, which are supposed to be even. The assumption that the dissipation potential be even is also natural - see Sec. 1.1.5, where it is shown that this property of dissipation potential is needed to make all the three definitions of irreversibility equivalent. This property of the dissipation potential is fulfilled for all dissipation potentials used in this manuscript, and the author is not aware of any non-even dissipation potential describing real systems.

Application of TRT on Eq. (1.16) then yields

$$-\mathcal{P}\left(x_i\right)\frac{\mathrm{d}x_i}{\mathrm{d}\tau} = \sum_j \mathcal{P}\left(L_{ij}\right)L_{ij}\mathcal{P}\left(x_j\right)E_{x_j} + \sum_j \mathcal{P}\left(M_{ij}\right)M_{ij}\mathcal{P}\left(x_j\right)S_{x_j}, \quad (1.25)$$

since functionals E and S are assumed to be even. This last equation can be rewritten as

$$\frac{\mathrm{d}x_i}{\mathrm{d}\tau} = -\sum_j \mathcal{P}\left(L_{ij}\right)\mathcal{P}\left(x_i\right)\mathcal{P}\left(x_j\right)L_{ij}E_{x_j} - \\ -\sum_j \mathcal{P}\left(M_{ij}\right)\mathcal{P}\left(x_i\right)\mathcal{P}\left(x_j\right)M_{ij}S_{x_j}. \quad (1.26)$$

The first term on the r.h.s. of equation (1.16) causes reversible evolution in the sense of Definition 4 while the second term causes irreversible evolution. For the two definitions 3 and 4 to be compatible, it is necessary that after application of TRT the first term does not alter structure of the equation while the second does. In other words, the first term on the r.h.s. of equation (1.26) must be the same as the first term on the r.h.s. of equation (1.16) while the second term must have opposite sign than the second term on the r.h.s. of equation (1.16), i.e.

$$\mathcal{P}\left(L_{ij}\right) = -\mathcal{P}\left(x_i\right)\mathcal{P}\left(x_j\right) \quad (1.27a)$$

$$\mathcal{P}\left(M_{ij}\right) = \mathcal{P}\left(x_i\right)\mathcal{P}\left(x_j\right). \quad (1.27b)$$

These two equations are the necessary and sufficient conditions for the notion of reversibility within GENERIC, Definition 4, to be equivalent to the definition of reversibility in the sense of Definition 3. This conclusion may be formulated as the following theorem

Theorem 1 (Equivalence of definitions of reversibility)**.** *Under these assumptions:*

1. *All variables have definite parities.*
2. *Assumption 2 holds true.*
3. *Relations* (1.27) *are fulfilled.*

the three definitions of reversibility/irreversibility 3, 4 and 5 are equivalent.

Note that the second relation (1.27b) can be seen as a consequence of that the dissipation potential is even. Indeed, parity of the quadratic dissipation potential (1.14) can be written as

$$1 = \mathcal{P}\left(S_{x_i} M_{ij} S_{x_j}\right) = \mathcal{P}\left(x_i\right) \mathcal{P}\left(x_j\right) \mathcal{P}\left(M_{ij}\right), \tag{1.28}$$

which is equivalent to the second relation of (1.27).

In section 1.1.5 the Definition 3 is formulated geometrically and Theorem 1 is generalized. Moreover, it is shown that Assumption 2 is sufficient to replace the second relation from (1.27) not only in case of dissipative bracket. In other words, dissipation potential generates only irreversible evolution automatically, and the second relation in (1.27) is redundant if we work with dissipation potential instead of dissipative bracket.

1.1.4 Onsager-Casimir reciprocal relations (OCRR)

In this section we show that OCRR are implied by GENERIC with conditions (1.27) near equilibrium. Near equilibrium the general evolution equation (1.19) becomes, see [38],

$$\dot{\xi}_i = \sum_j \sum_k \left(T L_{ij}(x_{th}) - M_{ij}(x_{th})\right) \frac{\delta^2 \Phi}{\delta x_j \delta x_k}(x_{th}) \xi_k \tag{1.29}$$

where the thermodynamic potential is approximated by quadratic terms and both brackets are evaluated at equilibrium. Symbol ξ_i denotes the deviation of variable x_i from the equilibrium value of the variable. This equation can be rewritten in the standard form of near-equilibrium evolution

$$\dot{\xi}_i = \sum_j K_{ij} X_j \tag{1.30}$$

where matrix of phenomenological coefficients $\mathbf{K}$ is defined as

$$K_{ij} = T L_{ij}(x_{th}) - M_{ij}(x_{th}) \tag{1.31}$$

and thermodynamic force $\mathbf{X}$ as

$$X_j = \sum_k \frac{\delta^2 \Phi}{\delta x_j \delta x_k}(x_{th}) \xi_k. \tag{1.32}$$

The matrix $\mathbf{K}$ depends only on equilibrium values of state variables (hence not evolving with time). Usually, the equilibrium values are even under TRT because odd variables, e.g. momentum, vanish at equilibrium. Therefore, each element of the matrix is even as well

$$\mathcal{P}\left(\mathbf{K}\right) = 1. \tag{1.33}$$

Analogously, the same is true for matrices $\mathbf{L}$ and $\mathbf{M}$ evaluated at equilibrium, i.e.

$$\mathcal{P}\left(L_{ij}(x_{th})\right) = \mathcal{P}\left(M_{ij}(x_{th})\right) = 1. \tag{1.34}$$

Comparing to parities indicated in relations (1.27), it follows that all terms corresponding to state variables with $\mathcal{P}(x_i)\mathcal{P}(x_j) = 1$, i.e. with the same parities, vanish in $L_{ij}(x_{th})$ while all terms corresponding to state variables with $\mathcal{P}(x_i)\mathcal{P}(x_j) = -1$, i.e. with opposite parities, vanish in $M_{ij}(x_{th})$.

Therefore, we have derived that $L_{ij}(x_{th})$ is responsible for coupling between state variables of different parities only while $M_{ij}(x_{th})$ is responsible for coupling only between state variables with the same parities. Now from the antisymmetry of $\mathbf{L}$ and symmetry of $\mathbf{M}$ we obtain Onsager-Casimir reciprocal relations, which say that state variables with the same parities are coupled through an symmetric matrix while state variables with opposite parities are coupled through an antisymmetric matrix. OCRR can be thus regarded as a consequence of GENERIC and the behavior of GENERIC with respect to TRT. Let us now formulate these conclusions as a theorem:

Theorem 2. *Let us assume that*

1. *Assumption 1 holds.*

2. *Parity may be assigned to each state variable x_i, i.e. $\mathcal{P}(x_i)$ is well defined for each x_i.*

3. *Both matrices L_{ij} and M_{ij} are even with respect to TRT if evaluated at equilibrium. This is true, for example, if the matrices are constructed from spatial gradients and state variables.*

4. *Relations* (1.27) *are valid.*

5. *Assumption 2 holds and thus definitions of reversibility 3, 4 and 5 are equivalent according to Theorem 1.*

Then state variables with opposite parities are coupled through the antisymmetric part of matrix K_{ij} in Eq. (1.30) *while state variables with the same parity are coupled through the symmetric part in the near-equilibrium regime. This is the statement of Onsager-Casimir reciprocal relations, which are thus proved for any system near equilibrium.*

Corollary 1. *Since the symmetric part is given by the dissipative bracket and the antisymmetric by the Poisson bracket, it follows that state variables with opposite parities are coupled only through the Poisson bracket while state variables with the same parities are coupled only through the dissipative bracket near equilibrium.*

We have, therefore, shown that the structure of GENERIC and its behavior with respect to TRT implies OCRR near equilibrium. This means that we have identified the general structure which contains OCRR and which is valid far from equilibrium. In this sense, GENERIC intrinsically contains OCRR and thus can be considered as a generalization of OCRR into the far-from-equilibrium regime. Note that other thermodynamic theories like CIT or EIT do not posses this property, and OCRR have to be supplied to them.

1.1.5 Geometrical interpretation of reversibility and irreversibility

The hitherto derived results can be formulated more rigorously within differential geometry. Generally, an evolution equation is an equality between time derivative of state variables and a vector field on tangent bundle of the manifold[32] of state variables $\mathcal{M}$, i.e.

$$\frac{\mathrm{d}\mathbf{x}}{\mathrm{d}t} = V^i(\mathbf{x})\frac{\partial}{\partial x^i} = \mathcal{V}(\mathbf{x}) \tag{1.35}$$

where state variables were denoted as coordinates $\mathbf{x}$. Note that we use Einstein's summation convention in this section. Time-reversal transformation $\mathbf{I}$ provides a diffeomorphism of manifold $\mathcal{M}$ to itself. This diffeomorphism then induces a push-forward of the vector field on the r.h.s. of equation (1.35)

$$\mathbf{I}_\star\left(V^i\frac{\partial}{\partial x^i}\right) = \frac{\partial \mathbf{I}^i}{\partial x^j}(\mathbf{x})V^j(\mathbf{x})\frac{\partial}{\partial \mathbf{I}(\mathbf{x})^i}. \tag{1.36}$$

This push-forward then acts on equation (1.35) as follows

$$\frac{\mathrm{d}\mathbf{I}(\mathbf{x})}{\mathrm{d}\tau} = -\mathbf{I}_\star\mathcal{V}|_{\mathbf{I}(\mathbf{x})} \tag{1.37}$$

where $\mathrm{d}t$ was replaced by $-\mathrm{d}\tau$ as in Definition 3. Definition 3 can be then reformulated as follows

Definition 6. *Vector field $\mathcal{V}$ is called reversible if and only if the push-forward only adds a minus sign in front of the vector field*

$$\mathbf{I}_\star\mathcal{V} = -\mathcal{V}|_{\mathbf{I}(\mathbf{x})}. \tag{1.38}$$

Roughly speaking, it means that all "arrows" along integral curves of the vector field are inverted if TRT is applied to the state variables. Recall that in the sense of Definition 3 the reversible part of the r.h.s of the evolution equation keeps the same form as the l.h.s with respect to TRT and that a minus sign is added in front of the l.h.s. due to transformation of $\mathrm{d}t$ to $\mathrm{d}\tau$. This is the minus sign which appears on r.h.s. of equation (1.38). Therefore, both definitions of reversibility 3 and 6 are equivalent.

Lemma 2. *Definitions of reversibility 3 and 6 are equivalent.*

Definition 6 is, however, more rigorous since it is formulated as a differentially geometric identity.

Let us now formulate conditions (1.27), which ensured that the Poisson and the dissipative bracket generate only reversible and irreversible evolution in the sense of Definition 3, geometrically. Assume, therefore, as well as in the derivation of the conditions, that all state variables have definite parities. That means that TRT acts on state variables as follows

$$\mathbf{I}(\mathbf{x})^i = P(x^i)x^i. \tag{1.39}$$

Jacobi matrix of this transformation is then

$$\frac{\partial \mathbf{I}(\mathbf{x})^i}{\partial x^j} = P(x^i)\delta^i_j \tag{1.40}$$

where δ is Kronecker delta. The Poisson vector field, which generates the reversible evolution, can be expressed as

$$\mathcal{V} = L^{ij}(\mathbf{x})\frac{\partial E}{\partial x^j}\frac{\partial}{\partial x^i} \tag{1.41}$$

where summation stands generally for scalar product and indices i and j may be also continuous as within the Boltzmann equation in section A.1. Condition (1.38) can be then rewritten as

$$L^{ij}|_{\mathbf{I}(\mathbf{x})} = -P(x^i)P(x^j)L^{ij}|_{\mathbf{x}}, \tag{1.42}$$

which is the geometrical interpretation of relation (1.27a).

But does any Poisson bracket satisfy this relation? To author's best knowledge this is an open problem. All the examples of Poisson brackets formulated in this manuscript satisfy the relation. To proof general validity of the relation, one would have to formulate how a Poisson bracket on a level of description can generally be inherited from Poisson bracket on the most microscopic level of description, e.g. from the Hamiltonian dynamics, because TRT on the more macroscopic level is inherited from TRT on the most microscopic level and Poisson bracket on the most microscopic level is reversible (Hamiltonian dynamics and its dual formulation A.2.2 are reversible). A method how to obtain a Poisson bracket on the more macroscopic level from a Poisson bracket of Hamiltonian dynamics by projection operators was formulated by H. C. Öttinger[75], and it is easy to show that any Poisson bracket obtained by this method fulfills relation (1.42) and thus is reversible. Nevertheless, validity of Jacobi identity for the Poisson bracket has not been derived in general and hence one can not regard the method as generally valid yet.

On the other hand, a very similar method for constructing Poisson brackets is proposed in this work, see A.2, where Poisson brackets on lower levels of description are derived from the Poisson bracket of Liouville equation, which is equivalent to the standard Poisson bracket of Hamiltonian dynamics, by geometrical means. Jacobi identity is fulfilled automatically, and the condition of reversibility of the constructed Poisson bracket is inherited from reversibility of the Poisson bracket on the Liouville level of description.

In summary, it is still an open problem to show that any Poisson bracket on any level of description fulfills relation (1.38), and it is still necessary to prove that any Poisson bracket generates only reversible evolution. However, if the method of construction of Poisson brackets developed in A.2 turns out to be generally valid, the problem will be solved because Poisson brackets constructed by the method automatically satisfy condition (1.42). Moreover, it can be shown by means of quantum master equation that condition (1.42) is satisfied at least at equilibrium, see our paper [78].

Analogically to the reversible evolution, irreversible evolution is generated by a vector field which is invariant to the push-forward $\mathbf{I}_\star$ induced by TRT. This leads to the following definition

Definition 7. *A vector field generates irreversible evolution if the push-forward induced by TRT acts on the field as follows*

$$\mathbf{I}_\star\mathcal{V} = \mathcal{V}|_{\mathbf{I}(\mathbf{x})} \tag{1.43}$$

Therefore, if all state variables have definite parities, a condition analogical to (1.42) holds also for the $\mathbf{M}$ matrix

$$M^{ij}|_{\mathbf{I}(\mathbf{x})} = +P(x^i)P(x^j)M^{ij}|_{\mathbf{x}}, \tag{1.44}$$

which is the geometrical interpretation of relation (1.27b).

In the more general setting where irreversible evolution is described by dissipation potential instead of dissipative matrix, the irreversible part of evolution equations transforms as follows

$$\begin{aligned}
\mathbf{I}_\star\left(\frac{\partial\Xi}{\partial\frac{\partial S}{\partial x^i}}\frac{\partial}{\partial x^i}\right) &= \frac{\partial\mathbf{I}^i}{\partial x^j}\frac{\partial\Xi}{\partial\frac{\partial S}{\partial x^j}}\Big|_{\mathbf{x}}\frac{\partial}{\partial\mathbf{I}^i(\mathbf{x})} = \frac{\partial\mathbf{I}^i}{\partial x^j}\frac{\partial\Xi}{\partial\frac{\partial S}{\partial\mathbf{I}^k}\frac{\partial\mathbf{I}^k}{\partial x^j}}\Big|_{\mathbf{x}}\frac{\partial}{\partial\mathbf{I}^i(\mathbf{x})} = \\
&= \frac{\partial\mathbf{I}^i}{\partial x^j}\frac{\partial\Xi}{\partial\frac{\partial S}{\partial\mathbf{I}^l}}\frac{\partial\frac{\partial S}{\partial\mathbf{I}^l}}{\partial\frac{\partial S}{\partial\mathbf{I}^k}\frac{\partial\mathbf{I}^k}{\partial x^j}}\Big|_{\mathbf{x}}\frac{\partial}{\partial\mathbf{I}^i(\mathbf{x})} = \frac{\partial\mathbf{I}^i}{\partial x^j}\frac{\partial\Xi}{\partial\frac{\partial S}{\partial\mathbf{I}^l}}\frac{\partial x^j}{\partial\mathbf{I}^k}\delta^k_l\Big|_{\mathbf{x}}\frac{\partial}{\partial\mathbf{I}^i(\mathbf{x})} = \\
&= \frac{\partial\Xi}{\partial\frac{\partial S}{\partial\mathbf{I}^i(\mathbf{x})}}\frac{\partial}{\partial\mathbf{I}^i(\mathbf{x})}
\end{aligned} \tag{1.45}$$

because both dissipation potential and entropy are even under TRT in accordance to Assumption 2. We have thus proven the following lemma

Lemma 3. *Any even dissipation potential satisfies relation* (1.38) *and thus generates only irreversible evolution.*

Note that dissipation potential (as a function on manifold $\mathcal{M}$) is even if it is not altered by the push-forward induced by TRT.

1.2 Discussion

The purpose of this section is to give a brief overview in the development of OCRR. More detailed discussion can be found in our paper [78].

The Onsager–Casimir reciprocal relations were originally formulated by Onsager[72, 73] and Casimir[20]. Later, they have been derived within quantum mechanics by van Kampen[47], and a very detailed derivation was given by de Groot and Mazur[28]. These reciprocity relations have been typically derived from the microscopic time reversibility and the hypothesis that equilibrium fluctuations and macroscopic state variables close to equilibrium follow the same time evolution. Moreover, only scalar state variables are usually admitted [28] in the derivation.

Despite these rather restrictive assumptions in the derivation, OCRR are often employed in phenomenological non-equilibrium thermodynamics. That is why much effort has been spent on a more general derivation of the relations. There are two classes of such derivations, one starting from statistical physics while the other being purely phenomenological. The statistical derivations, see e.g. [43], however, usually suffer from a hidden assumption of being close to global equilibrium, see the discussion in our paper [78]. The phenomenological derivations, e.g. [69], usually suffer from requiring an independent identification of thermodynamic forces and fluxes. An attempt to distinguish between forces and fluxes in general was given for example by Bothe and Dryer in [16], but the method is not invariant to change of physical units. For example, if one decides to divide a diffusion flux

by speed of light, one changes the resulting Onsager-Casimir coupling between the diffusion flux and other diffusion fluxes from symmetric to antisymmetric.

The advantage of our derivation of OCRR within GENERIC, the original idea of which comes from [35], is that no identification of forces and fluxes is required, and that it clearly indicates the range of validity of OCRR. OCRR in the original sense are only valid near global equilibrium as shown in Sec. 1.1.4. But since they are just an implication of GENERIC near equilibrium, GENERIC far from equilibrium can be considered a generalization of the OCRR into the far-from-equilibrium regime.

1.3 Conclusion

In Sec. 1.1.1 we introduce the concept of time-reversal transformation (TRT), which is specified rigorously in Sec. 1.1.5. Reversible evolution is identified as the part of evolution which is not altered by TRT while irreversible evolution changes its sign after applying TRT, see Def. 3. This concept of reversibility based on TRT is equivalent to the entropic definition of reversibility, Def. 4, where irreversible evolution is identified as the part of evolution which raises entropy. Yet another definition comes from GENERIC, where reversible evolution is identified as the evolution generated by a Poisson bracket while irreversible evolution is generated by a dissipation potential or dissipative bracket, see Def. 5. While it can be shown that under certain assumptions all these definitions of irreversible evolution coincide, see Sec. 1.1.5, it is not clear how to prove the analogical statement for the reversible evolution in full generality. To author's best knowledge this is an open problem although it is quite likely that the definitions coincide as well as for the irreversible evolution, since the author is not aware of any counterexample and because the proposed hierarchy of Poisson brackets in Sec. A.2 indeed generates only reversible evolution.

After introducing time-reversal transformation (TRT) properly, Onsager-Casimir reciprocal relations (OCRR) are shown to be implied by the structure of GENERIC in the near-equilibrium regime without limitations to finite-dimensional dynamics or continuum thermodynamics. The symmetric part of the relations is given by the dissipative bracket (or dissipation potential) while the antisymmetric part is given by the Poisson bracket. This way, OCRR can be regarded as a near-equilibrium consequence of the structure of GENERIC. OCRR are generalized into far-from-equilibrium regime in the sense that a far-from-equilibrium structure (GENERIC) which implies them is identified.

2. Classical Irreversible Thermodynamics

2.1 General theory

Classical irreversible thermodynamics (CIT) is one of the simplest forms of continuum non-equilibrium thermodynamics. The theory was first developed by Onsager [72, 73] and subsequently generalized by Meixner [64] and Prigogine [83], Meixner and Reik [65] and finally by de Groot and Mazur [28]. The last mentioned book can be regarded as perhaps the most complete treatment of CIT. For recent developments one should refer to a book by Signe Kjelstrup and Dick Bedeaux [48], where numerous application within chemistry and engineering are demonstrated, and a book by Lebon et al. [55], where also another theories of non-equilibrium thermodynamics are reviewed. Interesting applications can also be found in [61]. CIT has become one of the most frequently used forms of non-equilibrium thermodynamics due to its relative simplicity and due to the possibility to describe experiments efficiently.

State variables of CIT are densities of all species, overall momentum (or barycentric velocity) and energy (or entropy) density, and so CIT can be regarded as a particular level of description of a mixture of fluids. It can also be formulated within GENERIC, see [76]. A generalization of CIT, where also diffusion fluxes are among state variables, was proposed in our paper [81]. To avoid repetition, some details of the derivation which can be found in [28] or [81] are omitted in this work.

2.1.1 Balance equations

The starting point of CIT are continuum balance equations, which become evolution equations of the state variables after supplying all necessary constitutive relations. Balance equation of density of species α is

$$\frac{\partial \rho_\alpha}{\partial t} = -\mathrm{div}(\rho_\alpha \mathbf{v}_\alpha) + \widehat{\rho}_\alpha \tag{2.1}$$

where ρ_α is density of the species and $\mathbf{v}_\alpha$ is its velocity. $\widehat{\rho}_\alpha$ denotes density of production of species α in chemical reactions. Total density is given by

$$\rho = \sum_\alpha \rho_\alpha, \tag{2.2}$$

and barycentric velocity is defined as

$$\rho \mathbf{v} = \sum_\alpha \rho_\alpha \mathbf{v}_\alpha. \tag{2.3}$$

Diffusion flux of species α, $\mathbf{j}_\alpha$, can be then defined as

$$\mathbf{j}_\alpha = \rho_\alpha(\mathbf{v}_\alpha - \mathbf{v}). \tag{2.4}$$

Balance equation of momentum is

$$\frac{\partial \rho \mathbf{v}}{\partial t} = -\mathrm{div}(\rho \mathbf{v} \otimes \mathbf{v}) - \nabla p + \mathrm{div}\mathbf{t}^{irr} + \sum_{\alpha} \rho_\alpha \mathbf{f}_\alpha \tag{2.5}$$

where p is pressure, $\mathbf{t}^{irr}$ is the irreversible part of total Cauchy stress tensor, which is defined as being odd with respect to TRT, and $\mathbf{f}_\alpha$ is external force density acting on species α. We suppose that there are potentials satisfying

$$\mathbf{f}_\alpha = -\nabla \varphi_\alpha \tag{2.6}$$

for each force $\mathbf{f}_\alpha$.

Balance equation of total energy density is

$$\begin{aligned} \frac{\partial}{\partial t}\left(\frac{1}{2}\rho \mathbf{v}^2 + \rho\varepsilon + \sum_{\alpha} \rho_\alpha \varphi_\alpha\right) = \\ = -\mathrm{div}\left(\tilde{\mathbf{j}}_q + \rho \mathbf{v}\varepsilon + \sum_{\alpha} \rho_\alpha \mathbf{v}_\alpha \varphi_\alpha - \mathbf{t}\cdot\mathbf{v}\right) + \sum_{\alpha} \rho_\alpha \frac{\partial \varphi_\alpha}{\partial t} \end{aligned} \tag{2.7}$$

where ε is the internal energy density. Note that heat flux $\tilde{\mathbf{j}}_q$ consists of certain amount of energy carried by diffusion of particles and of conductive heat flux, e.g. carried by phonons. It can be shown that energy carried by diffusion of particles is equal to diffusion of enthalpy, see for example [81]. Hence we introduce the conductive heat flux[1]

$$\mathbf{j}_q = \tilde{\mathbf{j}}_q - \sum_{\alpha} \mathbf{j}_\alpha h_\alpha \tag{2.8}$$

where h_α is partial specific enthalpy given by

$$h_\alpha = T s_\alpha + \mu_\alpha. \tag{2.9}$$

This last formula follows from equilibrium thermodynamics, see e.g. [81].

Using (2.5) and (2.1), balance of total energy can be rewritten in the form of balance equation of internal energy

$$\frac{\partial \rho\varepsilon}{\partial t} = -\mathrm{div}(\tilde{\mathbf{j}}_q + \rho\mathbf{v}\varepsilon) + \mathbf{t} : \nabla\mathbf{v} - \sum_{\alpha} \mathbf{j}_\alpha \cdot \nabla\varphi_\alpha - \sum_{\alpha} \varphi_\alpha \widehat{\rho}_\alpha. \tag{2.10}$$

General balance of entropy can be written as

$$\frac{\partial \rho s}{\partial t} = -\mathrm{div}(\rho s \mathbf{v} + \mathbf{j}_s) + \sigma_s \tag{2.11}$$

where entropy density per kilogram s is equal to $\sum_\alpha \frac{\rho_\alpha}{\rho} s_\alpha$.

[1] In [28] the conductive heat flux is referred to as reduced heat flux, and it can be related to the measurable heat flux from [48], see section 3.1.1 for details.

2.1.2 Gibbs relation

Hitherto, we have formulated balance equations for densities, momentum density and energy density, and the balance equations can be regarded as evolution equations for the corresponding state variables. Therefore, state variables are ρ_α, $\mathbf{v}$ and ε. Entropy can, in general, depend on all the state variables, but since it should be Galilean invariant, it should not depend on $\mathbf{v}$. Therefore, entropy is a function of ρ_α and ε only, and we can write Gibbs relations as follows

$$\frac{\partial \rho s}{\partial t} = T^{-1}\frac{\partial \rho \varepsilon}{\partial t} - \sum_\alpha \frac{\mu_\alpha}{T}\frac{\partial \rho_\alpha}{\partial t} \tag{2.12}$$

where temperature T and chemical potentials μ_α were identified as the corresponding partial derivatives. This equation can be rewritten with ∇ substited for the partial time-derivatives as shown in [81]. Besides this relation we also recall the Euler relation, see [19] or [81],

$$T\rho s = \rho\varepsilon + p - \sum_\alpha \mu_\alpha \rho_\alpha \tag{2.13}$$

and the Gibbs-Duhem relation, which follows from the Euler relation and from the Gibbs relation,

$$0 = s\nabla T - \frac{1}{\rho}\nabla p + \sum_\alpha \rho_\alpha \nabla \mu_\alpha. \tag{2.14}$$

Alternatively, the Gibbs relation may be rewritten as

$$0 = \sum_\alpha \rho_\alpha s_\alpha \nabla T - \nabla p + \sum_\alpha \rho_\alpha \nabla \mu_\alpha = -\nabla p + \sum_\alpha \rho_\alpha \nabla (\mu_\alpha)_T \tag{2.15}$$

where $(\nabla \tilde{\mu}_\alpha)_T$ is gradient of electrochemical potential of species α at constant temperature,

$$(\nabla \tilde{\mu}_\alpha)_T = \nabla \tilde{\mu}_\alpha - \left(\frac{\partial \mu_\alpha}{\partial T}\right)_{p,m_\beta} \nabla T = \nabla \tilde{\mu}_\alpha + s_\alpha \nabla T, \tag{2.16}$$

with s_α being partial specific entropy,

$$s_\alpha = \left(\frac{\partial S}{\partial m_\alpha}\right)_{T,p,m_{\beta\neq\alpha}} = -\left(\frac{\partial \mu_\alpha}{\partial T}\right)_{p,m_\beta} \tag{2.17}$$

where S is the total entropy of the system, see [81].

2.1.3 Entropy production and entropy flux

Plugging balance equation of energy (2.10) and balance of mass (2.1) into the Gibbs relation (2.12) and using (2.12) and (2.14), we obtain balance equation of entropy in the form (2.11), where entropy production is

$$\sigma_s = \mathbf{j}_q \cdot \nabla \frac{1}{T} - \frac{1}{T}\sum_\alpha \mathbf{j}_\alpha \cdot (\nabla \tilde{\mu}_\alpha)_T + \frac{1}{T}\mathbf{t}^{irr} : \nabla \mathbf{v} + \frac{1}{T}\sum_r \tilde{\mathcal{A}}_r \dot{\xi}_r \tag{2.18}$$

and entropy flux is

$$\mathbf{j}_s = \frac{\mathbf{j}_q}{T} + \sum_\alpha \mathbf{j}_\alpha s_\alpha. \tag{2.19}$$

In these two last equations, $\mathbf{j}_q$ is the conductive heat flux, and $\tilde{\mu}_\alpha$ is electrochemical potential of species α defined as

$$\tilde{\mu}_\alpha = \mu_\alpha + \varphi_\alpha. \tag{2.20}$$

Electrochemical affinity $\tilde{\mathcal{A}}_r$, which constitutes the driving force for electrochemical reactions, is defined as

$$\tilde{\mathcal{A}}_r = -\sum_\alpha \nu_{r\alpha}\tilde{\mu}_\alpha \tag{2.21}$$

where $\nu_{r\alpha}$ is the stoichiometric coefficient of species α in chemical reaction r. Rate of reaction r is denoted by $\dot{\xi}_r$.

Entropy production (2.18) can be rewritten alternatively as

$$\sigma_s = -\frac{1}{T}\mathbf{j}_s \cdot \nabla T - \frac{1}{T}\sum_\alpha \mathbf{j}_\alpha \cdot \nabla\tilde{\mu}_\alpha + \frac{1}{T}\mathbf{t}^{irr} : \nabla\mathbf{v} + \frac{1}{T}\sum_r \tilde{\mathcal{A}}_r\dot{\xi}_r. \tag{2.22}$$

2.1.4 Force-flux relations

The formula for entropy production rate (2.18) usually serves for suggesting thermodynamically consistent constitutive relations between the unknown quantities ($\mathbf{j}_q$, $\mathbf{j}_\alpha$, $\mathbf{t}^{irr}$ and $\dot{\xi}_r$) and the state variables. The formula is regarded as a sum of products of thermodynamic forces and fluxes, and the fluxes are assumed to be proportional to the forces (assuming that they are identified correctly, see the Sec. 1.2). Moreover, from the Curie-Prigogine principle, see [55], it follows that only forces and fluxes of the same tensorial character are coupled in an isotropic medium, and we assume that the systems under consideration are isotropic.

Force-flux relations between scalar forces and fluxes are then expressed by assuming the reaction rates be proportional to the electrochemical affinities and (after splitting the $\mathbf{t}^{irr}$ term into its isotropic and deviatoric part) to divergence of velocity. Bulk viscosity and reaction rate constants come into play this way. However, proportionality between reaction rates and electrochemical affinities is too restrictive for usual chemical reactions, which are often described the law of mass action, see for example [36]. The linear dependence is thus often replaced by a nonlinear relation as in Sec. 3.2.

Force-flux relations between vectorial quantities are given by

$$\mathbf{j}_\alpha = L_{q\alpha}\nabla\frac{1}{T} - \frac{1}{T}\sum_\beta L_{\alpha\beta}(\nabla\tilde{\mu}_\beta)_T \tag{2.23a}$$

$$\mathbf{j}_q = L_{qq}\nabla\frac{1}{T} - \frac{1}{T}\sum_\alpha L_{q\alpha}(\nabla\tilde{\mu}_\alpha)_T \tag{2.23b}$$

with $L_{\alpha q} = L_{q\alpha}$ according to OCRR. Strictly speaking, one should use OCRR only in the near-global-equilibrium regime while CIT works in the local equilibrium regime, which may be relatively far from the global equilibrium. We suppose, however, that this symmetry, that holds near global equilibrium, also holds near local equilibrium. More details on this topic are given in Sec. 2.2.

Finally, force-flux relations between tensors of second order express that the deviatoric part of the irreversible Cauchy stress tensor is proportional to the deviatoric part of gradient of velocity, the proportionality coefficient being the shear viscosity. This way the classical hydrodynamics is derived within CIT, see [28]. Let us now illustrate the derivation of OCRR from Sec. 1.1.4 on classical hydrodynamics.

2.2 Classical hydrodynamics

The purpose of this section is to illustrate the derivation of OCRR from Sec. 1.1.4 on classical hydrodynamics. Classical hydrodynamics, where state variables are[2] density field $\rho(\mathbf{r})$, field of momentum density $\mathbf{u}(\mathbf{r})$ and field of internal energy density $\epsilon(\mathbf{r})$, was formulated within GENERIC in [77].

Energy of the whole system is specified as[3]

$$E = \int_V \frac{\mathbf{u}(\mathbf{r})^2}{2\rho(\mathbf{r})} + \epsilon(\mathbf{r}) \, \mathrm{d}\mathbf{r}. \tag{2.24}$$

Entropy of the whole system is given by

$$S = \int_V s(\epsilon(\mathbf{r}), \rho(\mathbf{r})) \, \mathrm{d}\mathbf{r}. \tag{2.25}$$

Poisson bivector is[77]

$$L(\mathbf{r}, \mathbf{r}') = \begin{pmatrix} 0 & \rho(\mathbf{r}')\frac{\partial\delta}{\partial\mathbf{r}'} & 0 \\ -\rho(\mathbf{r})\frac{\partial\delta}{\partial\mathbf{r}} & \mathbf{u}(\mathbf{r}')\frac{\partial\delta}{\partial\mathbf{r}'} - \frac{\partial\delta}{\partial\mathbf{r}}\mathbf{u}(\mathbf{r}) & -\epsilon(\mathbf{r})\frac{\partial\delta}{\partial\mathbf{r}} + \frac{\partial\delta}{\partial\mathbf{r}'}p(\mathbf{r}') \\ 0 & \epsilon(\mathbf{r}')\frac{\partial\delta}{\partial\mathbf{r}'} - \frac{\partial\delta}{\partial\mathbf{r}}p(\mathbf{r}) & 0 \end{pmatrix} \tag{2.26}$$

where $\delta = \delta(\mathbf{r} - \mathbf{r}')$ and δ denotes Dirac distribution[4]. The dissipative bracket is specified as[77]

$$M(\mathbf{r}, \mathbf{r}') = \begin{pmatrix} 0 & 0 & 0 \\ 0 & \left(\frac{\partial}{\partial\mathbf{r}'}\frac{\partial}{\partial\mathbf{r}} + \mathbf{1}\frac{\partial}{\partial\mathbf{r}'}\cdot\frac{\partial}{\partial\mathbf{r}}\right)\eta T\delta + & \frac{\partial}{\partial\mathbf{r}}\cdot\eta T\dot{\gamma}\delta + \frac{\partial}{\partial\mathbf{r}}\hat{k}T\mathrm{tr}\dot{\gamma}\delta \\ & +2\frac{\partial}{\partial\mathbf{r}}\frac{\partial}{\partial\mathbf{r}'}\hat{k}T\delta & \\ 0 & \frac{\partial}{\partial\mathbf{r}'}\cdot\eta T\dot{\gamma}\delta + \frac{\partial}{\partial\mathbf{r}'}\hat{k}T\mathrm{tr}\dot{\gamma}\delta & \frac{1}{2}\eta T\dot{\gamma} : \dot{\gamma}\delta + \frac{\partial}{\partial\mathbf{r}}\cdot\frac{\partial}{\partial\mathbf{r}'}\lambda T^2\delta + \\ & & +\frac{1}{2}\hat{k}T\mathrm{tr}\dot{\gamma}^2\delta \end{pmatrix} \tag{2.27}$$

where $\dot{\gamma}$ is the symmetric gradient of velocity field, η is shear viscosity, $\hat{k}$ is bulk viscosity and λ is thermal conductivity.

Poisson matrix (2.26) is obviously antisymmetric with respect to simultaneous transposition and swapping arguments $\mathbf{r}$ and $\mathbf{r}'$. Hydrodynamic state variables have the following parities

$$\mathcal{P}(\rho) = 1, \qquad \mathcal{P}(\mathbf{u}) = -1, \qquad \mathcal{P}(\epsilon) = 1. \tag{2.28}$$

[2]For compactness of notation, time dependence of state variables is not indicated explicitly.

[3]The variable with respect to which a function is integrated either follows directly the integral sign, or it follows the integrand. Moreover, instead of indicating the action of the delta-distribution on a function by duality, see [84], the action is expressed in a form of an integral, as usual in physics. Since function spaces are often unspecified, most calculations in this work have to be taken as formal or valid for sufficiently regular functions.

[4]Gradient of δ-distribution $\frac{\partial\delta}{\partial\mathbf{r}'}$ can be expressed as $\frac{\partial\delta_{\mathbf{r}}(\mathbf{r}')}{\partial\mathbf{r}'}$ more rigorously.

It can be easily checked that parities of the Poisson matrix are

$$\mathcal{P}\left(\mathbf{L}\right) = \begin{pmatrix} 0 & 1 & 0 \\ 1 & -1 & 1 \\ 0 & 1 & 0 \end{pmatrix}, \tag{2.29}$$

which is in agreement with result (1.27a), and the Poisson bracket generates reversible evolution, consequently.

Dissipative matrix is obviously symmetric with respect to transposition and swapping arguments $\mathbf{r}$ and $\mathbf{r}'$. The matrix has the following parities

$$\mathcal{P}\left(\mathbf{M}\right) = \begin{pmatrix} 0 & 0 & 0 \\ 0 & 1 & -1 \\ 0 & -1 & 1 \end{pmatrix}, \tag{2.30}$$

which is in agreement with result (1.27b) as well, and thus the dissipative bracket generates irreversible evolution.

Hitherto, we have shown that classical hydrodynamics is consistent with relations (1.27). Let us now show how the results of the near-equilibrium treatment apply to classical hydrodynamics. To do so we substitute equilibrium values of state variables (ρ_{th}, 0, ε_{th}) into both the matrices. Since the system is considered isolated, equilibrium value of momentum is zero everywhere. This way the Poisson matrix simplifies to

$$L(x_{th})(\mathbf{r},\mathbf{r}') = \begin{pmatrix} 0 & \rho_{th}\frac{\partial\delta}{\partial\mathbf{r}'} & 0 \\ -\rho_{th}\frac{\partial\delta}{\partial\mathbf{r}} & 0 & -\epsilon_{th}\frac{\partial\delta}{\partial\mathbf{r}} + \frac{\partial\delta}{\partial\mathbf{r}'}p_{th} \\ 0 & \epsilon_{th}\frac{\partial\delta}{\partial\mathbf{r}'} - \frac{\partial\delta}{\partial\mathbf{r}}p_{th} & 0 \end{pmatrix}, \tag{2.31}$$

and the dissipative matrix simplifies to

$$M(x_{th})(\mathbf{r},\mathbf{r}') = \begin{pmatrix} 0 & 0 & 0 \\ 0 & \left(\frac{\partial}{\partial\mathbf{r}'}\frac{\partial}{\partial\mathbf{r}} + \mathbf{1}\frac{\partial}{\partial\mathbf{r}'}\cdot\frac{\partial}{\partial\mathbf{r}}\right)\eta T\delta + 2\frac{\partial}{\partial\mathbf{r}}\frac{\partial}{\partial\mathbf{r}'}\hat{k}T\delta & 0 \\ 0 & 0 & \frac{\partial}{\partial\mathbf{r}}\cdot\frac{\partial}{\partial\mathbf{r}'}\lambda T^2\delta \end{pmatrix}. \tag{2.32}$$

It can be easily checked that the terms corresponding to state variables with the same parities have vanished in the Poisson matrix while terms corresponding to state variables with different parities have vanished in the dissipative matrix. Therefore, OCRR are fulfilled for near-equilibrium classical hydrodynamics, which is the result of Theorem 2, proof of which we have just retraced. Explicit form of the near-equilibrium evolution equations can be found in our paper [78].

We have thus shown validity of OCRR near global equilibrium. But classical hydrodynamics (and the whole CIT) is based on the assumption of local equilibrium only. Are OCRR valid for local equilibrium as well? To answer the question one would at first have to specify the meaning of OCRR in a regime not near global equilibrium. If the meaning were that coupling of state variables with the same parities is symmetric while coupling of state variables with different parities is antisymmetric, then OCRR are clearly violated in the regime. Indeed, dissipative matrix (2.27) provides symmetric coupling between momentum and energy, which have opposite parities. On the other hand, if the coupling coefficients (e.g. coefficient of thermodiffusion in CIT[28, 76]) are constant, that is the same as in

equilibrium, coupling keeps its symmetricity or antisymmetricity also out of the near global equilibrium regime. In summary, one should bear in mind that OCRR are valid near global equilibrium and that GENERIC is the far-from-equilibrium extension of OCRR, which may have the same symmetry/antisymmetry as near global equilibrium also far from equilibrium.

3. Mechanical Equilibrium

Mechanical equilibrium is the level of description, where state variables consist of densities of all species and overall energy (or entropy) while momentum is no more among the state variables because it already has relaxed to a value constant through space. This level of description is of enormous importance in description of real systems. Indeed, for example the whole book [48] is formulated on this level. The phenomena that prevail on this level consist of heat flux, diffusion, and (electro)chemical reactions.

As the level of mechanical equilibrium is more macroscopic than the level of CIT, evolution equations on the former level can be derived from evolution equations on the latter level by letting the overall momentum relax. In particular, there is no Poisson bracket on the level of mechanical equilibrium as shown in Sec. A.2.9. The requirement of relaxed overall momentum is typically fulfilled in porous media. Let us, therefore, have a look at formulation of porous media within mechanical equilibrium at first.

3.1 Transport through porous media

When describing diffusion through a porous medium, the diffusing species generally interact with the medium, and concentration of the medium, therefore, affects electrochemical potential of the species. Hence, the medium should be treated as one component of the mixture, let us say the zeroth component as already suggested in [28].

Let us suppose that the whole mixture is in mechanical equilibrium, i.e. barycentric velocity is constant in time and space. This means that Eq. (2.5) becomes

$$0 = -\nabla p + \sum_{\alpha} \rho_\alpha \mathbf{f}_\alpha. \tag{3.1}$$

Then from Gibbs-Duhem relation (2.15) it follows that

$$\sum_{\alpha} \rho_\alpha (\nabla \tilde{\mu}_\alpha)_T = 0. \tag{3.2}$$

Therefore, if we expand diffusion fluxes according to their definition, the term with barycentric velocity in the diffusion part of entropy production disappears. Moreover, we can add any constant velocity to the actual velocities $\mathbf{v}_\alpha$. This means that we can even set $v = 0$ without loss of generality.

Let us further suppose that the porous medium is static, i.e. its velocity is zero everywhere, and that it is in equilibrium, i.e. $(\nabla \tilde{\mu}_0)_T = 0$. Diffusion fluxes can be then expressed with respect to the medium, velocity of which is zero,

$$\mathbf{j}_\alpha = \rho_\alpha \mathbf{v}_\alpha. \tag{3.3}$$

Let us also suppose that $L_{0q} = 0$, which means that gradient of temperature does

not cause diffusion of the medium. Finally, force-flux relations (2.23) become

$$\mathbf{j}_\alpha = L_{\alpha q}\nabla\frac{1}{T} - \frac{1}{T}\sum_{\beta\neq 0} L_{\alpha\beta}(\nabla\tilde{\mu}_\beta)_T \quad \forall\alpha\neq 0 \tag{3.4a}$$

$$\mathbf{j}_q = L_{qq}\nabla\frac{1}{T} - \frac{1}{T}\sum_{\alpha\neq 0} L_{q\alpha}(\nabla\tilde{\mu}_\alpha)_T, \tag{3.4b}$$

and diffusion can be, therefore, described effectively without explicitly concerning the porous medium.

3.1.1 Electrochemistry

Flux of total energy, which is represented by the term inside the divergence in Eq. (2.7), becomes

$$\mathbf{j}_{en} = \mathbf{j}_q + \sum_\alpha \mathbf{j}_\alpha(h_\alpha + \varphi_\alpha) \tag{3.5}$$

on the level of mechanical equilibrium (by setting the barycentric velocity equal to zero). Using relation (2.9), the formula for energy flux can be rewritten as

$$\mathbf{j}_{en} = \mathbf{j}'_q + \sum_{\alpha\in n}\mathbf{j}_\alpha h_\alpha + \sum_{\alpha\in c}\mathbf{j}_\alpha z_\alpha F\Phi_\alpha \tag{3.6}$$

where measurable heat flux[1] was defined as

$$\mathbf{j}'_q = \mathbf{j}_q + T\sum_{\alpha\in c}\mathbf{j}_\alpha s_\alpha \tag{3.7}$$

and where $\sum_{\alpha\in n}$ denotes sum over all neutral species (except for the porous medium), $\sum_{\alpha\in c}$ sum over all charged species, z_α denotes amount of elementary charge per particle and Φ_α is electric potential closely related to electrochemical potential through

$$\tilde{\mu}_\alpha \overset{def}{=} z_\alpha F\Phi_\alpha \qquad \forall\alpha\in c. \tag{3.8}$$

This definition of electric potential is free of any inconsistencies mentioned in [70]. Note that we assumed that potential energy of neutral species is negligible in Eq. (3.6). The electrochemical potential can be further specified as

$$\tilde{\mu}_\alpha = \mu^\circ_\alpha + RT\ln\underbrace{\left(\gamma_\alpha\frac{b_\alpha}{b^\circ}\right)}_{a_\alpha} + z_\alpha F\varphi \tag{3.9}$$

where μ°_α is the standard chemical potential of the species (for example in an aqueous solution in Sec. 4.2), b_α is its molality, i.e. number of moles of the species per $1kg$ of water in the solution, γ_α is activity coefficient, see [5], a_α is activity, z_α is charge number and φ is the Maxwell potential, see [48].

Finally, from Eqs. (2.19) and (3.7) it follows by setting $v = 0$ that the total entropy flux is given by

$$\mathbf{j}_{s,tot} = \frac{\mathbf{j}'_q}{T} + \sum_{\alpha\in n}\mathbf{j}_\alpha s_\alpha. \tag{3.10}$$

[1] These terminology and notation are compatible with [48].

Exploiting these new definitions, entropy production in the porous medium becomes

$$\sigma_s = \mathbf{j}'_q \cdot \nabla \frac{1}{T} - \frac{1}{T} \sum_{\alpha \in n} \mathbf{j}_\alpha \cdot (\nabla \mu_\alpha)_T - \frac{1}{T} \sum_{\alpha \in c} \mathbf{j}_\alpha z_\alpha F \cdot \nabla \Phi_\alpha + \frac{1}{T} \sum_r \tilde{\mathcal{A}}_r \dot{\xi}_r. \quad (3.11)$$

This form of entropy production is particularly favorable because of the presence of the measurable heat flux and electric potentials, which can be measured by voltmeter (more details are given in the next section), and also due to the presence of electrochemical affinities, which drive electrochemical reactions. Formula (3.11) can be rewritten in an equivalent form similar to Eq. (2.22)

$$\sigma_s = -\mathbf{j}_{s,tot} \cdot \nabla T - \frac{1}{T} \sum_{\alpha \in n} \mathbf{j}_\alpha \cdot \nabla \mu_\alpha - \frac{1}{T} \sum_{\alpha \in c} \mathbf{j}_\alpha z_\alpha F \cdot \nabla \Phi_\alpha + \frac{1}{T} \sum_r \tilde{\mathcal{A}}_r \dot{\xi}_r, \quad (3.12)$$

where Eq. (3.10) was used.

3.1.2 Steady state

Finally, real electrochemical devices, e.g. fuel cells, are often studied in a state such that no property of the device changes with time, i.e. the device is in a steady state. Let us now have a look at steady balance equations.

Steady balance of total energy and steady balance of entropy in mechanical equilibrium can be written as

$$0 = -\int_{\partial V} \mathbf{j}_{en} \cdot \mathrm{d}\mathbf{S} \quad (3.13)$$

$$0 = -\int_{\partial V} \mathbf{j}_{s,tot} \cdot \mathrm{d}\mathbf{S} + \int_V \sigma_s \mathrm{d}V, \quad (3.14)$$

respectively, where the total energy flux $\mathbf{j}_{en}$ is given by Eq. (3.6) and the total entropy flux by Eq. (3.10).

By introducing partial currents

$$I_\alpha = \frac{z_\alpha F}{M_\alpha} \mathbf{j}_\alpha, \quad (3.15)$$

the total energy flux can be rewritten as

$$\mathbf{j}_{en} = \mathbf{j}'_q + \sum_{\alpha \in n} h_\alpha \mathbf{j}_\alpha + \sum_{\alpha \in c} I_\alpha \Phi_\alpha. \quad (3.16)$$

Note that potentials of neutral species, e.g. gravity, have been neglected. The total current is then given by

$$I = \sum_{\alpha \in c} I_\alpha. \quad (3.17)$$

Let us now return to the question which potential is measured by a voltmeter. Consider balance of total energy (3.13). Electrical work is the flux of energy due to electrons leaving and entering a device, i.e. passing to and from an external circuit. Electrical work is thus given by

$$\Delta W_{el} = \int_{\partial V} (h_e + \varphi_e) \mathbf{j}_e \cdot \mathrm{d}\mathbf{S}. \quad (3.18)$$

From equilibrium thermodynamics, see for example [53], it follows that partial specific enthalpy of electrons, as well as of any other species, can be expressed as

$$h_e = Ts_e + \mu_e \tag{3.19}$$

with s_e being partial specific entropy of electrons and μ_e chemical potential of electrons. Formula for electrical work (3.18) can be then rewritten as

$$\Delta W_{el} = \int_{\partial V} Ts_e \mathbf{j}_e \cdot \mathrm{d}\mathbf{S} + I(\Phi^c - \Phi^a), \tag{3.20}$$

where definition (3.8) was used. Total electric current leaving and entering the device was denoted by I and it was supposed that electrons leave the device at electric potential Φ^a (denoting the anode) and re-enter the device at potential Φ^c (denoting the cathode). The last term on r.h.s. of this equation is the standard expression for electrical work. But how to understand the first term? Firstly, the term is incorporated into the measurable heat flux, $\mathbf{j}'_q$. Secondly, the term is negligible compared with the last term as discussed in our paper [80]. Therefore, we can use electrical work in the standard form

$$\Delta W'_{el} = I(\Phi^c - \Phi^a). \tag{3.21}$$

Hence, a voltmeter indeed measures difference between electric potentials of electrons, which is proportional to difference between electrochemical potentials of electrons.

Let us put this differently. The voltmeter measures, in fact, the small electric current passing through it. Indeed, the current then moves the coil in the voltmeter. Regarding force-flux stemming from (3.11), the electric current is proportional to the difference between electrochemical potentials of the charged species, and thus the voltmeter measures this difference.

It should be borne in mind, however, that if the first term on r.h.s. of equation (3.20) were not negligible or if one wished to exploit the term to produce useful work, one should perhaps prefer formula (3.20). In this work, we use formula (3.21) since the first term on r.h.s. of equation (3.20) is negligible.

Defining the total measurable heat flux into the device and the total flux of enthalpy into the device as

$$\Delta Q' = \int_{\partial V} -\mathbf{j}'_q \cdot \mathrm{d}\mathbf{S} \tag{3.22}$$

$$\Delta H = \int_{\partial V} -\sum_{\alpha \in n} \mathbf{j}_\alpha h_\alpha \cdot \mathrm{d}\mathbf{S}, \tag{3.23}$$

respectively, allows to rewrite balance of energy (3.13) as

$$\Delta W'_{el} = \Delta Q' + \Delta H. \tag{3.24}$$

This formula is quite useful in concrete applications, see Sec. 3.7. Note that it is supposed that electrons are the only charged species leaving and entering the device.

3.2 Butler-Volmer equation

3.2.1 Thermodynamic formulation

In the standard CIT from [28] thermodynamic fluxes are supposed to be proportional to thermodynamic forces. In particular, rates of a chemical reactions are supposed to be proportional to chemical affinities of the reactions. On the other hand, electrochemical reactions are often well described by Butler-Volmer equation, see [18, 30, 5, 8, 70], where rate of an electrochemical reaction is given by

$$j = j_0 \left(e^{(1-\alpha)\tilde{\eta}F/RT} - e^{-\alpha\tilde{\eta}F/RT} \right) \tag{3.25}$$

where j_0 is called exchange current, α is transfer coefficient, F is Faraday constant, R is universal gas constant and $\tilde{\eta}$ is overpotential, which represents the driving force of the electrochemical reaction. Overpotential $\tilde{\eta}$ has the property that if positive, the reaction proceeds in the direction of oxidation while if negative the direction proceeds in the direction of reduction. In particular, the net reaction does not proceed in any direction if and only if the overpotential is zero. But this is exactly the behavior of electrochemical affinity and so we can conclude that overpotential is proportional to electrochemical affinity, i.e.

$$\tilde{\eta} = \frac{\tilde{\mathcal{A}}}{nF} \tag{3.26}$$

where n is number of electrons involved in the electrochemical reaction. See [15] for a survey on Butler-Volmer equation.

The purpose of this section is to formulate the Butler-Volmer equation within non-equilibrium thermodynamics, in particular in the GENERIC framework. The advantage of such formulation is that the equation can then be combined with other results of non-equilibrium thermodynamics consistently. Consider therefore the following assumptions

1. Entropy is the same as in CIT [28].

2. Dissipation potential is specified as

$$\Xi = \frac{j_0 a_c R}{nF} \left(\frac{e^{(1-\alpha)\tilde{\mathcal{A}}/RT}}{1-\alpha} + \frac{e^{-\alpha\tilde{\mathcal{A}}/RT}}{\alpha} - \frac{1}{\alpha(1-\alpha)} \right) \tag{3.27}$$

where $\tilde{\mathcal{A}}$ is electrochemical affinity of the reaction introduced in [28] and [81], which is minus the reaction Gibbs energy. It can be also expressed as

$$\tilde{\mathcal{A}} = T\frac{\partial S}{\partial \xi} \tag{3.28}$$

where ξ is extent of the reaction in the direction of oxidation. A concrete example of electrochemical affinity is given below. Phenomenological constant α, which is referred to as a charge transfer coefficient and which is between 0 and 1, is usually near to 0.5, see [33]. Active area density, i.e. the area of active reaction surface per m^3 of the electrode, is denoted by a_c.

Note that although construction of the dissipation potential (3.27) might seem rather artificial at first sight, it is quite natural. Indeed, the dissipation

potential in CIT is just a quadratic function of the affinity since the reaction rate is then proportional to the affinity. How to extend the quadratic function into the far-from-equilibrium regime described by Butler-Volmer equation? Hyperbolic cosine seems to be a natural choice. More generally, any convex combination of the two exponentials present in the hyperbolic cosine can be considered, which leads to the presence of parameters α in arguments of the exponentials. When expanding the dissipation potential near equilibrium up to the second order in affinities, however, the result must be compatible with CIT, i.e. the dissipation potential must become a quadratic function without any linear contribution. This leads to the presence of parameters α in the denominators. Moreover, arguments of the exponentials must be dimensionless which leads to the presence of RT. Finally, the dissipation potential has to be zero for affinity equal to zero without any loss of generality, and it can be multiplied by a constant with proper physical dimension. This concludes the construction of dissipation potential (3.27).

According to the GENERIC framework [38], reaction rate in the direction of oxidation is then given by

$$\dot{\xi} = \frac{\partial \Xi}{\partial \frac{\partial S}{\partial \xi}} = \frac{a_c}{n} \frac{j}{F} \tag{3.29}$$

where current density due to the electrochemical reaction is defined as

$$j = j_0 \left(e^{(1-\alpha)\tilde{\mathcal{A}}/RT} - e^{-\alpha \tilde{\mathcal{A}}/RT} \right) \tag{3.30a}$$

or equivalently as

$$j = j_0 \left(e^{(1-\alpha)n\tilde{\eta}\frac{F}{RT}} - e^{-\alpha n \tilde{\eta}\frac{F}{RT}} \right) \tag{3.30b}$$

when using Eq. (3.26). Formulas (3.29) and (3.30a) or (3.30b) represent the non-equilibrium thermodynamic form of Butler-Volmer equation[2].

3.2.2 Solid oxide fuel cells

Let us now specify the electrochemical affinity for hydrogen oxidation reaction (HOR) and oxygen reduction reaction (ORR) within SOFC. For HOR

$$H_2 + O^{2-} \rightarrow H_2O + 2e^- \tag{3.31}$$

the electrochemical affinity can be expressed as

$$\tilde{\mathcal{A}} = \mu_{H_2} + \tilde{\mu}_{O^{2-}} - \mu_{H_2O} - 2\tilde{\mu}_{e^-}. \tag{3.32}$$

Note that electrochemical potentials of hydrogen and water are equal to the corresponding chemical potentials, since neither hydrogen nor water are charged. The

[2]Butler-Volmer equation was derived within Mesoscopic Non-Equilibrium Thermodynamics [85], but the derivation seems to be consistent only for $\alpha = 0.5$. Equation (44) in the paper implies that sign of reaction rate is inverted if the reaction itself is inverted (electrochemical potentials at both ends of the reaction coordinate are swapped). This symmetric behavior is, however, only consistent with the symmetric Butler-Volmer equation, i.e. $\alpha = 0.5$.

reaction proceeds in the direction depicted by the arrow in equation (3.31) if and only if affinity (3.32) is positive, i.e. Gibbs energy decreases as the reaction proceeds. According to definition (3.8), the electrochemical affinity can be expressed in terms of electric potential of oxygen ions in the ion-conductive phase, Φ_i, and electric potential of electrons in the electron-conductive phase, Φ_e. Expressing electrochemical affinity in terms of the overpotential, according to (3.26), then leads to

$$\tilde{\eta}^a = (\Phi_e - \Phi_i) + \frac{\mu_{H_2} - \mu_{H_2O}}{2F}. \tag{3.33}$$

Chemical potential of water vapor and hydrogen can be approximated by chemical potentials of ideal gases

$$\mu_{H_2} = \mu^\circ_{H_2}(T) + RT \ln \frac{p_{H_2}}{p^\circ} \tag{3.34}$$

$$\mu_{H_2O} = \mu^\circ_{H_2O}(T) + RT \ln \frac{p_{H_2O}}{p^\circ} \tag{3.35}$$

where μ° denotes standard chemical potential at given temperature and standard pressure, p° denotes the standard pressure and where p_{H_2} and p_{H_2O} denote partial pressures of hydrogen and water, respectively. This way, the electrochemical affinity becomes

$$\tilde{\eta}^a = \Phi_e - \Phi_i - E^{\circ,a}(T) + \frac{RT}{2F} \ln \left(\frac{p_{H_2}}{p^\circ} \frac{p^\circ}{p_{H_2O}} \right) \tag{3.36}$$

with

$$E^{\circ,a}(T) = \frac{\mu^\circ_{H_2O}(T) - \mu^\circ_{H_2}(T)}{2F}. \tag{3.37}$$

Rate of HOR is then given by

$$\begin{aligned} j^a = \quad & j^a_0 \left(\left(\frac{p_{H_2}}{p^\circ} \right)^{\frac{1}{2}} \left(\frac{p_{H_2O}}{p^\circ} \right)^{-\frac{1}{2}} e^{(\Phi_e - \Phi_i - E^{\circ,a}(T)) \frac{F}{RT}} - \right. \\ & \left. - \left(\frac{p_{H_2O}}{p^\circ} \right)^{\frac{1}{2}} \left(\frac{p_{H_2}}{p^\circ} \right)^{-\frac{1}{2}} e^{-(\Phi_e - \Phi_i - E^{\circ,a}(T)) \frac{F}{RT}} \right) \end{aligned} \tag{3.38}$$

where charge transfer coefficient was approximated by 0.5 in accordance with [33].

ORR at the cathode in the direction of oxidation, i.e. the opposite direction than in fuel cells,

$$O^{2-} \rightarrow \frac{1}{2} O_2 + 2e^- \tag{3.39}$$

can be treated analogously. Cathode overpotential is then

$$\tilde{\eta}^c = \frac{1}{2F} \left(\tilde{\mu}_{O^{2-}} - \frac{1}{2} \mu_{O_2} - 2\tilde{\mu}_{e^-} \right) = \Phi_e - \Phi_i - E^{\circ,c}(T) + \frac{RT}{2F} \ln \left(\frac{p_{O_2}}{p^\circ} \right)^{-\frac{1}{2}} \tag{3.40}$$

where $E^{\circ,c}$ is equal to $\frac{\mu^\circ_{O_2}(T)}{4F}$. Rate of ORR in the direction of reduction, i.e. opposite than in (3.39), is then

$$\begin{aligned} -j^c = \quad & j^c_0 \left(\left(\frac{p_{O_2}}{p^\circ} \right)^{\frac{1}{4}} e^{-(\Phi_e - \Phi_i - E^{\circ,c}(T)) \frac{F}{RT}} - \right. \\ & \left. - \left(\frac{p_{O_2}}{p^\circ} \right)^{-\frac{1}{4}} e^{(\Phi_e - \Phi_i - E^{\circ,c}(T)) \frac{F}{RT}} \right). \end{aligned} \tag{3.41}$$

Note that in equilibrium or in a steady isothermal state with disconnected external circuit, when reaction rates are zero, electric potential of ions has no gradient and equations (3.38) and (3.41) lead to the standard Nernst relation, see for example [101],

$$\Phi_e^c - \Phi_e^a = -\frac{\mu^\circ_{H_2O} - \mu^\circ_{H_2} - \frac{1}{2}\mu^\circ_{O_2}}{2F} + \frac{RT}{2F} \ln \frac{\frac{p_{H_2}}{p^\circ}\left(\frac{p_{O_2}}{p^\circ}\right)^{\frac{1}{2}}}{\frac{p_{H_2O}}{p^\circ}}. \tag{3.42}$$

Entropy production can be expressed in terms of overpotentials easily. Indeed, the last term in formula (3.11) can be rewritten as

$$\frac{1}{T} a^a j^a \tilde{\eta}^a \quad \text{in the anode and as} \quad \frac{1}{T} a^c j^c \tilde{\eta}^c \quad \text{in the cathode.} \tag{3.43}$$

Note also that equations (3.38) and (3.41) are not completely equivalent with the form of Butler-Volmer equation in literature, for example [71] or [3], which are, however, not completely equivalent with each other either. From the thermodynamic point of view, equation (3.30a) seems to be the simplest equation leading to a Butler-Volmer-like constitutive relation for reaction rate. Moreover, equation (3.30a) is guaranteed to be compatible with thermodynamics since it is a realization of GENERIC.

Equations (3.38) and (3.41) represent constitutive relations for reaction rates of electrochemical reactions in SOFC. These equations are compatible with non-equilibrium thermodynamics and, therefore, can be used in the preceding considerations. Completing the dissipation potential with quadratic terms corresponding to the standard linear force-flux relations between diffusion, heat flux and shear rate, see [76], then yields the full set of constitutive relations which are to be supplemented to balance equations of CIT.

3.2.3 PEM fuel cells

As with SOFC, electrochemical reactions in a PEM fuel cell can also be described by a Butler-Volmer equation. Hydrogen oxidation reaction (HOR)

$$H_2 \to 2H^+ + 2e^- \tag{3.44}$$

takes place in the anode catalyst layer (ACL) while oxygen reduction reaction (ORR)

$$\frac{1}{2}O_2 + 2H^+ + 2e^- \to H_2O(l) \tag{3.45}$$

takes place in the cathode catalyst layer (CCL) of the PEM fuel cell.

The transfer coefficient is taken as equal to 0.5 for both the reactions and the number of electrons participating in the reactions is 2 in accordance with [101]. Flux of protons in the anode is then equal, in accordance with Eq. (3.30b), to

$$j_p|_{ACL} = j_0^{HOR} a_C L_C \left(e^{\eta^a \frac{F}{RT}} - e^{-\eta^a \frac{F}{RT}} \right) \tag{3.46}$$

where η^a is the overpotential in the ACL, which is defined as

$$\begin{aligned}\eta^a &= \frac{\tilde{\mathcal{A}}}{2F} = \frac{1}{2F}\left(\mu^a_{H_2} - 2\tilde{\mu}^a_{H^+} - 2\tilde{\mu}^a_{e^-}\right) = \\ &= \frac{1}{2F}\left(\underbrace{\mu^{\ominus}_{H_2}}_{0} + RT\ln\frac{p^a_{H_2}}{p^\circ} - 2F\Phi^a + 2F\Phi^a_e\right) = \\ &= \frac{RT}{2F}\ln\frac{p^a_{H_2}}{p^\circ} - \Phi^a + \Phi^a_e \end{aligned} \tag{3.47}$$

where Φ^a_e is the electric potential of electrons in the ACL, i.e. the potential of electrons at the anode side of the external circuit, and Φ^a is the electric potential of protons at the anode side of the membrane. Constants $j_0^{HOR} = 7.21 \cdot 10^{-3}\frac{A}{cm^2}$, $a_C = 1000\frac{cm^2}{mgPt}$ and $L_C = 0.5\frac{mgPt}{cm^2}$ represent exchange current of HOR (the value is taken from [101]), active surface per amount of platinum (a typical value taken from [7]) and platinum loading per area of the catalyst layer (a typical value taken from [7] as well). Note that cm^2 in a_C stand for the active area, where the reaction takes place, while in the expression for L_C it stands for total catalyst layer cross section. The standard chemical potential of hydrogen is equal to zero because hydrogen is an element.

Similarly, proton flux in the CCL is given by

$$j_p|_{CCL} = -j_0^{ORR} a_C L_C \left(e^{\eta^c \frac{F}{RT}} - e^{-\eta^c \frac{F}{RT}}\right) \tag{3.48}$$

where the overpotential in the CCL is given by

$$\begin{aligned}\eta^c &= \frac{\tilde{\mathcal{A}}^c}{2F} = \frac{1}{2F}\left(\mu^c_{H_2O(l)} - \frac{1}{2}\mu^c_{O_2} - 2\tilde{\mu}^c_{H^+} - 2\tilde{\mu}^c_e\right) = \\ &= \frac{1}{2F}\left(\mu^\bullet_w + RT\ln a^c_w - \frac{1}{2}\underbrace{\mu^{\ominus}_{O_2}}_{0} - RT\ln\left(\frac{p^c_{O_2}}{p^\circ}\right)^{\frac{1}{2}} - 2F\Phi^c + 2F\Phi^c_e\right) = \\ &= \frac{\mu^\bullet_w}{2F} + \frac{RT}{2F}\ln\left(a^c_w\sqrt{\frac{p^\circ}{p^c_{O_2}}}\right) + \Phi^c_e - \Phi^c \end{aligned} \tag{3.49}$$

where Φ^c_e is the electric potential of electrons in the CCL, i.e. the electric potential at the cathode side of the external circuit. The difference $\Phi^c_e - \Phi^a_e$ is the voltage of the external circuit. Constants a_C and L_C can be taken the same as in the case of HOR and the exchange current is equal to $j_0^{ORR} = 2.8 \cdot 10^{-7}\frac{A}{cm^2}$ in accordance with [101].

3.3 Transport of water and protons in Nafion membranes

On the level of mechanical equilibrium, total fluxes of protons and water in a membrane are proportional to the corresponding thermodynamic forces (gradients of electrochemical potentials at constant temperature). For an isothermal

membrane, force-flux relations (3.4a) for flux of water and flux of protons are given by

$$j_p = L_{pp}X_p + L_{pw}X_w \tag{3.50a}$$
$$j_w = L_{wp}X_p + L_{ww}X_w \tag{3.50b}$$

where $X_p = -\frac{1}{T}F\nabla\Phi$ and $X_w = -\frac{1}{T}\nabla\mu_w$.

Moreover, Onsager-Casimir reciprocity relations yield that

$$L_{pw} = L_{wp}. \tag{3.51}$$

Finally, to fulfill the second law of thermodynamics for arbitrary fluxes it is necessary that L_{pp} and L_{ww} are nonnegative and that

$$L_{pp}L_{ww} - L_{pw}L_{wp} \geq 0. \tag{3.52}$$

Expressing X_p in equation (3.50b) by means of equation (3.50a) and X_w in (3.50a) by means of (3.50b), yields

$$j_w = \frac{L_{ww}L_{pp} - L_{wp}L_{pw}}{L_{pp}}X_w + \frac{L_{wp}}{L_{pp}}j_p \tag{3.53a}$$
$$j_p = \frac{L_{ww}L_{pp} - L_{wp}L_{pw}}{L_{ww}}X_p + \frac{L_{wp}}{L_{ww}}j_w. \tag{3.53b}$$

Usually, the cross coefficient L_{pw} is expressed in terms of a drag coefficient defined as

$$\xi = \left(\frac{j_w}{j_p}\right)_{X_w=0} = \frac{L_{wp}}{L_{pp}}, \tag{3.54}$$

where the second equality follows from equation (3.53a). From the concept that protons and water molecules drag each other it follows that the drag coefficient should be nonnegative. Therefore, it follows from the second law of thermodynamics (3.52) that

$$\xi \in \left[0, \sqrt{\frac{L_{ww}}{L_{pp}}}\right]. \tag{3.55}$$

Let us, moreover, introduce the coupling coefficient q

$$q = \sqrt{\frac{L_{wp}L_{pw}}{L_{ww}L_{pp}}}. \tag{3.56}$$

Due to the restrictions imposed by the second law of thermodynamics and Onsager reciprocal relations, (3.51) and (3.52), the coupling coefficient is always between 0 and 1.

3.3.1 Proton conductivity

Proton conductivity is defined as

$$\sigma_p = F^2\left(\frac{j_p}{X_p}\right)_{X_w=0} = \frac{F^2L_{pp}}{T}. \tag{3.57}$$

Experimental proton conductivity can be found for example in paper [13], where the data can be fitted by

$$\sigma_p = \sigma_p^0 a_w^2 \tag{3.58}$$

with

$$\sigma_p^0 = 0.1 \exp\left(-3500\left(\frac{1}{T} - \frac{1}{273.15+20}\right)\right)\frac{S}{cm} \tag{3.59}$$

where T is temperature in K. This fit was approved by author of paper [13] in our private communication.

3.3.2 Proton diffusivity

Proton diffusivity is defined as

$$\frac{D_p c_p}{R} = \left(\frac{j_p}{X_p}\right)_{j_w=0} = L_{pp} - \frac{L_{pw}L_{wp}}{L_{ww}} \tag{3.60}$$

where c_p is concentration of protons. It is necessary to distinguish between proton diffusivity and proton conductivity because the former is measured at $j_w = 0$ while the latter at $X_w = 0$.

Proton diffusivity was theoretically estimated by Choi in [25] from Grothuss mechanism of proton hopping as

$$D_p = 7 \cdot 10^{-5}\frac{cm^2}{s}. \tag{3.61}$$

As proton transport was estimated in the frame of reference of water, i.e. water not moving, the diffusivity was estimated rather than conductivity. It should be borne in mind, however, that to the best of the author's knowledge, no experimental data on proton diffusivity are available in the literature.

3.3.3 Water diffusivity

Diffusivity expresses how gradient of concentration affects diffusion flux, and it is defined as

$$\frac{D_w c_w}{R} = \left(\frac{j_w}{X_w}\right)_{j_p=0} = L_{ww} - \frac{L_{pw}L_{wp}}{L_{pp}}. \tag{3.62}$$

Using Eq. (3.56), it can also be rewritten as

$$D_w \frac{c_w}{R} = L_{ww}\left(1 - q^2\right). \tag{3.63}$$

Self-diffusivity of water in Nafion was determined in [13] and [102] by pulse gradient spin-echo nuclear magnetic resonance (PGSE-NMR), where the experimental data were fitted by the curve

$$D_w^{self} = D_\infty^0 a_w^2 \tag{3.64}$$

with

$$D_\infty^0 = 0.265 \exp\left(-\frac{3343K}{T}\right)\frac{cm^2}{s}. \tag{3.65}$$

But self-diffusivity can not be used as the macroscopic (thermodynamic) diffusivity D_w in general, since the thermodynamic diffusivity also takes into account correlations between water molecules in contrast to self-diffusivity as demonstrated in [58]. Several theories have been proposed to convert self-diffusivity into the thermodynamic diffusivity, see [9, 95, 96]. A mutual diffusion coefficient defined as

$$j_w = -\frac{D_{mutual}}{1 - c_w v_w} \frac{\partial c_w}{\partial x} \tag{3.66}$$

was introduced in [9], where c_w and v_w are concentration $[mol/cm^3]$ of water in the polymer and partial molar volume of water in the polymer, respectively. The mutual diffusion coefficient was estimated by Vrentas and Duda in [95, 96] by

$$D_{mutual} = \frac{D_w^{self} c_N v_N c_w}{RT} \left(\frac{\partial \mu_w}{\partial c_w} \right)_{T,p} \tag{3.67}$$

where c_N and v_N are concentration and partial molar volume of the polymer. Using the general thermodynamic relation, see e.g. [81],

$$1 = c_w v_w + c_N v_N, \tag{3.68}$$

flux of water becomes

$$j_w = -\frac{D_w^{self}}{RT} c_w \left(\frac{\partial \mu_w}{\partial c_w} \right)_{T,p} \frac{\partial c_w}{\partial x} = -\frac{D_w^{self} c_w}{RT} \left(\frac{\partial \mu_w}{\partial x} \right)_{T,p}. \tag{3.69}$$

If there is no electric current (no flux of protons), formula (3.53a) can be rewritten as follows

$$j_w|_{j_p=0} = L_{ww}(1 - q^2) \left(-\frac{1}{T} \left(\frac{\partial \mu_w}{\partial x} \right)_T \right) = -\frac{D_w c_w}{RT} \left(\frac{\partial \mu_w}{\partial x} \right)_T. \tag{3.70}$$

By comparison with Eq. (3.69) it follows, assuming no pressure gradient, that in the approximation proposed by Vrentas and Duda, the thermodynamic diffusivity is equal to the self-diffusivity of water in Nafion, i.e.

$$D_w = D_w^{self}. \tag{3.71}$$

Finally, using the experimental formula (3.64) and the general formula for chemical potential of water in the membrane (4.3), water flux can be written (in case of zero electric current) explicitly as

$$j_w = -D_\infty^0 \cdot c_w a_w \frac{\partial a_w}{\partial x}. \tag{3.72}$$

It will be shown later that concentration c_w can be expressed as a function of a_w, see formula (4.8).

When introducing the diffusivity coefficient in formula (3.66), it was assumed that no other species moves. Therefore, this diffusion coefficient indeed represents the thermodynamic diffusivity (3.62).

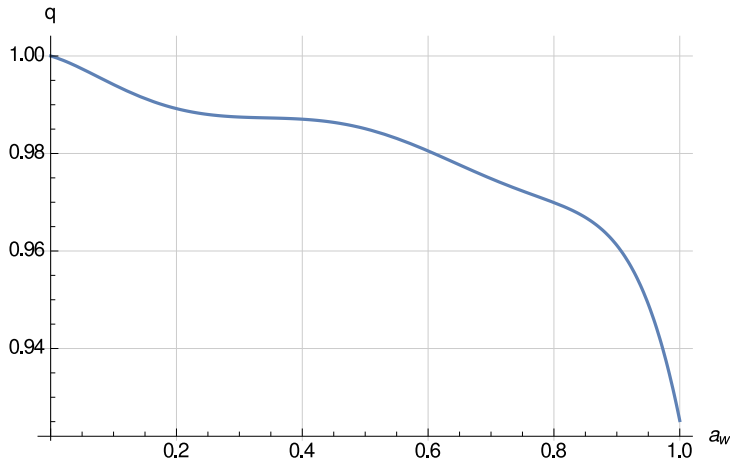

Figure 3.1: Coupling coefficient q as a function of water activity while ξ equal to 2. Eq. (3.55) is solved for each value of a_w, and the above dependencies of the phenomenological coefficients on q and a_w are used.

3.3.4 Drag coefficient

By combining proton conductivity, proton diffusivity and water diffusivity, one could determine the drag coefficient ξ. Conversely, by taking proton conductivity, water diffusivity and the drag coefficient, one can calculate proton diffusivity. The drag coefficient was determined experimentally many times, but the experimental data are rather inconsistent as the coefficient varies between approximately 1 and 3. A comprehensive review of experimental measurements of the drag coefficient is given in [22]. Therefore, we do not consider any particular value of the drag coefficient in this work, but we rather explore implications of various values of the coefficient (or of the coupling coefficient q), see Sec. 3.5.

However, for example for the drag coefficient equal to 2, Eq. (3.55) can be solved (with the above specified data for D_w and σ) which yields Fig. 3.1, where the dependence of the coupling coefficient on water activity for that particular value of the drag coefficient is demonstrated. The coupling coefficient is between 0 and 1, which means that the ξ being equal to 2 is thermodynamically admissible. Interestingly, this typical value of the drag coefficient leads to coupling coefficient higher than 0.9 for all activities.

3.3.5 Explicit expressions for fluxes

The above presented definitions and experimental data can be now summarized in the final explicit form of water and proton fluxes. Having water diffusivity D_w, proton conductivity σ_p and the coupling coefficient q, the phenomenological

coefficients become

$$L_{ww} = D_w \frac{c_w}{R} \frac{1}{1-q^2} \tag{3.73a}$$

$$L_{pp} = \frac{T}{F^2}\sigma_p \tag{3.73b}$$

$$L_{pw} = L_{wp} = q\sqrt{L_{ww}L_{pp}} = \sqrt{\frac{Tc_w D_w \sigma_p}{RF^2}} \frac{q}{\sqrt{1-q^2}}, \tag{3.73c}$$

where formulas (3.56), (3.57) and (3.63) were used.

Force-flux relations (3.50a) and (3.50b) then become, after plugging formulas (3.58) and (3.71) into the coefficients (3.73),

$$j_w = -\frac{D^0_\infty c_w a_w}{1-q^2}\nabla a_w - \sqrt{\frac{c_w D^0_\infty \sigma^0_p}{RT}} \frac{q}{\sqrt{1-q^2}} a_w^2 \nabla\Phi \tag{3.74a}$$

$$j_p = -\frac{\sqrt{RTc_w D^0_\infty \sigma^0_p}}{F} \frac{q}{\sqrt{1-q^2}} a_w \nabla a_w - \frac{\sigma^0_p}{F} a_w^2 \nabla\Phi. \tag{3.74b}$$

3.4 Time-dependent sorption

It has been observed experimentally [88] that when a dry Nafion membrane is immersed into saturated water vapor, absorption takes much longer than when a fully hydrated membrane is immersed into dry nitrogen. Attempts to explain such asymmetry include for example formation of a hydration front [88]. The purpose of this section is to explain the asymmetry by a model as simple as possible while being thermodynamically consistent.

Note that Sec. 4.1 is referenced many times in this section, and thus could be favorable to read it first.

3.4.1 Balance of mass

General balance of mass of water in the membrane reads, in accordance with Eq. (2.1),

$$\frac{\partial c_w}{\partial t} = -\mathrm{div} j_w \tag{3.75}$$

where concentration c_w is expressed in mol/cm^3 and water flux j_w in $mol/cm^2 s$. Assuming no electric current in the membrane, the water flux is given by formula (3.72).

Boundary conditions are prescribed as

$$j_w|_0 = k_w(RH^L - a_w|_0) \tag{3.76a}$$

$$j_w|_{x_m} = k_w(a_w|_{x_m} - RH^R) \tag{3.76b}$$

where k_w represents a phenomenological constant which is to be determined by comparing the resulting sorption curves to experiments. Constants RH^L and RH^R denote relative humidities of vapor on the left and right side of the membrane, respectively. Note that in the thermodynamic sense these boundary conditions can be constructed from an exponential dissipation potential similarly to the Bulter-Volmer equation in Sec. 3.2 or as in case of Boltzmann equation, see Sec. A.1.

3.4.2 Lagrangian coordinates

Let us now restrict to one-dimensional calculations, i.e. the membrane is supposed to be a very thin rectangular parallelepiped, which is, however, always the case for Nafion membranes, and it is homogeneous in the longer directions, let us say y and z, so that a_w or any other physical quantity only vary in the x direction (in which the membrane is thin).

The membrane is swelling when absorbing water. For the sake of simplicity of numerical simulation, it is advantageous to transform the spatial (Eulerian) coordinates to Lagrangian coordinates attached to the dry membrane. The physical spatial (Eulerian) coordinates have already been denoted by x, y and z, and let us denote by $x_m(t)$, $y_m(x,t)$ and $z_m(x,t)$ boundaries of the membrane. In other words,

$$x \in [0, x_m(t)],\ y \in [0, y_m(x,t)] \text{ and } z \in [0, z_m(x,t)]. \tag{3.77}$$

The Lagrangian coordinates

$$X \in [0, X_m], Y \in [0, Y_m] \text{ and } Z \in [0, Z_m] \tag{3.78}$$

which are attached to the membrane in the dry state are related to the Eulerian coordinates as follows, see Eq. (4.10),

$$\begin{aligned}
x(X,Y,Z,t) &= \int_0^X (1+\varepsilon(A_w(X',t)))\,\mathrm{d}X' && (3.79)\\
y(X,Y,Z,t) &= \int_0^Y (1+\varepsilon(A_w(X,t)))\,\mathrm{d}Y' = (1+\varepsilon(A_w(X,t)))Y && (3.80)\\
z(X,Y,Z,t) &= \int_0^Z (1+\varepsilon(A_w(X,t)))\,\mathrm{d}Z' = (1+\varepsilon(A_w(X,t)))Z && (3.81)\\
& && (3.82)
\end{aligned}$$

where Lagrangian activity of water is defined as

$$A_w(X,t) = a_w(x(X,t),t). \tag{3.83}$$

Jacobi matrix of the transformation from Eulerian to Lagrangian coordinates is then

$$\begin{array}{lll}
\frac{\partial x}{\partial X} = 1+\varepsilon(A_w(X,t)) & \frac{\partial x}{\partial Y} = 0 & \frac{\partial x}{\partial Z} = 0\\
\frac{\partial y}{\partial X} = \varepsilon'(A_w(X,t))\frac{\partial A_w(X,t)}{\partial X}Y & \frac{\partial y}{\partial Y} = 1+\varepsilon(A_w(X,t)) & \frac{\partial y}{\partial Z} = 0\\
\frac{\partial z}{\partial X} = \varepsilon'(A_w(X,t))\frac{\partial A_w(X,t)}{\partial X}Z & \frac{\partial z}{\partial Y} = 0 & \frac{\partial z}{\partial Z} = 1+\varepsilon(A_w(X,t)).
\end{array} \tag{3.84}$$

3.4.3 Lagrangian concentration

Lagrangian concentration of water in the slice of the membrane with Lagrangian coordinate X at time t is equal to

$$\begin{aligned}
C(X,t) &= \int_0^{y_m(x(X,t),t)} \int_0^{z_m(x(X,t),t)} c_w(x(X,t),y,z,t)\,\mathrm{d}y\,\mathrm{d}z && (3.85)\\
&= c_w(x(X,t),t)(1+\varepsilon(A_w(X,t)))^2 \underbrace{Y\cdot Z}_{\Delta A} && (3.86)
\end{aligned}$$

where area of the dry membrane ΔA was introduced. Lagrangian area concentration of water is then defined as

$$C_s(X,t) = \frac{C(X,t)}{\Delta A} = c_w(x(X,t),t)(1+\varepsilon(A_w(X,t)))^2. \tag{3.87}$$

Concentration $c_w(x,y,z,t)$ can be expressed in terms of water activity a_w. Indeed, as $c_w(x,y,z,t)$ gives the number of moles of water per cm^3 of the swollen membrane, it can be related to water uptake λ by Eq. (4.8), and water uptake λ can be expressed in terms of activity according to Eq. (4.2). Converting also density of the polymer into density of the dry Nafion by using Eqs. (4.8) and (4.19) then leads to the Lagrangian expression for concentration

$$c_w(x(X,t),t) = \frac{\lambda(A_w(X,t))}{(1+\varepsilon(A_w(X,t)))^3}\frac{\rho_{dry}}{EW}. \tag{3.88}$$

Comparing this formula with Eq. (3.87) yields a relation between the Lagrangian area concentration and the Lagrangian activity

$$C_s(X,t) = \frac{\lambda(A_w(X,t))}{1+\varepsilon(A_w(X,t))}\frac{\rho_{dry}}{EW}. \tag{3.89}$$

Finally, the total amount (in moles) of water in the membrane can be calculated as follows

$$\begin{aligned} n_w &= \int_0^{x_m(t)}\int_0^{y_m(x,t)}\int_0^{z_m(x,t)} c_w(x,y,z,t)\,\mathrm{d}x\,\mathrm{d}y\,\mathrm{d}z = \int_0^{x_m(t)} C(X(x,t),t)\,\mathrm{d}x = \\ &= \int_0^{X_m} C(X,t)\frac{\partial x}{\partial X}\,\mathrm{d}X = \int_0^{X_m} C(X,t)(1+\varepsilon(A_w(X,t)))\,\mathrm{d}X = \\ &= \frac{\rho_{dry}}{EW}\int_0^{X_m}\lambda(A_w(X,t))\,\mathrm{d}X\cdot\Delta A. \end{aligned} \tag{3.90}$$

3.4.4 Lagrangian evolution equation

Let us now rewrite the evolution equation (3.75) in the Lagrangian coordinates. Plugging relations (3.72) and (3.88) into Eq. (3.75), the evolution equation becomes

$$\begin{aligned} &\frac{\partial}{\partial t}\left(\frac{\lambda(a_w(X,t))}{(1+\varepsilon(A_w(X,t)))^3}\frac{\rho_{dry}}{EW}\right) = \\ &\quad = \frac{1}{1+\varepsilon(A_w(X,t))}\frac{\partial}{\partial X}\left(D_\infty^0\frac{\lambda(A_w(X,t))A_w(X,t)}{(1+\varepsilon(A_w(X,t)))^4}\frac{\rho_{dry}}{EW}\frac{\partial A_w(X,t)}{\partial X}\right) \end{aligned} \tag{3.91}$$

where derivatives with respect to x were replaced with derivatives with respect to X by formula

$$\frac{\partial}{\partial x} = \frac{\partial X}{\partial x}\frac{\partial}{\partial X} = \frac{1}{1+\varepsilon}\frac{\partial}{\partial X}. \tag{3.92}$$

It is, moreover, convenient to introduce a dimensionless coordinate

$$\hat{X} = \frac{X}{X_m}. \tag{3.93}$$

Activity can be then expressed in the dimensionless coordinate

$$\hat{A}_w(\hat{X},t) = A_w(X(\hat{X}),t), \tag{3.94}$$

and derivatives with respect to $\hat{X}$ are given by

$$\frac{\partial}{\partial X} = \frac{1}{X_m}\frac{\partial}{\partial \hat{X}}. \tag{3.95}$$

This way Eq. (3.91) becomes

$$\begin{aligned}\frac{\partial}{\partial t}\left(\frac{\lambda(\hat{A}_w(\hat{X},t))}{(1+\varepsilon(\hat{A}_w(\hat{X},t)))^3}\frac{\rho_{dry}}{EW}\right) = \\ = \frac{1}{X_m(1+\varepsilon(\hat{A}_w(\hat{X},t)))}\frac{\partial}{\partial \hat{X}}\left(D_\infty^0\frac{\rho_{dry}}{EW}\frac{\lambda(\hat{A}_w(\hat{X},t))\hat{A}_w(\hat{X},t)}{X_m(1+\varepsilon(\hat{A}_w(\hat{X},t)))^4}\frac{\partial \hat{A}_w(\hat{X},t)}{\partial \hat{X}}\right).\end{aligned} \tag{3.96}$$

Note that this equation can be simplified by neglecting the swelling, i.e. putting $\varepsilon = 0$, so that it becomes

$$\frac{\partial}{\partial t}\left(\lambda(\hat{A}_w(\hat{X},t))\right) = \frac{1}{X_m^2}\frac{\partial}{\partial \hat{X}}\left(D_\infty^0\lambda(\hat{A}_w(\hat{X},t))\hat{A}_w(\hat{X},t)\frac{\partial \hat{A}_w(\hat{X},t)}{\partial \hat{X}}\right). \tag{3.97}$$

Numerical calculations then demonstrate that solutions to this simplified equation are qualitatively the same as solutions to the full Eq. (3.91), e.g. desorption is still faster than absorption (see the results). On the other hand, the solutions are not completely the same, and quantitative agreement between experimental data and theoretical prediction requires using the full Eq. (3.91). In Sec. 3.4.9 Eq. (3.97) is further approximated by an ordinary differential equation giving also qualitatively the same results as the full Eq. (3.91).

3.4.5 Time-discretization

Eq. (3.96) can be solved numerically. The time derivative is discretized using the backward Euler scheme. This yields the following equation

$$\begin{aligned}\left(\frac{\lambda(\hat{A}_w^k)}{(1+\varepsilon(\hat{A}_w^k))^3} - \frac{\lambda(\hat{A}_w^{k-1})}{(1+\varepsilon(\hat{A}_w^{k-1}))^3}\right)\frac{\rho_{dry}}{EW} = \\ = \mathrm{d}t\frac{1}{X_m(1+\varepsilon(\hat{A}_w^k))}\frac{\partial}{\partial \hat{X}}\left(D_\infty^0\frac{\lambda(\hat{A}_w^k)\hat{A}_w^k}{X_m(1+\varepsilon(\hat{A}_w^k))^4}\frac{\rho_{dry}}{EW}\frac{\partial \hat{A}_w^k}{\partial \hat{X}}\right)\end{aligned} \tag{3.98}$$

where $\hat{A}_w^k = \hat{A}_w(\hat{X},t_k)$, $t_k = t_0 + k\cdot \mathrm{d}t$, and $\mathrm{d}t$ is the time-step.

3.4.6 Weak formulation

Eq. (3.98) is then multiplied by a test-function $\varphi(\hat{X})$ from the $H^1(0,1)$ Sobolev space, see e.g. [31]. After integrating by parts, one obtains the weak formulation:

Find $\hat{A}_w^k \in H^1(0,1)$ such that:

$$S(\hat{A}_w^k, \hat{A}_w^{k-1}, \varphi) = 0 \qquad \forall \varphi \in H^1(0,1) \tag{3.99}$$

where the functional S is defined as

$$\begin{aligned} S(\hat{A}_w^k, \hat{A}_w^{k-1}, \varphi) &= \int_0^1 \left(\frac{\lambda(\hat{A}_w^k)}{(1+\varepsilon(\hat{A}_w^k))^3} - \frac{\lambda(\hat{A}_w^{k-1})}{(1+\varepsilon(\hat{A}_w^{k-1}))^3} \right) \frac{\rho_{dry}}{EW} \varphi \, \mathrm{d}\hat{X} + \\ &+ \int_0^1 \frac{\mathrm{d}t}{X_m^2} D_\infty^0 \frac{\rho_{dry}}{EW} \frac{\lambda(\hat{A}_w^k)\hat{A}_w^k}{(1+\varepsilon(\hat{A}_w^k))^4} \frac{\partial \hat{A}_w^k}{\partial \hat{X}} \frac{\partial}{\partial \hat{X}} \frac{\varphi}{1+\varepsilon(\hat{A}_w^k)} \, \mathrm{d}\hat{X} + \\ &+ \frac{\mathrm{d}t}{X_m} \frac{\varphi(1)}{1+\varepsilon(\hat{A}_w^k(1))} k_w \left(\hat{A}_w^k(1) - RH^R \right) - \\ &- \frac{\mathrm{d}t}{X_m} \frac{\varphi(0)}{1+\varepsilon(\hat{A}_w^k(0))} k_w \left(RH^L - \hat{A}_w^k(0) \right). \end{aligned} \tag{3.100}$$

This problem is then solved by finite element method using Lagrangian elements of second order implemented within the FEniCS environment [56]. The algebraic equations stemming from the space discretization are solved by the standard Newton solver implemented within FEniCS. Note that the values at the boundary are interpreted in the sense of traces in accordance with [31]. Time step was set to $0.1s$ and the mesh consisted of 100 equal elements.

3.4.7 Results

Let us now demonstrate results of the simulations obtained by solving problem (3.99). Absorption started with a membrane equilibrated with water vapor at $RH = 18.3\%$. RH of the surrounding water vapor was equal to 96.0%. After equilibrium had been reached[3], relative humidity of the surrounding vapor was suddenly changed to 13.3% and the desorption started. These values were taken from paper [88] and from the datasets used in the paper, which were kindly provided by J. Benziger in our personal communication.

The state of sorption is defined as follows

$$s(t) = \frac{n_w(t) - n_w(0)}{n_w(\infty) - n_w(0)} \tag{3.101}$$

where $n_w(t)$ is the number of moles of water in the membrane at time t. A sorption curve is then the curve $s(t)$. The absorption and desorption curves for N115 and N1110 membranes obtained by the numerical simulation of processes described in the preceding paragraph are shown in Fig. 3.2 and Fig. 3.3, respectively. The numerical results are compared to experimental data from [88] in the figures with only one fitted constant, namely the constant k_w introduced in Eqs. (3.76). The constant was equal to

$$k_w = 3.0 \cdot 10^{-7} \frac{mol}{cm^2 s} \tag{3.102}$$

for all membranes and for both absorption and desorption.

3.4.8 Discussion of the results

It has been demonstrated that Eq. (3.96) describes the sorption experiments well. The only fitting parameter was the k_w constant, which was taken the same

[3] the amount of water in the membrane less than 1% lower than the amount of water corresponding to a membrane in equilibrium with $RH = 96\%$

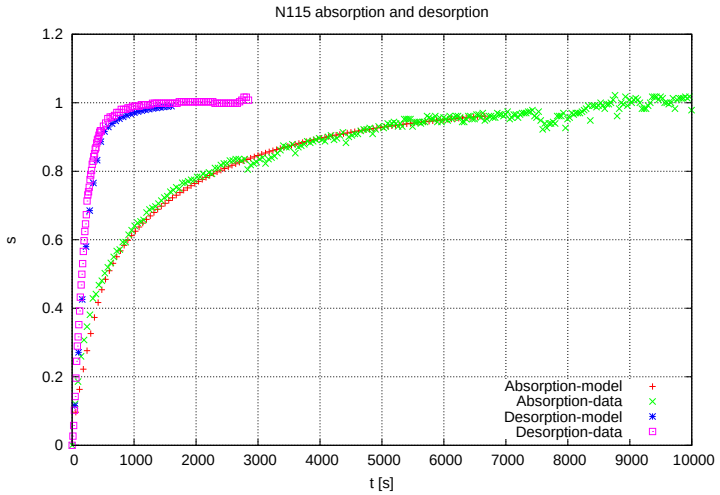

Figure 3.2: Absorption and desorption in a N115 membrane. Absorption (curve Absorption-model) started at $RH = 18.3\%$ and finished at $RH = 96.0\%$, where desorption (curve Desorption-model) started. Desorption finished at $RH = 13.3\%$. The resulting sorption curves, which are solutions to Eq. 3.98 are compared to experimental data from [88] (curves Absorption-data and Desorption-data). Quantitative agreement between the theory and the data is obvious. The desorption curve is clearly faster than the absorption curve.

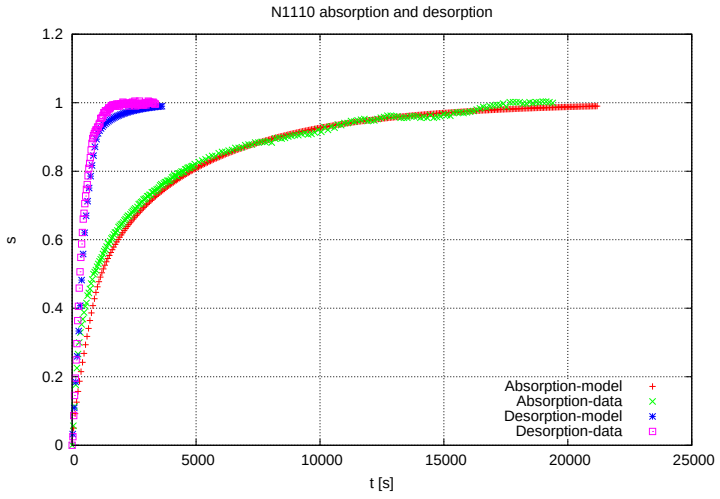

Figure 3.3: Absorption and desorption in a N1110 membrane. Absorption (curve Absorption-model) started at $RH = 18.3\%$ and finished at $RH = 96.0\%$, where desorption (curve Desorption-model) started. Desorption finished at $RH = 13.3\%$. These parameter are the same as in case of the N115 membrane in Fig. 3.2. The resulting sorption curves, which are solutions to Eq. 3.98 are compared to experimental data from [88] (curves Absorption-data and Desorption-data). Quantitative agreement between the theory and the data is obvious. The desorption curve is clearly faster than the absorption curve.

for all membranes and all simulated processes. An interesting observation is that desorption is faster than absorption. Several explanations of this asymmetry were suggested in the literature. Evolution equation (3.96), which is just a transformation of balance of mass (3.75), is, however, the simplest possible evolution equation describing the sorption respecting swelling and the dependence of water uptake on water activity. No additional phenomena like case-II diffusion [88] or special boundary conditions [67] need to be incorporated to reconstruct the asymmetry.

The reason for the asymmetry is simply the nonlinear dependence of water uptake on activity in Eq. (4.2). Indeed, if the dependence of λ on a_w were taken linear, the asymmetry would disappear because (when neglecting swelling and neglecting the $c_w a_w$ prefactor in j_w) Eq. (3.75) would describe the standard Fick's diffusion, which does not exhibit the asymmetry as shown in [27]. Note that neither neglecting swelling nor dropping the term $c_w a_w$ in the formula for j_w leads to disappearance of the asymmetry if Eq. (4.2) is taken into account. The effect of the dependence of λ on a_w on the asymmetry is further elucidated in Sec. 3.4.9.

3.4.9 A simplified sorption modeling

The purpose of this section is to elucidate the origin of the asymmetry in absorption and desorption (absorption being much slower than desorption). Let us, therefore, simplify the evolution equation (3.96) as much as possible. Firstly, the swelling is to be neglected by putting $\varepsilon = 0$, which leads to Eq. (3.97). Secondly, integrating the equation with respect to space yields an evolution equation for the total amount of water in the membrane

$$\frac{\mathrm{d}}{\mathrm{d}t}\int_0^1 \lambda(\hat{A}_w(\hat{X},t))\frac{\rho_{dry}}{EW}\,\mathrm{d}\hat{X} = \frac{1}{X_m}\left(j_w|_0 - j_w|_{X_m}\right) = \\ = \frac{k_w}{X_m}\left(RH^L - \hat{A}_w|_0 + RH^R - \hat{A}_w|_1\right), \quad (3.103)$$

where boundary conditions (3.76) were used. Assuming that $RH^L = RH^R = RH$ and that diffusion is fast enough so that activity can be considered equal to a constant in space function $\hat{A}_w(t)$, equation (3.103) becomes

$$\frac{\mathrm{d}}{\mathrm{d}t}\hat{A}_w(t) = \frac{2k_wEW}{\rho_{dry}X_m}\frac{RH - \hat{A}_w(t)}{\lambda'(\hat{A}_w(t))}, \quad (3.104)$$

which is just an ordinary differential equation. Once the dependence $\lambda(a_w)$ is known, as for example in the experimental formula (4.2), this equation can be solved. Let us now have a look at solution to this simple differential equation.

Consider the same setting as in the preceding section, i.e. $EW = 1100$, $k_w = 3.0 \cdot 10^{-7}\frac{mol}{cm^2 s}$ and $X_m = t_{N115,dry}$. Initial and final activities during absorption and desorption are also taken the same as in the preceding section. Eq. (3.104) with the dependence of λ on a_w given by (4.2) can be then solved numerically. The solution was acquired by the NDSolve solver in Wolfram Mathematica 10, and it is plotted plotted in Fig. (3.4).

Desorption is clearly much faster than absorption in Fig. 3.4. This means that Eq. (3.104) is sufficient to recover the asymmetry, and thus the cause of the asymmetry is identified as the nonlinear dependence of λ on a_w. Indeed, if we replace this dependence in Eq. (3.104) by the linear dependence

$$\lambda_{linear} = \lambda(1)a_w, \quad (3.105)$$

Eq. (3.104) can be solved analytically. Let us, for simplicity, assume that the absorption starts with a dry membrane and that the desorption starts with a membrane in equilibrium with saturated water vapor. Sorption curves then become

$$s_{abs}(t) = \frac{\lambda(\hat{A}_w(t))}{\lambda(1)} \quad (3.106)$$

for absorption and

$$s_{des}(t) = 1 - \frac{\lambda(\hat{A}_w(t))}{\lambda(1)} \quad (3.107)$$

for desorption. The solution to Eq. (3.104) is then

$$\hat{A}_w(t) = RH - (RH - \hat{A}_w(0))\exp\left(-\frac{2k_wEW}{\rho_{dry}X_m\lambda(1)}t\right), \quad (3.108)$$

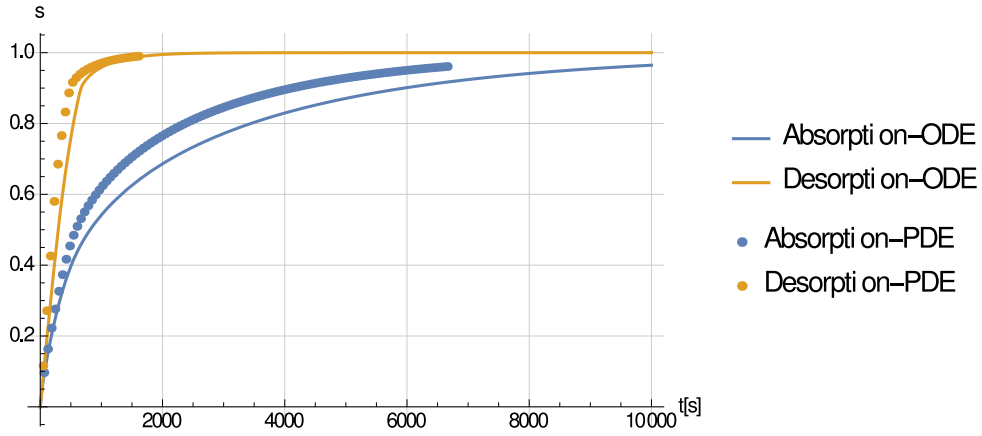

Figure 3.4: Numerical solution to Eq. (3.104) for absorption and desorption. Absorption curve (3.106) and desorption curve (3.107) are plotted (curves Absorption-ODE and Desorption-ODE). The solution to the ordinary differential equation (ODE) is compared with the solution of problem (3.99) from Fig. 3.2 (curves Absorption-PDE and Desorption-PDE). The two sets of solutions are similar and so Eq. (3.104) represents a good approximation of the full PDE (3.91).

and the absorption and desorption curves (3.106) and (3.107) become identical.

$$s_{abs}(t) = s_{des}(t) = 1 - \exp\left(-\frac{2k_w EW}{\rho_{dry} X_m \lambda(1)} t\right). \tag{3.109}$$

Therefore, the absorption is as fast as the desorption if the nonlinear dependence of λ on a_w is replaced by a linear dependence.

In summary, the simplified sorption equation (3.104), where diffusion is neglected completely, is sufficient to recover the asymmetry between absorption and desorption, and the asymmetry is caused by the nonlinear dependence $\lambda(a_w)$ because if the dependence were linear, the asymmetry would disappear.

3.4.10 Conclusion

A simple thermodynamically consistent model of sorption in Nafion membranes has been developed. The model is able to reproduce experimental data, and it predicts that desorption is much faster than absorption in Nafion membranes in accordance with experimental observations.

ODE (3.104) approximates the original PDE (3.91) well (including the asymmetry), and if λ were a linear function of a_w, the asymmetry would disappear in solutions to the ODE[4]. Therefore, the asymmetry is caused by the nonlinear dependence (4.2).

[4]Numerical experiments show that the asymmetry disappers also from the solutions to the full PDE if the dependence of λ on a_w is taken linear.

3.5 STR PEM Fuel Cell

3.5.1 Description of the fuel cell

In this section a stirred tank reactor (STR) polymer-electrolyte membrane (PEM) fuel cell (FC), which consists of three basic parts: anode gas diffusion layer (AGDL), membrane-electrode assembly (MEA) and cathode gas diffusion layer (CGDL), see [14] for details, is modeled. The AGDL is in contact with the anode channel (AC), which provides the hydrogen feed, while CGDL is in contact with the cathode channel (CC), which provides the oxygen feed. Besides hydrogen and oxygen, water vapor is transported into and out of the fuel cell also through the channels. Each of the channels is constructed as an open plenum, which simplifies the experimental observation (this leads to the name STR). The MEA, moreover, consists of a thin membrane and two even thinner catalyst layers on each side of the membrane. The fuel cell is taken as one-dimensional, stationary, isothermal and isobaric. Moreover, swelling of the membrane is neglected because the membrane is typically fixed from both sides by solid parts of the fuel cell.

The advantage of such simplified fuel cells is that the number of unknown parameters is lower than when modeling the whole "real life" fuel cell[5], where the for example serpentine flow channels are used instead of the open plenum. An even simpler experimental fuel cell has recently been investigated by Cheah et al. [22], where only hydrogen, nitrogen and water vapor are present in both the channels (thus the fuel cell working effectively as a hydrogen pump). Such experiments are of great importance because the simpler they are, the more precise knowledge of the MEA can be gained from them. Therefore, it is important to develop thermodynamically correct models of such simple fuel cells. The purpose of this section is to develop a thermodynamically consistent model of such fuel cell. The model, however, should be referred to as a "toy model" as it has not been compared to experiments.

The MEA consists of a Nafion membrane, the anode catalyst layer (ACL), which is a thin layer at the left boundary of the membrane, and the cathode catalyst layer (CCL), which is formed by a thin layer at the right boundary of the membrane. ACL is in contact with the AGDL, where a mixture of hydrogen and water vapor is present. Transport resistance of the gases through the AGDL is neglected, in accordance with [14], so that the AC contains mixture of vapor and hydrogen of the same composition as AGDL. CCL is in contact with the CGDL, that contains a mixture of oxygen, nitrogen and water vapor. The CGDL is in contact with the CC. While it is assumed that water vapor has the same partial pressure in both CGDL and CC, the amount of oxygen in the CC is different than in the CGDL in accordance with [14]. Finally, electrons can leave the MEA from the ACL and re-enter the MEA in the CCL while performing useful work in an external circuit.

The fuel cell works as follows: Hydrogen is transported from the AC to the ACL through the AGDL. It splits into protons and electrons at the ACL. Electrons pass to the CCL through the external circuit, and protons pass to the CCL through the membrane. Oxygen is transported from the CC to the CCL through

[5]Book [7] is a good reference for the actually used fuel cells.

the CGDL. It is reduced by the electrons (from the external circuit) in the CCL and reacts with the protons (from the membrane) while forming condensed water at boundary of the membrane. Besides these processes, water is transported from CC to AC and vice versa through the AGDL, the membrane and the CGDL.

3.5.2 Thermodynamic modeling

Transport of protons through the membrane is prescribed by Eq. (3.74b) while transport of water by Eq. (3.74a).

Transport of water from the channels to the MEA is described by boundary conditions (3.76) but with the constant k_w equal to $3.6{\cdot}10^{-5} mol\, cm^{-2} s^{-1}$, which is more appropriate when the gases are flowing around the MEA, see [59]. Transport of oxygen to the CCL is prescribed by a boundary condition analogical to Eqs. (3.76)

$$j_{O_2} = \frac{k_{O_2}}{4F}\left(a_{O_2}^{CCL} - a_{O_2}^{CC}\right) \tag{3.110}$$

where $a_{O_2}^{CCL}$ and $a_{O_2}^{CC}$ are the thermodynamic activities, see Eq. (4.6), of oxygen in the CCL and in the CC, respectively, i.e. equal to

$$a_{O_2}^{CCL} = \frac{p_{O_2}^{c}}{p^{\circ}}, \qquad \text{and} \quad a_{O_2}^{CC} = \frac{p_{O_2}^{CC}}{p^{\circ}} \tag{3.111}$$

with $p_{O_2}^{c}$ and $p_{O_2}^{CC}$ being partial pressure oxygen in the CCL and in the CC, respectively. The constant k_{O_2} is equal to $6.3 \cdot 10^{-5} \frac{A}{cm^2}$ in accordance with experimental results from [14].

Finally, there are electrochemical reactions taking place in the catalyst layers. These electrochemical reactions are described by the Butler-Volmer equation in Sec. 3.2.3.

3.5.3 Weak formulation

Applying derivative with respect to x to Eqs. (3.74b) and (3.74a), that describe transport of protons and water through the membrane, multiplying the resulting equations by test functions $\varphi_p(x)$ and $\varphi_w(x)$, and integrating with respect to x, leads to

$$0 = \int_0^{X_m} \frac{\partial j_w(x)}{\partial x}\varphi_p(x)\,\mathrm{d}x \tag{3.112a}$$

$$0 = \int_0^{X_m} \frac{\partial j_p(x)}{\partial x}\varphi_w(x)\,\mathrm{d}x. \tag{3.112b}$$

By integrating by parts it follows that

$$0 = -\int_0^{X_m} j_w(x)\frac{\partial \varphi_p(x)}{\partial x}\,\mathrm{d}x + \left[j_p\varphi_p\right]_0^{X_m} \tag{3.113a}$$

$$0 = -\int_0^{X_m} j_p(x)\frac{\partial \varphi_w(x)}{\partial x}\,\mathrm{d}x + \left[j_w\varphi_w\right]_0^{X_m}. \tag{3.113b}$$

Eq. (3.74b) and Eq. (3.74a) are then substituted for proton flux $j_p(x)$ and water flux $j_w(x)$ under the integration signs, respectively. Boundary conditions (3.46)

Parameters of the simulations	
Φ_e^a	$0V$
Φ_e^c	$\in [0V, 1.23V]$
RH^L	50%
RH^R	50%
$p_{O_2}^{CC}$	$\in [0.2bar, 1.0bar]$
T	$50°C$

Table 3.1: Parameters used in the numerical simulations. Other parameters, e.g. diffusivity and proton conductivity, have already been specified in Section 3.3. In the experiments [14] the feeds were dry while both the effluents were saturated with water vapor. RH in the channels is thus taken as average between the inputs and outputs, i.e. equal to 50%. Partial pressure of oxygen was varied between $0.2bar$ and $1.0bar$.

and (3.48) are substituted for proton fluxes j_p at the boundaries. Since water is not only created in the CCL but also transported to the CC, balance of water in the CCL,

$$j_w|_{X_m} + \dot{\xi}_{ORR} = j_w|_{CCL}, \tag{3.114}$$

has to be taken into account. Flux $j_w|_{X_m}$ in this last equation stands for water flux at the cathode edge of the membrane, $\dot{\xi}_{ORR} = j_p/2$ is the rate of reaction (3.45) and $j_w|_{CCL}$ is the water flux given by (3.76). Water flux $j_w|_{X_m}$ is then substituted for the water flux at X_m in Eq. (3.113a). The test functions are from the $H^1(0, X_m)$ Sobolev space, and the solution consists of functions $\Phi(x)$ and $a_w(x)$ which also belong to that Sobolev space [31]. The weak formulation of the problem follows:

Find $\Phi(x)$ and $a_w(x)$ from $H^1(0, X_m)$ such that:
Eqs. (3.113) hold for each $\varphi_p(x)$ and $\varphi_w(x)$ from $H^1(0, X_m)$. (3.115)

3.5.4 Numerical solution

To solve the problem (3.115), it is necessary to specify all the constants from the boundary conditions explicitly. Boundary condition (3.46) requires specifying electric potential at the anode end of the external circuit, Φ_e^a, and partial pressure of hydrogen in the ACL, $p_{H_2}^a$, on the anode side. Similarly, boundary condition (3.48) requires electric potential at the cathode side of the external circuit, Φ_e^c, and partial pressure of oxygen in the CCL, $p_{O_2}^c$. Finally, Eq. (3.110) has to be solved at the boundary to obtain $p_{O_2}^c$ from the oxygen partial pressure in the CC, $p_{O_2}^{CC}$. This means that instead of prescribing $p_{O_2}^c$, pressure $p_{O_2}^{CC}$ is set. Values of these parameters used in the numerical simulations can be found in Table 3.1. Besides these pressures, partial pressure of nitrogen in the CC was chosen so that the total pressure is equal to $1bar$ in the channel. The fuel cell was considered isothermal and temperature was set to $50°C$.

Problem (3.115) is then solved by finite element method implemented in the FEniCS [56] environment with Lagrange elements of second order. The algebraic equations resulting from the approximation of the Sobolev space are solved by a Newton solver.

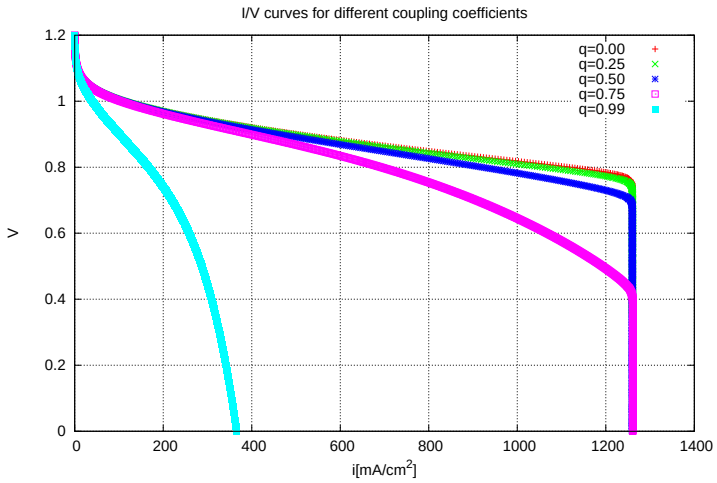

Figure 3.5: I/V (or polarization) curves of the fuel cell for different coupling coefficients. Partial pressure of oxygen in the CC was $0.2bar$. The coupling coefficients does not affect the limiting current (except for $q = 0.99$, where no limiting current appears), but it alters slope of the curve.

Problem (3.115) needs the value of $p^c_{O_2}$ to be given. But this pressure is determined by solving Eq. (3.110) from partial pressure of oxygen in the CC. If solution to this equation were substituted for $p^c_{O_2}$ in boundary condition (3.48), one would obtain an algebraic equation of third order in proton flux. Instead of carrying on such substitution and solving the equation, the solution is obtained numerically by a fixed-point iteration as follows.

The numerical solution is obtained so that $p^c_{O_2}$ starts at an initial value ($p^{CC}_{O_2}$ or $p^c_{O_2}$ of a previous iteration). Problem (3.115) is then solved and proton flux is calculated according to (3.74b). If the value is near enough to the value of the flux calculated from Eq. (3.110), the solution has been reached. If not, pressure $p^c_{O_2}$ is altered as follows

$$p^c_{O_2,new} = p^c_{O_2,old} + k_{O_2}(j_p^{CC} - j_p^{MEA}) \tag{3.116}$$

where $p^c_{O_2,new}$ is the new value of the pressure, $p^c_{O_2,old}$ is the previous value, j_p^{CC} is the proton flux given by Eq. (3.110) and j_p^{MEA} is the proton flux determined by solving problem (3.115).

3.5.5 Results

Problem (3.115) is solved as described in the preceding section for different values of the coupling coefficient q. The resulting I/V curves are plotted in Fig. 3.5.

The I/V curve of a PEM fuel cell also depends on the oxygen partial pressure (or molar fraction) in the CC, see Fig. 3.6.

Eventually, let us demonstrate how the electric potential of protons in the membrane, Φ, varies through the fuel cell. In Fig. 3.7 the electric potential is plotted for different values of the applied voltage. The potential is nearly zero (indicated) near the anode edge of the membrane, and it decreases through the membrane. At the cathode edge of the membrane, there is a wide gap between the

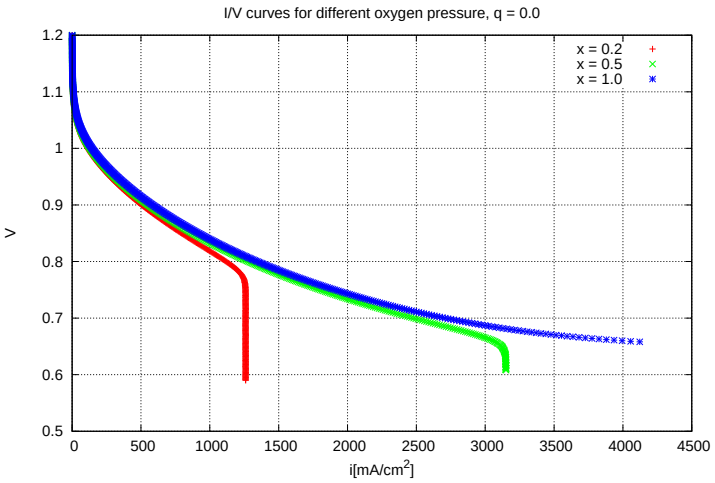

Figure 3.6: I/V curves of the MEA for zero coupling coefficient, i.e. $q = 0$, and varying mole fraction of oxygen in CC equal to 0.2, 0.5, and 1.0. The limiting current is not present in the case of pure oxygen (or it appears for unrealistically high currents) while it appears for lower mole fractions. The limiting current is thus given by partial pressure of oxygen in the CC.

value of the electric potential in the membrane (proportional to the electrochemical potential of protons in the membrane) and the value of the electric potential in the electron-conductive part of the CCL (proportional to the electrochemical potential of electrons therein). When there is no electric current passing through the fuel cell, i.e. the cathode overpotential from Eq. (3.49) is zero, the gap is given by Gibbs energy of formation of liquid water (assuming a_w equal to unity).

Note that the model has to be regarded as a "toy model" for two reasons. Firstly, it has not been compared with experiments. Secondly, several processes were neglected. For example, creation of liquid water in the CCL and its evaporation to the CCL was not assumed. To overcome this simplification, one should consider for example the model from [86]. Moreover, the fuel cell was considered isothermal although non-uniform temperature can also be treated on the level of mechanical equilibrium efficiently as in [50]. Finally, as the gases are passing through the fuel cell, their composition is varying, which is not included in the 1D approximation. All these drawbacks have to be solved at first before trying to compare the model with experiments. The purpose of the model is to provide means how to demonstrate the analysis of efficiency developed in the following section.

3.5.6 Conclusion

A one-dimensional stationary non-equilibrium thermodynamic model of STR PEM fuel cells has been developed. The model contains transport of oxygen from the cathode channel (CC) to the cathode catalyst layer (CCL), which causes that the fuel cell exhibits a limiting current. The model also contains coupling between transport of water and protons inside the membrane, and the effect of

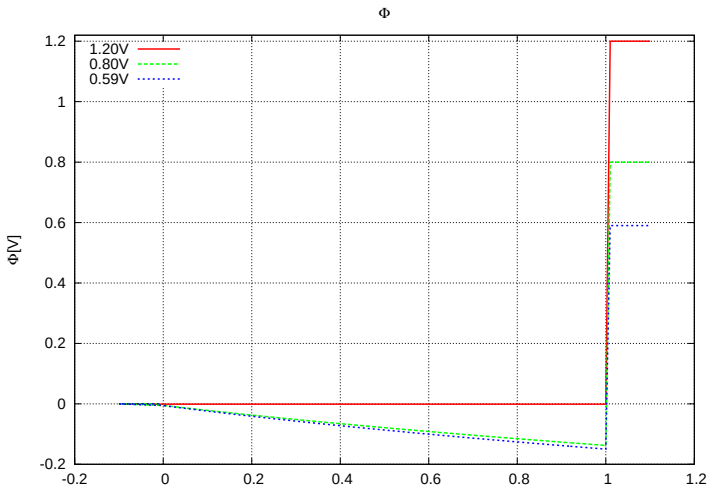

Figure 3.7: Electric potential in the fuel cell with $q = 0.0$ and $p_{O_2}^{CC} = 0.2bar$ at three different loads.

this coupling is demonstrated.

3.6 Analysis of efficiency

Consider a device producing useful work, e.g. a fuel cell, that produces electricity. Suppose that the device is in a steady state, i.e. its thermodynamic state is not varying in time. It is difficult to overestimate importance of the two following questions:

1. What is the maximum work possibly produced by the device?

2. The actual work is lower than the maximum work. Where exactly in the device is the work being lost and how much exactly at each point of the device?

An answer to the first question provides a measure of how efficient the device is. An answer to the second question identifies parts of the device that should be enhanced.

Answers to those two questions may seem to be provided by standard exergy analysis presented for example in [10, 6, 11, 44], which has become a widely used tool among engineers. See our paper [79] for review of applications of exergy analysis. The total exergy destruction, which is proportional to the total entropy production inside the device, is, according to the theory, the measure of lost work. In particular, local entropy production rate indicates how much useful work is being lost at each point of the device. Entropy production can be then minimized by altering some parameters of the device, which leads to the minimum entropy production method of optimization, see [49].

However, we show that the standard exergy analysis relies on an inherently present assumption that resticts the range of validity of the theory. For example, the theory ceases to apply in fuel cells with non-isothermal boundary. Therefore, we develop a more general theory which covers also the cases where the standard theory fails, and so provides answers to those two questions.

3.6.1 Standard exergy analysis

Let us at first briefly review some results of standard exergy analysis which can be found for example in the following works: [10], [12], [6], [49] and [53]. Although this section mainly reviews known facts, it is important to include it so that we are able to compare the new theory with the standard theory efficiently.

Steady state

Let us consider a device in a steady state. The device is in contact with reservoirs of both heat and matter and the device produces useful work (e.g. electricity). Exergy analysis provides answers to the questions what is the maximum possible useful work and where exactly the useful work is being lost. There is, however, an assumption inherently incorporated into exergy analysis which restricts validity of the theory to some extent. The assumption is identified later in this section and a generalization of exergy analysis free of the assumption is then proposed in Sec. 3.7.

A very precise formulation of exergy analysis was given by Adrian Bejan [10], where also the enormous importance of exergy analysis was discussed. Let us

briefly recapitulate the main results. Consider a device in thermal contact with environments $0 \dots n$, see our paper [79] for an illustration, and assume that the device is in a steady state. Besides heat transfer also mass transfer occurs at boundaries of the device.

Balance equations of energy and entropy of the device in a steady state can be written as

$$0 = \frac{\mathrm{d}E}{\mathrm{d}t} = \sum_{i=0}^{n} \Delta Q^i - \Delta W - \int_{\partial V} \sum_{\alpha} (h_\alpha + \varphi_\alpha) \mathbf{j}_\alpha \cdot \mathrm{d}\mathbf{S} + \Delta KE \quad (3.117)$$

$$0 = \frac{\mathrm{d}S}{\mathrm{d}t} = \sum_{i=0}^{n} \frac{\Delta Q^i}{T^i} - \int_{\partial V} \sum_{\alpha} s_\alpha \mathbf{j}_\alpha \cdot \mathrm{d}\mathbf{S} + \mathrm{d}_{irr} S \quad (3.118)$$

where ΔW denotes steady state useful work being produced by the device, i.e. energy leaving the device per unit of time. Symbol φ_α denotes potential energy of species α, $\mathbf{j}_\alpha$ is mass flux of species α and ΔQ^i denotes conductive heat flux from the i-th environment into the device, e.g. transmitted by phonons. Symbol ΔKE denotes flux of kinetic energy into the device. Finally, s_α denotes partial specific entropy of species α, h_α stands for partial specific enthalpy of the species, see also (2.9), and $\mathrm{d}_{irr}S$ is total entropy production in the device, i.e.

$$\mathrm{d}_{irr} S = \int_V \sigma_s \mathrm{d}V \quad (3.119)$$

with σ_s being entropy production, which can be evaluated at each point of the device. Eliminating ΔQ^0 from balance of energy (3.117) and balance of entropy (3.118), a formula for useful work is obtained

$$\Delta W = \underbrace{\sum_i \left(1 - \frac{T^0}{T^i}\right) \Delta Q^i}_{\text{heat exergy}} \underbrace{- \int_{\partial V} \sum_{\alpha} (h_\alpha + \varphi_\alpha - T^0 s_\alpha) \mathbf{j}_\alpha \cdot \mathrm{d}\mathbf{S} + \Delta KE}_{\text{flow exergy}} \underbrace{- T^0 \mathrm{d}_{irr} S}_{\text{exergy destruction}} . \quad (3.120)$$

From the second law of thermodynamics, which can be formulated in the sense that entropy production is non-negative, it follows that the maximum work one can obtain from the device is given by this last equation with $\mathrm{d}_{irr}S$ equal to zero. That means that the maximum useful work is a function of the following quantities

$$\Delta W_{max}(\Delta Q^1, \dots, \Delta Q^n, \mathbf{j}_\alpha|_{\partial V}, (h_\alpha + \varphi_\alpha - T^0 s_\alpha)|_{\partial V}, \Delta KE). \quad (3.121)$$

Thus, it is a function of all energy fluxes through the boundary except for ΔQ^0. Therefore, we can draw the conclusion that exergy analysis gives the maximum useful work one can obtain from a device when heat flux from the environment with temperature T^0 is not well controlled and when it is simultaneously the only not well controlled energy flux through the boundary of the device. Indeed, heat flux ΔQ^0 is the only energy flux through the boundary of the device which is not present in the final formula for maximum work (3.121).

The assumption that only ΔQ^0 is not known is important because it restricts validity of exergy analysis for example in fuel cells with non-isothermal boundary, which is shown in the next section.

On the other hand, if exergy analysis is applicable to the device, entropy production σ_s evaluated at a point gives the amount of useful work which is being lost at the point. This means that plotting σ_s at each point of the device provides a map of losses which tells where exactly the useful work is being lost and thus identifies places where optimization can be done. This provides a very useful tool for efficient design of industrial devices, see for example [12, 49].

Note that if the boundary of the device is isothermal, i.e. there is only the heat reservoir with temperature T^0, the formula for useful work (3.120) simplifies to

$$\Delta W = \Delta G - T^0 \int_V \sigma_s \mathrm{d}V \tag{3.122}$$

if kinetic and potential energies can be neglected. ΔG denotes steady flux of Gibbs energy of neutral species into the device

$$\Delta G = -\int_{\partial V} \sum_{\alpha \in n} \mu_\alpha \mathbf{j}_\alpha \cdot \mathrm{d}\mathbf{S}. \tag{3.123}$$

Only neutral species have been incorporated into ΔG since Gibbs energy of the charged species is supposed to be incorporated into the useful (electrical) work. See Sec. 3.1 for more details. Therefore, exergy analysis implies that flux of Gibbs energy into a device with isothermal boundary gives the maximum useful work one can obtain from the device. This is a common point with the generalized version of the theory formulated below.

Restriction of standard exergy analysis

In the context of standard exergy analysis, the maximum useful work was given by a function of energy fluxes through the boundary except for heat flux from environment at temperature T^0 and losses of the work were given by entropy production, see formulas (3.121) and (3.120).

Consider now a device which has non-isothermal boundary (similarly to Sec. 3.6.1). What if one does not wish to express the maximum useful work in terms of heat fluxes $\Delta Q^1 \dots \Delta Q^n$ because neither those fluxes nor ΔQ^0 are known a priori? In other words, expressing the maximum useful work in terms of heat fluxes restricts validity of formula (3.121) because one may wish to seek a formula for maximum useful work in a form where no heat fluxes are present. See Sec. 3.7.1 for an example where one does not wish to keep heat fluxes fixed.

In summary, there is an assumption inherently incorporated into exergy analysis which says that heat flux ΔQ^0 is the only energy flux through boundary of the device which is not well controlled. Consequently, this is the only energy flux not present in the final formula for maximum useful work, (3.121), and if one wishes to let also some other energy fluxes to be not well controlled, one can not use the results of standard exergy analysis. In particular, entropy production ceases to be the functional which should be minimized in order to maximize the useful work as shown later in section 3.7.1. Similarly, if mass fluxes are not well controlled, e.g. phase transitions, reactions occurring at the interface or when leakages cannot be prevented, one could generalize the above idea with uncontrolled heat fluxes to take care of all uncontrolled fluxes accordingly. As the procedure is analogous, we shall limit the analysis hereafter to the most typical

case, i.e. uncontrollable heat fluxes through the boundary, and we propose a generalization of exergy analysis in the next section. Eventually, a general algorithm of thermodynamic optimization is proposed in Sec. 3.7.3.

3.7 Generalization of exergy analysis

In the preceding section we recalled the standard results of exergy analysis on maximum useful work that one can obtain from a device in a steady state. The maximum work was a function of all energy fluxes through the boundary of the device except for heat flux from the environment at temperature T^0. But what if one does not wish to express the maximum work in terms of all those fluxes?

3.7.1 PEM fuel cells

Consider polymer-electrolyte membrane (PEM) fuel cells, which are very well presented for example in book [7]. Fuel cell is a device which converts chemical energy into electrical work. For example, hydrogen fuel cells convert chemical energy of the reaction (3.38) into electrical energy. That is also why fuel cell efficiency is usually expressed as[6]

$$\eta = \frac{\Delta W'_{el}}{\Delta H} \tag{3.124}$$

where flux of enthalpy into the fuel cell, i.e. enthalpy flux of the fuel (hydrogen, oxygen and water flowing into the fuel cell) diminished by enthalpy flux of the exhausts (water and unconsumed gases leaving the fuel cell), is calculated by formula (3.23). Consequently, maximum useful work is the maximum electrical work the fuel cell can produce from chemical energy of the fuel. In other words, the maximum useful work should be expressed as a function of enthalpy flux into the fuel cell

$$\Delta W_{max}(\Delta H) \tag{3.125}$$

letting heat fluxes between the fuel cell and its surroundings uncontrolled. Therefore, formula (3.121), which follows from exergy analysis, is not consistent with the notion of useful work in fuel cells because the maximum useful work of a fuel cell should not depend, besides kinetic energy, on heat flux through the boundary. As mentioned above, if the boundary is not isothermal, exergy analysis is thus not compatible with the notion of useful work in fuel cells and a more general theory should be used instead. Let us now proceed to the more general theory, which was first noticed in [80] and which is re-derived here in a slightly more convenient way[7].

It has been shown that exergy analysis does not apply for fuel cells with non-isothermal boundary. Let us, therefore, analyze a steady state fuel cell within classical irreversible thermodynamics (CIT), which reviewed in Sec. 3.1 briefly. The analysis proceeds in agreement with Sec. 3.7.3, where a general algorithm of thermodynamic optimization is proposed.

[6] An alternative definition with enthalpy replaced by Gibbs energy is discussed later.

[7] as in our recent paper [79]

1. Boundary of the fuel cell ∂V is defined to enclose both backings[8], gas diffusion layers and membrane-electrode assembly, see [7] or [50] for terminology. It means that there are two electric contacts at the boundary, one at the anode and one at the cathode, with the external circuit. Moreover, hydrogen, oxygen and water enter and leave the fuel cell through the boundary of the backings.

2. Consequently, there are the following energy fluxes through the boundary, see Fig. 3.8: energy flux due to flux of electrons from the anode contact to the external circuit, energy flux due to electrons moving from the external circuit to the cathode contact, energy flux due to flux of hydrogen into the anode backing and possibly also out of the cathode backing (in case of fuel crossover), energy flux due to flux of oxygen into the cathode backing and possibly from the anode backing and energy flux due to flux of water in or out of the anode or cathode backings. Besides all these fluxes, there is flux of conductive heat, i.e. heat flux not accompanied by transport of matter[9], through the whole boundary. All these energy fluxes are incorporated into balance of total energy (3.13), where they are also defined within the framework of CIT.

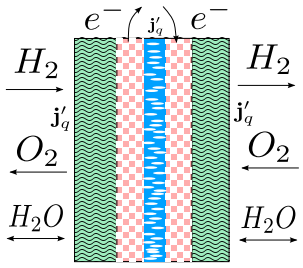

Figure 3.8: An illustration of energy fluxes through the boundary of a PEM fuel cell. The inner parts represent MEA with anode (left) catalyst layer, membrane and cathode (right) catalyst layer. The outer parts represent backings through which gases and liquids flow.

3. Efficiency is defined in the standard way (3.124).

4. We suppose that CIT is precise enough in order to describe all experimental results in fuel cells. Note that it is straightforward to generalize linear force-flux relations to incorporate also Butler-Volmer equation, see Sec. 3.2. This is the only generalization of CIT we use here. It should be borne in mind, however, that for high diffusion velocities, one should go beyond the level of mechanical equilibrium or CIT using for example the extended irreversible thermodynamics, see [46] and [81], or even GENERIC if another phenomena become important, see [38] and [77]. Nevertheless, no matter how detailed theory of non-equilibrium thermodynamics is used, the procedure of thermodynamic optimization remains the same.

[8] AC and CC in the STR PEM FC

[9] except for electrons, entropy of which is incorporated into the measurable heat flux, see Sec. 3.1 for more details

5. According to equation (3.24), electrical work can be expressed as

$$\Delta W'_{el} = \Delta H - \int_V \mathrm{div}\mathbf{j}'_q \mathrm{d}V. \tag{3.126}$$

This means that electrical work is given by enthalpy flux into the fuel cell and by a functional (the second term on r.h.s.) which gives the map of losses. Note that the map of losses is in fact given by heat sources inside the fuel cell.

6. The map of losses may now be evaluated for a given set of boundary conditions consistent with given value of ΔH. Note that it is not necessary to set Dirichlet boundary conditions for fluxes of matter but one can use any boundary conditions leading to the same value of ΔH.

7. To conclude the thermodynamic analysis, an iterative procedure should follow now. Within the procedure only ΔH is kept fixed while material parameters and boundary conditions of the fuel cell are varied. This way the maximum electrical work may be found together with the map of losses elucidating where exactly the useful work is being lost. Note, however, that it is not necessary to find the global maximum of useful work, since it depends on the possible ranges of material parameters, like heat conductivity, or boundary conditions which may be varied. Anyway, if the useful work is raised, the optimization serves its purpose. Note also that if a change of boundary conditions or material parameters leads to a change in ΔH, some information may still be gained as the new set of parameters (leading to the new value of ΔH) may be compared with a different set leading to the same value of ΔH.

We have shown that the standard definition of efficiency leads to a functional quite different from entropy production, compare formulas (3.126) and (3.120), and thus the proposed theory leads to different results than exergy analysis.

Instead of definition (3.124) it is possible to use an alternative definition with flux of enthalpy replaced by flux of Gibbs energy, i.e.

$$\eta = \frac{\Delta W'_{el}}{\Delta G} \tag{3.127}$$

where ΔG is flux of Gibbs energy into the fuel cell calculated according to formula (3.123). Stationary balance of entropy (3.14) can be written as

$$0 = -\mathrm{div} \underbrace{\left(\frac{\mathbf{j}'_q}{T} + \sum_{\alpha \in n} s_\alpha \mathbf{j}_\alpha \right)}_{\mathbf{j}_{s,tot}} + \sigma_s \tag{3.128}$$

for fuel cells. Note that the terms inside divergence represent the total entropy flux $\mathbf{j}_{s,tot}$. Using this equation, the total measurable heat flux into the fuel cell can be expressed as follows

$$\begin{aligned} \Delta Q' &= -\int_{\partial V} \left(T\mathbf{j}_{s,tot} - \sum_{\alpha \in n} T s_\alpha \mathbf{j}_\alpha \right) \cdot \mathrm{d}\mathbf{S} \\ &= \int_{\partial V} \sum_{\alpha \in n} T s_\alpha \mathbf{j}_\alpha \cdot \mathrm{d}\mathbf{S} - \int_V T\sigma_s + \mathbf{j}_{s,tot} \cdot \nabla T \mathrm{d}V. \end{aligned} \tag{3.129}$$

Using this last equation and equation (2.9), the measurable heat flux can be eliminated from formula for electrical work (3.24), which gives

$$\Delta W'_{el} \;=\; \Delta G - \int_V T\sigma_s + \mathbf{j}_{s,tot} \cdot \nabla T \mathrm{d}V. \tag{3.130}$$

Both σ_s and $\mathbf{j}_{s,tot}$ in equation (3.130) can be easily evaluated in terms of heat flux, diffusion fluxes and reaction rates, see Eq. (3.12). The integrand in Eq. (3.130) is the sought map of losses if one wishes to keep ΔG constant.

Formula (3.130) might seem similar to the formula developed within exergy analysis, (3.122), but there are some substantial differences. Indeed, the last term in Eq. (3.130), $\mathbf{j}_{s,tot} \cdot \nabla T$, is not negligible if high gradient of temperature is present, see Sec. 3.7.2. Moreover, it is not σ_s but $T\sigma_s$ which is integrated over volume of the fuel cell. Thus, the two formulas (3.122) and (3.130) are different, and the difference is important if high gradients of temperature are present in the fuel cell.

Note, however, that if the boundary of the fuel cell is isothermal, i.e. $T_{\partial V} = T^0$, the expression for work developed using CIT, (3.130), becomes

$$\Delta W'_{el} \;=\; \Delta G - T^0 \int_V \sigma_s \mathrm{d}V \tag{3.131}$$

which is identical to formula (3.122). Therefore, if the boundary of the fuel cell is isothermal and Gibbs energy is to be kept constant at the boundary, the proposed analysis of efficiency is equivalent to exergy analysis, which says that the maximum work one can obtain from a fuel cell is equal to flux of Gibbs energy into the fuel cell and that the work is being lost due to entropy production.

Moreover, using equation (3.12), one can discover that the functional in formula (3.130) contains only entropy production due to diffusion, electric current and electrochemical reactions, i.e.

$$\Delta W'_{el} = \Delta G - \int_V - \sum_{\alpha \in n} \mathbf{j}_\alpha \cdot \nabla \mu_\alpha - \sum_{\alpha \in c} I_\alpha \cdot \nabla \Phi_\alpha + \sum_r \dot{\xi}_r \tilde{\mathcal{A}}_r \mathrm{d}V. \tag{3.132}$$

Note that in the case of non-isothermal boundary, formula (3.130) does not provide any a priori bound for the useful work. Indeed, even if entropy production is equal to zero, the second term in the integral remains. Physically, it means that even if we know the flux of Gibbs energy into the fuel cell and if no entropy is being produced, heat fluxes through the fuel cell (between parts of the boundary with different temperatures) may raise or reduce the useful work. The maximum useful work is then obtained by some iterative procedure sketched above. In case of isothermal boundary, however, the bound exists, see equation (3.131), where the maximum useful work is obtained if entropy production is zero.

Since neither the optimization where ΔH is kept fixed at the boundary nor the optimization where ΔG is kept fixed at the boundary provide an a priori bound of useful work if the fuel cell has non-isothermal boundary, it is just a matter of convenience whether one chooses the former or the latter approach. The former has the advantage that it can be easily compared to work provided by heat engines while the latter has the advantage that if the fuel cell works isothermally, it is easily related to the experimental measurements, since the resulting voltage is

then given by Gibbs energy flux into the fuel cell. Note also that if and only if the boundary is isothermal, the latter approach gives the same results as exergy analysis.

An isothermal STR PEM fuel cell

Let us now apply the foregoing analysis to the STR PEM fuel cell model developed in Sec. 3.5. Since the fuel cell is considered isothermal, its boundary is isothermal as well, and the standard exergy analysis may be used. In particular, the map of losses is given by $T^0\sigma_s$ with T^0 being the temperature of the fuel cell.

The lost work, $T^0\int_0^{X_m}\sigma_s\,\mathrm{d}x$, in the fuel cell consists, in accordance with Eq. (3.132), of the following contributions:

- Proton flux passing through the membrane:

$$\int_0^{X_m} -Fj_p\cdot\nabla\Phi\,\mathrm{d}x \tag{3.133a}$$

- Water flux passing through the membrane:

$$\int_0^{X_m} -j_w\cdot\nabla\mu_w\,\mathrm{d}x = \int_0^{X_m} -\frac{RT}{a_w}j_w\cdot\nabla a_w\,\mathrm{d}x \tag{3.133b}$$

- HOR in the ACL:

$$j_pF\tilde{\eta}^a \tag{3.133c}$$

  with $\tilde{\eta}^a$ given by Eq. (3.47)

- ORR in the CCL:

$$-j_pF\tilde{\eta}^c \tag{3.133d}$$

  with $\tilde{\eta}^c$ given by Eq. (3.49)

- Water flux between the ACL and the membrane:

$$-j_w|_{ACL}\left(\mu_w^{\bullet}+RT\ln a_w(0)-\mu_w^{\ominus}-RT\ln\frac{p_w^{ACL}}{p^\circ}\right)=-Rj_w|_{ACL}\ln\frac{a_w(0)}{RH^L} \tag{3.133e}$$

- Water flux between the CCL and the membrane:

$$-Rj_w|_{CCL}\ln\frac{RH^R}{a_w(X_m)} \tag{3.133f}$$

The contributions are demonstrated in Fig. 3.9 for the coupling coefficient equal to zero, oxygen pressure in the CC $0.2bar$ and various values of voltage. The highest amount of useful work is clearly lost due to ORR in the CCL. The next greatest source of losses is proton conduction in the membrane. All the other sources are negligible compared with those two sources in that case.

For coupling coefficient $q = 0.99$ the situation is different as shown in Fig. 3.10. The loss due to proton conduction is highest due to the high drag caused by water activity being lower at the anode side than at the cathode side (while protons moving in the opposite direction). The loss due to water transport through

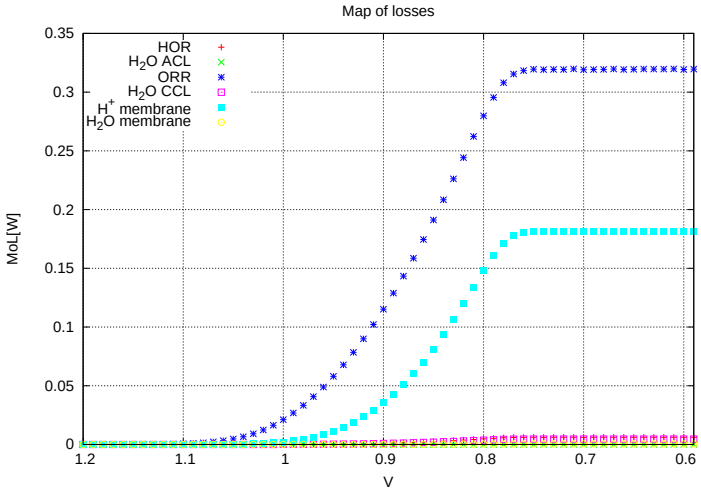

Figure 3.9: Map of losses (MoL) in the fuel cell with $q = 0.0$ and partial pressure of oxygen in the CC equal to $0.2bar$. Curves HOR and ORR represent the losses due to HOR in the ACL, described by formula (3.133c), and the losses due to ORR in the CCL, described by formula (3.133d), respectively. Curves $H_2O\,ACL$ and $H_2O\,CCL$ represent losses due to water transport between the membrane and the ACL, given by Eq. (3.133e), and the CCL, given by Eq. (3.133f), respectively. Finally, curves $H_2O\,membrane$ and $H^+\,membrane$ represent losses due to transport of water and protons through the membrane, given by Eq. (3.133b) and (3.133a), respectively. Highest loss of useful work is caused by ORR, followed by transport of protons through the membrane. Note that the plateau is caused by the limiting current.

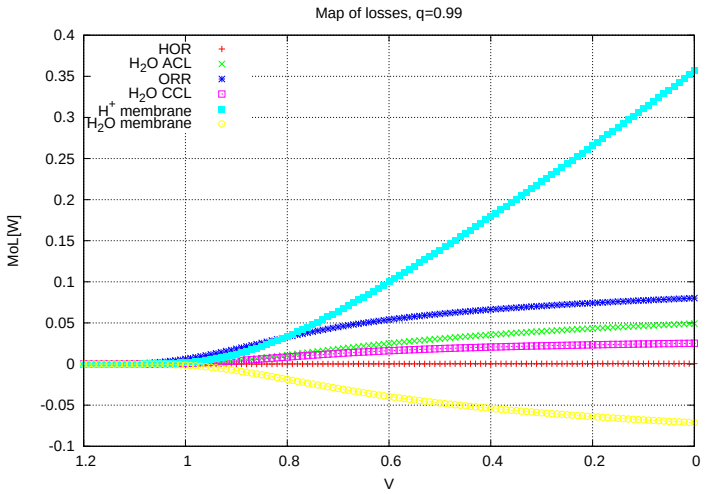

Figure 3.10: Map of losses in the fuel cell with $q = 0.99$ and partial pressure of oxygen in the CC equal to $0.2bar$. The curves are specified in the caption of Fig. 3.9. In this case, transport of protons causes highest losses, followed by ORR. The losses by water transport through the membrane are even negative since water is transported to regions with higher chemical potential (to the cathode).

the membrane is even negative, which means that water moves in the direction with higher chemical potential of water, i.e. to the cathode side[10]. The next highest loss of useful work is caused by ORR in the CCL. The coupling coefficient can thus affect the sources of useful work losses to great extent.

Finally, formula (3.132) is checked. In Fig. 3.11 the useful work, flux of Gibbs energy into the fuel cell, the total amount of losses, and the r.h.s. of Eq. (3.132) are plotted for $q = 0.0$ and oxygen pressure $0.2bar$. The curves ΔW and $\Delta G - MoL$, which represent the r.h.s. of Eq. (3.132), coincide, and so the equation is verified. Useful work is thus equal to the flux of Gibbs energy into the fuel cell diminished by the total amount of losses, which are given by Eq. (3.132).

In summary, all sources of losses in the fuel cell were demonstrated for $q = 0.0$ and $q = 0.99$. It could be now a matter optimization to alter some parameters of the fuel cell so that the losses are reduced, keeping ΔG constant. For example, Fig. 3.9 indicates that the optimization should be targeted on the ORR for $q = 0.0$. Finally, Eq. (3.132) was checked, which means that the useful work delivered by the fuel cell is equal to the flux of Gibbs energy into the fuel cell diminished by the total amount of losses given by the terms (3.133). Standard exergy analysis, which works with Eq. (3.131), thus applies to isothermal fuel cells.

3.7.2 A toy model of SOFC

In this section we illustrate the foregoing analysis on a 1D steady state toy model of SOFC (solid oxide fuel cell). The map of losses is found and compared with

[10]This is inconsistent with the observations made in [14], where water always flows to the anode. This inconsistency demonstrates the limitations of the 1D approximation.

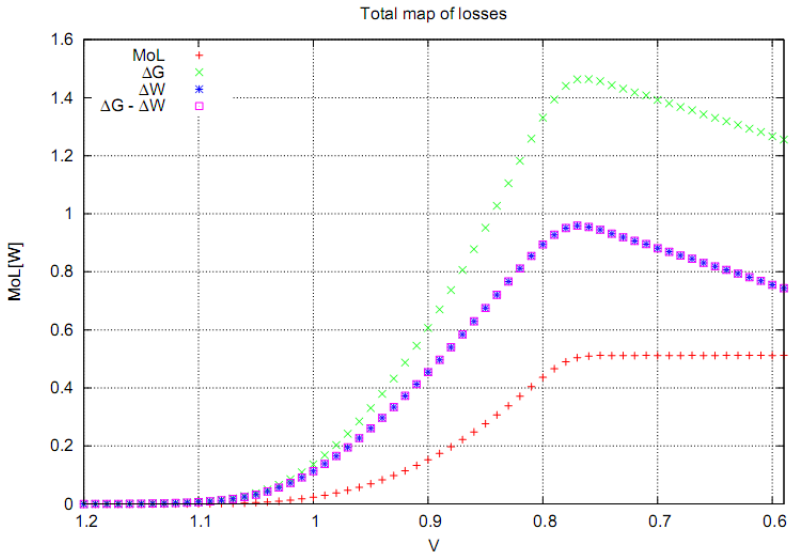

Figure 3.11: Total losses in the fuel cell with $q = 0.0$ and partial pressure of oxygen in the CC equal to $0.2bar$. Curve MoL denotes the total amount of losses for given applied voltage (integral of the map of losses, i.e. the integral in Eq. (3.132)). Curve ΔG represents the flux of Gibbs energy into the fuel cell. Curve ΔW represents the electrical work delivered by the fuel cell, i.e. voltage multiplied by electrical current, per cm^2. Finally, curve $\Delta G - MoL$ shows the difference between the curve ΔG and curve MoL, which is the r.h.s. of Eq. (3.132). This curve coincides with the curve ΔW, the l.h.s. of the equation. Eq. (3.132), which has thus been verified.

entropy production so that the difference between the generalized and standard exergy analysis is revealed, and the above theoretical considerations are validated.

The model is a simplification of a SOFC model presented[11] in master's thesis [94], and it has to be regarded as a toy model as it has not been validated by experiments and because transport of gases is oversimplified so that it is easy to formulate it on the level of mechanical equilibrium. As the goal of this section is not to present the model but rather to elucidate the foregoing analysis, we introduce the model very briefly. We refer the interested reader to the mentioned master thesis for detailed formulation of the model.

The fuel cell consists of an anode (left), an electrolyte (middle) and a cathode (right) as well as the fuel cell illustrated in Fig. 3.8 without the backings. The main difference between the PEM fuel cell in Fig. 3.8 and the solid oxide fuel cell described by this toy model of SOFC is that water is created in the anode according to reaction (3.31) and that oxygen is consumed by reaction (3.39). Moreover, we do not consider any crossover effects, which means that hydrogen and water vapor are present only in the anode while oxygen is present only in the cathode. Oxygen anions are transported to the left through all parts of the fuel cell while electrons are transported only in the anode and in the cathode (also to the left). Electrons from an external circuit enter the fuel cell at the boundary of the cathode and they leave the fuel cell from the boundary of the anode. Besides these fluxes of matter, measurable heat flows through the whole fuel cell. These are all physical processes that are taken into account in the model.

The processes are modeled on the level of mechanical equilibrium, rates of the electrochemical reactions are modeled in Sec. 3.2. All fluxes are proportional to the corresponding forces as in the force-flux relations (3.4). In particular, fluxes of the gases are proportional to gradients of corresponding chemical potentials, and the chemical potentials are approximated by ideal gas chemical potentials, see [5]. Fluxes of ions and electrons are proportional to gradients of electric potentials of ions and electrons, respectively. Finally, measurable heat flux is proportional to gradient of temperature. This way, balance equations of hydrogen, oxygen and water concentration and balance of total energy form a closed set of 1D partial differential equations. These equations were solved within the FEniCS simulation package [56] by the finite element method.

Let us now take a look at results of the simulation. At first we chose the following boundary conditions: Electric potential drop V across the fuel cell was $0.8V$. At the boundary of the anode partial pressures of hydrogen and water vapor were $0.5bar$, and at the other boundary partial pressure of oxygen was $1bar$. Temperature at both boundaries was set equal to $1073K$, i.e. the boundary was isothermal and formula (3.131) applied. Indeed, we obtained from the simulation that electric current I was equal to $503\frac{A}{m^2}$, which implies electric power

$$W'_{el} = V \cdot I = 402.3\frac{W}{m^2}. \tag{3.134}$$

Moreover, flux of Gibbs energy into the fuel cell, ΔG, was $492.0\frac{W}{m^2}$ and the lost

[11] The model from the thesis was altered a little as follows. The dusty-gas model was approximated by simple Fickian law for diffusion, i.e. only gradients of partial pressures were taken into account. Moreover, formula for enthalpy was corrected so that it is consistent with formula (2.9).

work,

$$T^0 \int_V \sigma_s \mathrm{d}V, \tag{3.135}$$

was equal to $89.7\frac{W}{m^2}$, which is equal to the difference between ΔG and W'_{el}. The only assumptions that were used to obtain W'_{el}, ΔG and the map of losses, which altogether satisfy relation (3.131), were that electrical work is defined as (3.21) and that mechanical equilibrium can be used.

Where exactly did the useful work get lost in the fuel cell? The answer to this question is given by map of losses, which is proportional to entropy production in this case (bear in mind that the boundary is isothermal). Entropy production is plotted in Fig. 3.12. The useful work is clearly lost mainly due to electrochemical reactions, which take place mostly in the electrodes near the electrolyte. This conclusion can be verified by plotting entropy production due to the reactions directly.

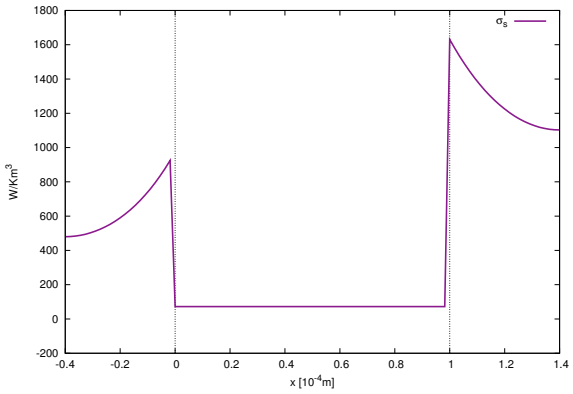

Figure 3.12: Entropy production in a fuel cell with isothermal boundary. Most entropy is being produced by electrochemical reactions in the electrodes. Since for isothermal boundary the map of losses is proportional to entropy production, most useful work is being lost due to the reactions.

Temperature at the boundary of the anode was then decreased by $5K$, and the equations were solved with this new boundary condition. The boundary was not isothermal any more, and so the more precise formula (3.130) had to be used. Electrical work became $W'_{el} = 397.5\frac{W}{m^2}$ and flux of Gibbs energy $\Delta G = 485.3\frac{W}{m^2}$. The lost work,

$$\int_V T\sigma_s + \mathbf{j}_{s,tot} \cdot \nabla T \mathrm{d}V, \tag{3.136}$$

was equal to $87.8\frac{W}{m^2}$, which is exactly the difference between ΔG and W'_{el} as expected. The map of losses given by equation (3.130) thus predicts the lost useful work precisely unlike exergy destruction (see below). As well as in the isothermal case, the only assumptions necessary for this verification were that electrical work is given by (3.21) and that mechanical equilibrium can be applied.

As well as in the case of isothermal boundary, we can ask where exactly in the fuel cell the useful work gets lost, and the answer is again provided the map of losses, i.e. the integrand of formula (3.136). One can see in Fig. 3.13 that curves for exergy destruction, $T^0\sigma_s$, and for $T\sigma_s$ coincide. The term $\mathbf{j}_{s,tot} \cdot \nabla T$ is negative

and similar in magnitude to $T\sigma_s$, and this term causes the big difference between the actual map of losses (MoL) and exergy destruction. Indeed, although most entropy is now being produced by heat flux in the electrolyte, most useful work is still lost due to the electrochemical reactions.

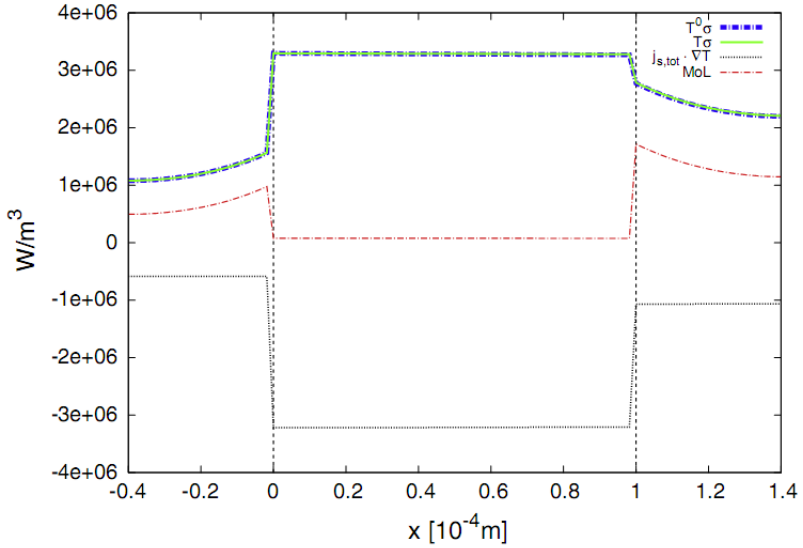

Figure 3.13: Analysis of map of losses for non-isothermal boundary. The curves for $T^0\sigma_s$ and $T\sigma_s$ coincide. The term $\mathbf{j}_{s,tot} \cdot \nabla T$ is negative and similar in magnitude to $T\sigma_s$. This term is quite important because it is responsible for the huge difference between the actual map of losses (MoL) and exergy destruction, $T^0\sigma_s$. Most entropy is now being produced by heat flux in the electrolyte. In other words, most exergy is being destroyed in the electrolyte. However, the map of losses indicates that most useful work is being lost by the electrochemical reactions in the electrodes as well as in the isothermal case. The standard exergy analysis is thus inapplicable in this case.

In summary, the generalization of exergy analysis has been illustrated on a toy model of 1D steady state SOFC. For isothermal boundary, both standard and generalized exergy analyses coincide as they should because they predict the same maps of losses (formula (3.131)). On the other hand, for non-isothermal boundary there is a significant difference between exergy destruction and the map of losses predicted by the generalized exergy analysis, see Fig. 3.13 as most useful work is lost due to electrochemical reactions in the electrodes (as well as in the case of isothermal boundary) while most exergy is destroyed (or most entropy is produced) by heat flux through the electrolyte. Therefore, the standard exergy analysis should not be used in case of non-isothermal boundary, and it is vital to adopt the generalized analysis.

3.7.3 General algorithm of thermodynamic optimization

Let us now summarize the above analysis of efficiency and suggest an algorithm of thermodynamic optimization based on the map of losses:

1. Define the system and its boundary ∂V.

2. Identify energy fluxes through ∂V. All steady state energy fluxes have to sum up to zero in order to fulfill the law of conservation of energy.

3. Define efficiency. Based on this definition, identify which energy fluxes through the boundary of the device should be kept fixed during the optimization.

4. Choose a level of description within non-equilibrium thermodynamics. In this step the set of state variables has to be chosen. The set of state variables then corresponds to an appropriate non-equilibrium thermodynamic theory. For examples, for densities, temperature and barycentric velocity one should use CIT [28]. In mechanical equilibrium, where barycentric velocity is no longer among state variables, one would prefer the theory presented in book [48]. If, however, diffusion velocities are large enough, extended irreversible thermodynamics [81] is the appropriate theory. The level of description has to be also compatible with the energy fluxes chosen in step 2 in the sense that energy fluxes should be formulated within the chosen thermodynamic theory.

5. Express useful work in terms of the energy fluxes present in definition of efficiency from step 3, which are kept constant, and in terms of a map of losses. This is the crucial and the most difficult step, since non-equilibrium theory of mixtures has to be employed. For example, in fuel cells this step leads to formula (3.130), from which it follows that the map of losses is the integrand in the second term on r.h.s. of the formula.

6. Evaluate the map of losses. This reveals where exactly useful work is being lost.

7. Modify boundary conditions or parameters, e.g. material parameters, of the device so that the energy fluxes through the boundary which are to be kept constant remain fixed, and reevaluate the useful work and the map of losses. If the new useful work is higher than the preceding, the new choice of boundary conditions and parameters should be preferred to the preceding. The new map of losses suggests at which place of the device an another iteration of the optimization should be focused.

   Note that information is gained even if the new set of boundary conditions and parameters leads to different values of the energy fluxes through the boundary which are to be kept constant. Indeed, if yet another set of boundary conditions or parameters leads to the same value of the energy fluxes, those two sets may also be compared. This way, one would optimize the device for different values of the energy fluxes.

3.7.4 Importance in engineering

Exergy analysis or its generalization are very useful tools for any engineer working with a continuous thermodynamic model of an industrial device. For example, in case of fuel cells, efficiency is usually evaluated from voltage produced by the fuel cell. This is perfectly consistent with the definition of fuel cell efficiency (3.124), but it does not provide the local map of losses. In other words, when one calculates

what the voltage will be using a continuous model, one knows the efficiency but one does not know where exactly the efficiency will be lost. To find out such information rigorously, one should evaluate the map of losses, which is given by entropy production in the standard exergy analysis or by a similar functional in the generalized theory. If the continuous model is thermodynamically consistent, e.g. fulfills condition (3.14) in steady state, the map of losses may be evaluated straightforwardly without any modification of the model.

With the map of losses, one can reveal where exactly in the device some enhancements are needed so that the total efficiency raises.

3.7.5 Conclusion

Results of exergy analysis were reviewed in Sec. 3.6.1, and all assumptions behind the theory were identified. It was shown that for fuel cells with non-isothermal boundary one of the assumptions is not fulfilled in general. Consequently, a general algorithm of thermodynamic optimization not relying on the assumption any more was formulated in Sec. 3.7.3 and illustrated in sections 3.7.1 and 3.7.2. Moreover, it was demonstrated on saline power plants and heat engines in our paper [79]. The generalization of exergy analysis is shown to be essential for non-isothermal fuel cell as shown in Sec. 3.7.2.

It should be stressed that whichever method (standard exergy analysis or the newly proposed method) is used, the outcome is of crucial importance for any engineer who predicts behavior of an energy producing device using a continuous thermodynamic model because, besides calculating the maximum work, it is possible to reveal where exactly in the device useful energy is being lost.

4. Equilibrium Thermodynamics

Equilibrium thermodynamics, very well described for example in classical textbooks [53] and [19], is the most macroscopic level of description, where no more evolution is present. The state variables are total energy (or entropy), volume and mass (or number of moles) of each species. Since this level is the oldest part of thermodynamics [55], it is also the most developed part of the theory. Results of equilibrium thermodynamics have been used implicitly or explicitly at many occasions in this work. Refer to our paper [81] for terminology and derivation of those results, which are not derived in this work.

This section consists of two parts. In Sec. 4.1 equilibrium properties of Nafion membranes are studied, which were necessary in Sec. 3.4. In Sec. 4.2 open circuit voltage (OCV) of vanadium redox flow batteries (VRFB) is derived, and that section constitutes more or less our paper [82], which has been submitted to the Journal of Power Sources but has not been reviewed at the time of writing yet.

4.1 Equilibrium water sorption in Nafion membranes

4.1.1 Water uptake

The amount of water in a Nafion membrane is usually expressed in terms of water uptake λ, which is defined as the ratio of the number of moles of water in the membrane to the number of moles of SO_3 groups in the membrane

$$\lambda = \frac{mol\, H_2O}{mol\, SO_3}. \tag{4.1}$$

The dependence of water uptake on relative humidity of the environment in which the membrane is immersed has been measured many times. However, not all experimentally obtained dependencies are equivalent. There are two basic groups of the experimental results, one where $\lambda \approx 14$ for saturated water vapor, i.e. $RH = 100\%$, see e.g. [89], the other where $\lambda \approx 21$, see e.g. [45]. These two groups are clearly inconsistent with each other. Water uptake of a Nafion membrane equilibrated with liquid water is approximately 22, see [100], which is compatible with the latter group, while the former group thus exhibits the so called Schröder's paradox.

Let us now explain the paradox. Consider two Nafion membranes, one equilibrated with liquid water and the other with saturated water vapor at the same pressure and temperature. Chemical potential of pure liquid water is equal to chemical potential of the saturated water vapor, and chemical potential of water in the membrane is equal to chemical potential of water in the surroundings after equilibrium has been reached. Therefore, chemical potential of water in the membrane equilibrated with liquid water is the same as chemical potential of water in the membrane equilibrated with saturated water vapor.

Conditions of thermodynamic stability require the second derivative of Gibbs energy of the membrane with respect to water content to be positive, see for example [53]. Since chemical potential of water in the membrane is the first

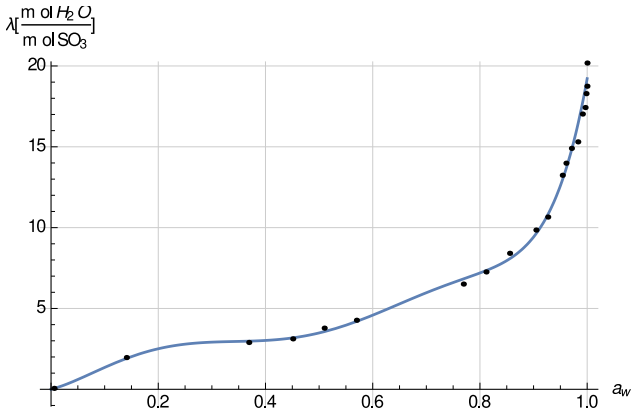

Figure 4.1: Water uptake as a function of water activity (or RH).

derivative, it has to be a monotonous function of water content. Hence, water uptake is a monotonous function of chemical potential and water uptakes in the two membranes also have to be equal as well, which contradicts the observation that $\lambda = 14$ for membranes equilibrated with saturated water vapor. This is a reason why the experiments without Schröder's paradox, i.e. with $\lambda \approx 21$ for saturated water vapor, are preferred in this work.

It should be borne in mind, however, that there are also theories supporting Schröder's paradox, where either surface effects play a role [25, 34] or where chemical potential of water is a non-monotonous function of water uptake [29]. The former works, however, often suffer from the impossibility to describe a membrane equilibrated on one side with liquid water and with saturated water vapor on the other side as they often predict non-zero water flux in such case. The latter works indicate an instability, e.g. phase transition taking place in the membrane, see [19].

In this work water uptake is taken from [45] for high RH and from [89] for low RH. As Jeck et al. [45] pointed out, a substantial part of water uptake from vapor appears for very high RH, which is the reason for such combination of sorption curves, see figure 4.1 for the data. According to that paper, Schröder's paradox is just an experimental artifact caused by not reaching sufficiently high RH. On the figure there is also a fitted function $\lambda(a_w)$ of the form

$$\begin{aligned} \lambda(a_w) &= -180402 + 194743e^{a_w} - \\ &\quad -15265e^{2a_w} + 924e^{3a_w} - \\ &\quad -166977a_w - 70904a_w^2 - \\ &\quad -16833a_w^3 - 0.0185816. \end{aligned} \tag{4.2}$$

This function is implemented in the time-dependent simulation in Section 3.4.

Activity of water and relative humidity are often taken as equivalent in this section. Is this equivalence consistent with thermodynamics? Indeed, it is as will be shown right away. Consider a membrane filled with water which is in equilibrium with water vapor in which the membrane is immersed, and suppose that the vapor can be treated as an ideal gas. The equilibrium between water in the membrane and water in the vapor is expressed as equality of chemical

potentials of the two kinds of water

$$\mu_w^{\bullet} + RT \ln a_w = \mu^{\ominus} + RT \ln \frac{p_w}{p^{\circ}} \tag{4.3}$$

where on the l.h.s. the standard state is the chemical potential of pure liquid water while on the r.h.s. the standard state is the chemical potential of pure water vapor at standard pressure and given temperature. Equilibrium of pure liquid water and pure water vapor is then expressed as

$$\mu_w^{\bullet} = \mu_w^{\ominus} + RT \ln \frac{p_w^{sat}}{p^{\circ}} \tag{4.4}$$

where p_w^{sat} is the saturated water vapor pressure at given temperature. Equality (4.3) can be then rewritten as

$$a_w = \frac{p_w}{p_w^{sat}} \equiv RH, \tag{4.5}$$

where the definition of relative humidity was employed. Therefore, activity of water in the membrane equilibrated with water vapor with certain relative humidity is equal to the relative humidity.

Note however, that RH is equal to activity of condensed water in the membrane and not to the activity of water vapor defined in the standard thermodynamic sense as

$$\mu_w^g = \mu^{\ominus} + RT \ln a_w^g = \mu^{\ominus} + RT \ln \frac{p_w}{p^{\circ}} \tag{4.6}$$

with μ_w^g being chemical potential of the vapor.

Water uptake can be converted to concentration of water (with units $mol\, cm^{-3}$). Dimension of the concentration is

$$[c] = \frac{mol\, H_2O}{cm^3} = \frac{mol\, H_2O}{mol\, SO_3} \frac{mol\, SO_3}{g_{Nafion}} \frac{g_{Nafion}}{cm^3}, \tag{4.7}$$

and thus

$$c = \lambda \cdot \frac{1}{EW} \cdot \rho_{Nafion} \tag{4.8}$$

where EW is the equivalent weight, which expresses weight of the Nafion polymer per $1\, mol$ of SO_3 groups, see [63], and ρ_{Nafion} is density of the Nafion polymer in the swollen membrane.

4.1.2 Swelling

Besides the dependence of water uptake on water activity one also needs to know how shape of the membrane varies during the sorption in order to be able to take swelling into account properly. Strain of the membrane is defined as

$$\varepsilon = \frac{\mathrm{d}x - \mathrm{d}X}{\mathrm{d}X}, \tag{4.9}$$

$\mathrm{d}x$ being a short segment of the swollen membrane and $\mathrm{d}X$ a short segment of the dry membrane. This equation can be rewritten as

$$\mathrm{d}x = (1 + \varepsilon)\, \mathrm{d}X. \tag{4.10}$$

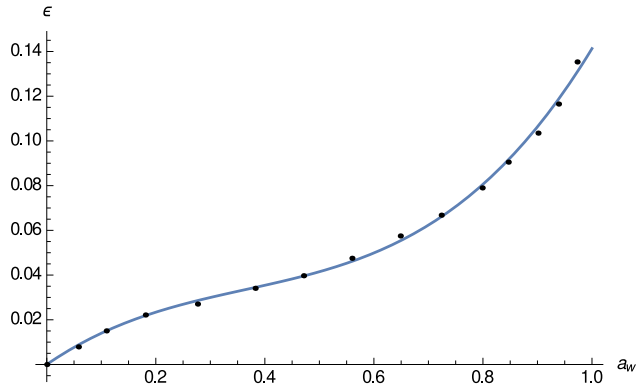

Figure 4.2: Strain of EW 1100 Nafion membrane at $30°C$ taken from [102].

Assuming isotropic swelling, the experimental dependence of strain on relative humidity was published in [102]. The experimental data can be fitted, see figure 4.2, as

$$\varepsilon(a_w) = 0.168426a_w - 0.314683a_w^2 + 0.287563a_w^3. \tag{4.11}$$

4.1.3 Thickness and density

Having the swelling and water uptake as functions of water activity (or relative humidity) it is now easy to calculate thickness and density of dry Nafion membranes. Such calculation is needed because thicknesses and densities of the membranes are usually measured at $RH = 50\%$. For example in [1] thickness and density of Nafion 115 were determined at $RH = 50\%$ and $23°C$ to be $\rho_{N115} = 1.969gcm^{-3}$ and $t_{N115} = 127\mu m$. Nafion N1110 has the same density as N115 and its thickness is $t_{N1110} = 254\mu m$. Using formula (4.11), thickness of dry Nafion $N115$ is given by

$$t_{N115,dry} = \frac{t_{N115}}{1 + \varepsilon(0.5)} = 121.6\mu m, \tag{4.12}$$

and thickness of dry Nafion N1110 is

$$t_{N1110,dry} = \frac{t_{N1110}}{1 + \varepsilon(0.5)} = 243.3\mu m. \tag{4.13}$$

To find density of dry Nafion, one can start with realizing that mass of water in the swollen Nafion can be expressed as

$$m_w = M_w \frac{\lambda}{EW} m_{membrane,dry} = M_w \frac{\lambda}{EW} \rho_{dry} V_{dry} \tag{4.14}$$

where ρ_{dry} and V_{dry} are density and volume of the dry Nafion, respectively, and M_w is the molar mass of water. V_{dry} is related to volume of the membrane at $RH = 50\%$ by

$$V_{RH=50\%} = (1 + \varepsilon(0.5))^3 V_{dry}. \tag{4.15}$$

Mass of the swollen Nafion is then equal to the sum of mass of the polymer and mass of water swollen in the polymer

$$\rho_{RH=50\%} V_{RH=50\%} = \rho_{dry} \frac{V_{RH=50\%}}{(1 + \varepsilon(0.5))^3} \left(1 + \frac{M_w \lambda(0.5)}{EW}\right) \tag{4.16}$$

so that density of the dry Nafion is

$$\rho_{dry} = \frac{(1+\varepsilon(0.5))^3 \rho_{RH=50\%}}{1+\frac{M_w \lambda(0.5)}{EW}}. \tag{4.17}$$

Density of dry Nafion N115 is equal to

$$\rho_{N115,dry} = \rho_{N1110,dry} = 2.12 \frac{g}{cm^3}, \tag{4.18}$$

which is also equal to density of dry Nafion N1110 as these two types of Nafion only differ by thickness, see [63] for the naming conventions. Finally, note that density of the polymer itself, i.e. without water, can be calculated from the dry density as

$$\rho_{Nafion} = \frac{\rho_{dry}}{(1+\varepsilon)^3}. \tag{4.19}$$

4.2 Thermodynamic derivation of open circuit voltage in vanadium redox flow batteries

4.2.1 Introduction

Vanadium redox flow batteries [92, 91] (VRFB) represent a promising way for storing electrical energy. In many aspects they are similar to fuel cells, where electric energy can also be stored into or produced from fuel (e.g. hydrogen). In VRFB, however, the energy is stored in the electrolytes. A VRFB single-cell consists of a positive half-cell, where V^{IV} ions are oxidized to V^V when charging, and of a negative half-cell, where V^{III} is reduced to V^{II} when charging. The two half-cells are separated by a membrane through which either cations or anions are transported. The former kind of membrane is referred to as cation-exchange (catex) membrane while the latter as anion-exchange (anex) membrane. The half-cells are also connected through an external circuit, which enables the flow of electrons (i.e., electric current).

The battery voltage, i.e. difference of the electrochemical potentials of electrons in the positive and the negative half-cell, is measured on the clamps of the cell. How does the voltage depend on the state of charge (SOC) of the battery in a steady state when no current is passing through the circuit? In other words, how does the open circuit voltage (OCV) depend on SOC? Although this fundamental question has been addressed many times due to its high importance, it seems that the precise quantitative description for the dependence of OCV on SOC has not been found so far, and this is the goal of this work.

Usually, the dependence of OCV on SOC is derived from Nernst relation [5, 51]. Probably the most frequently used dependence in literature is

$$E_{usual} = E^\circ + \frac{RT}{F} \ln \frac{c^P_{VO_2^+} c^N_{V^{2+}} (c^P_{H^+})^2}{c^P_{VO^{2+}} c^N_{V^{3+}}} \tag{4.20}$$

where c^P_α stands for concentration of species α in the positive electrolyte (N stands for negative). However, several possible dependencies have been suggested in the literature. For example, Al-Fetlawi et al. suggest a simple form where only

concentrations of vanadium ions are present. Corcuera and Skyllas-Kazacos [26], Heintz and Illenberger [39] and Hudak [42] include also concentration of protons in the positive half-cell (as in formula (4.20)) as well as Knehr and Kumbur [51], who moreover suggest the inclusion of Donnan potential due to different proton concentrations in both electrolytes. In all these works it was assumed that activity coefficients of all species taken into account can be neglected (i.e. be equal to unity). Is it possible to derive any even more accurate formula describing the OCV as a function of SOC?

This question is answered by equilibrium thermodynamics. Indeed, the Nernst relation itself [5, 70] is derived from thermodynamics. So what if we do not start with any form of Nernst relation but rather with thermodynamic equality of electrochemical potentials? This is the way followed in this manuscript. At first, conditions for the steady state where OCV is measured are carefully stated and complete electrochemical potentials of all species participating on the electrochemical reactions are written down. Consequently, a Nernst relation for VRFB is derived. In the derivation careful attention is paid to the definition of standard states so that thermodynamic data are used consistently. The here derived Nernst relation is different from the Nernst relations mentioned above, and it is free of any possible inconsistencies (at least in the form with activities), since it is derived directly from thermodynamics. Therefore, thermodynamics yields the final form of Nernst relation.

The thermodynamic Nernst relation is compared to our own experimental data[1]and good agreement is demonstrated. It is also shown how non-ideality affects the Nernst relation considerably, and a formula for the activity coefficients is proposed based on the Debye-Hückel theory [5]. Finally, it is shown that VRFB with an anex membrane follows a different Nernst relation than a battery with a catex membrane since bisulphates are equilibrated in the former case while protons are equilibrated in the latter case. To the best of author's knowledge this behavior has not been yet presented.

In summary, Sec. 4.2 provides careful thermodynamic derivation of Nernst relations for VRFB with both anex and catex membranes. Interestingly, these two Nernst relations are different since different species are equilibrated in both cases. The forms of the Nernst relations in terms of activities are free of any possible inconsistencies as there is no way how to enhance them (at least in the steady state), since otherwise they would not agree with thermodynamics. Uncertainties are introduced when rewriting activities in terms of concentrations or molalities and activity coefficients, since activity coefficients for the considered electrolytes are not available in general. However, a first approximation of the activity coefficients based on the Debye-Hückel theory is proposed. The here derived Nernst relations show good agreement with experimental data.

[1]Experiments were carried out at the New Technologies Research Centre, University of West Bohemia by Petr Mazur, co-author of paper [82], and at Fraunhofer ICT, Pfinztal by Frank Wandschneider, an another co-author of the paper. Author of this work did not assist with the experiments.

4.2.2 OCV for catex membranes

This section provides a thermodynamic calculation of OCV in all-vanadium VRFB with cation exchange membrane at standard temperature and pressure. The OCV is calculated in two ways differing in definition of the reference voltage. Both ways, however, are equivalent as they give the same dependence of OCV on SOC.

General Nernst relation

During discharging the following electrochemical reactions take place in the battery, see e.g. [51],

- Positive half-cell:

$$VO_2^+ + e^- + 2H^+ \rightarrow VO^{2+} + H_2O \tag{4.21}$$

- Negative half-cell:

$$V^{2+} \rightarrow V^{3+} + e^- \tag{4.22}$$

As shown in Sec. 2.1.3, electrochemical reactions are driven by their electrochemical affinities, which are negatives of the corresponding reaction Gibbs energies. An electrochemical reaction then proceeds in the direction from left to right if and only if its electrochemical affinity is positive, and in the opposite direction if the affinity is negative. In particular, it does not proceed in any direction (or it proceeds in both directions with the same rates) if and only if the affinity is zero.

Electrochemical affinity in the positive half-cell, which is equal to minus the corresponding reaction Gibbs energy written with electrochemical potentials, is defined as

$$\mathcal{A}^P = \tilde{\mu}^P_{VO_2^+} + \tilde{\mu}^P_{e^-} + 2\tilde{\mu}^P_{H^+} - \tilde{\mu}^P_{VO^{2+}} - \tilde{\mu}^P_{H_2O} \tag{4.23}$$

where $\tilde{\mu}_\alpha$ is electrochemical potential of species α, see for example [28], [5] or [79]. Superscripts P denote that the species are present in the positive half-cell. Note that this affinity is positive during discharging while negative during charging. Let us now have a closer look at the electrochemical potentials. Firstly, electrochemical potential of water is equal to chemical potential of water as water is not charged. Secondly, electrochemical potential of electrons can be identified with electric potential Φ as follows

$$\tilde{\mu}_{H_2O} = \mu_{H_2O} \qquad \text{and} \qquad \tilde{\mu}_{e^-} = -F\Phi. \tag{4.24}$$

See 3.1.1 for more details on the relation between electric and electrochemical potentials. Altogether, electrochemical affinity in the positive half-cell becomes

$$\mathcal{A}^P = \tilde{\mu}^P_{VO_2^+} - F\Phi^P + 2\tilde{\mu}^P_{H^+} - \tilde{\mu}^P_{VO^{2+}} - \mu^P_{H_2O}. \tag{4.25}$$

Analogically, the electrochemical affinity in the negative half-cell reads

$$\mathcal{A}^N = \tilde{\mu}^N_{V^{2+}} - \tilde{\mu}^N_{V^{3+}} + F\Phi^N. \tag{4.26}$$

Voltage of the battery can be then expressed as

$$E = \Phi^P - \Phi^N = \frac{1}{F}\left(\tilde{\mu}^P_{VO_2^+} + 2\tilde{\mu}^P_{H^+} - \tilde{\mu}^P_{VO^{2+}} - \mu^P_{H_2O} + \tilde{\mu}^N_{V^{2+}} - \tilde{\mu}^N_{V^{3+}}\right) - \frac{1}{F}\left(\mathcal{A}^P + \mathcal{A}^N\right). \tag{4.27}$$

Note that during discharging both the electrochemical affinities are positive which reduces the voltage provided by the battery. When the external circuit is disconnected and if we assume steady state, the electrochemical reactions do not proceed and, therefore, the electrochemical affinities are zero and the formula for OCV reads

$$E = \frac{1}{F}\left(\tilde{\mu}^P_{VO_2^+} + 2\tilde{\mu}^P_{H^+} - \tilde{\mu}^P_{VO^{2+}} - \mu^P_{H_2O} + \tilde{\mu}^N_{V^{2+}} - \tilde{\mu}^N_{V^{3+}}\right). \tag{4.28}$$

Moreover, protons can not move through the membrane because otherwise they would violate the steady state. Hence, electrochemical potential of protons has to be the same in both half-cells

$$\tilde{\mu}^P_{H^+} = \tilde{\mu}^N_{H^+}. \tag{4.29}$$

This equation expresses equilibrium between the half-cells separated by a catex membrane. Equation (4.28) represents the general form of Nernst relation in VRFB, where the electrochemical potentials still have to be specified. But let us at first have a look at standard electrode potentials in VRFB.

Positive half-cell with reference electrode

Consider the positive half-cell connected with a reference hydrogen electrode, where the following reaction proceeds

$$H_2 \rightarrow 2H^+ + 2e^-. \tag{4.30}$$

Electrochemical affinities are then

$$\mathcal{A}^P = \tilde{\mu}^P_{VO_2^+} - F\Phi^P + 2\tilde{\mu}^P_{H^+} - \tilde{\mu}^P_{VO^{2+}} - \mu^P_{H_2O} \tag{4.31}$$

for the positive half-cell and

$$\mathcal{A}^H = \mu_{H_2} + 2F\Phi^H - 2\tilde{\mu}^H_{H^+} \tag{4.32}$$

for the hydrogen electrode. OCV of such cell is then given by

$$E^{P,H} = \Phi^P - \Phi^H = \frac{1}{F}\left(\tilde{\mu}^P_{VO_2^+} + 2\tilde{\mu}^P_{H^+} - \tilde{\mu}^P_{VO^{2+}} - \mu^P_{H_2O} + \frac{1}{2}\mu_{H_2} - \tilde{\mu}^H_{H^+}\right). \tag{4.33}$$

Condition (4.29) also applies in the steady state, i.e.

$$\tilde{\mu}^P_{H^+} = \tilde{\mu}^H_{H^+}. \tag{4.34}$$

Moreover, from chemical equilibrium between water and protons and hydroxyl anions, we obtain

$$\mu_{H_2O} = \tilde{\mu}_{H^+} + \tilde{\mu}_{OH^-}. \tag{4.35}$$

Finally, chemical potential of hydrogen is zero in the standard state by definition as well as the standard chemical potential of protons, see for example [5],

$$\mu^{\circ}_{H_2} = 0 \qquad \text{and} \qquad \mu^{\circ}_{H^+} = 0. \tag{4.36}$$

Therefore, OCV becomes

$$E^{P,H} = \frac{1}{F}\left(\tilde{\mu}^{P}_{VO_2^+} - \tilde{\mu}^{P}_{VO^{2+}} - \tilde{\mu}^{P}_{OH^-}\right). \tag{4.37}$$

Expressing electrochemical potentials with respect to (3.9) then leads to

$$E^{P,H} = E^{P,\circ} + \frac{RT}{F}\ln\frac{a^{P}_{VO_2^+}}{a^{P}_{VO^{2+}}a^{P}_{OH^-}} \tag{4.38}$$

where standard electrode potential of the positive half-cell is defined as

$$E^{P,\circ} = \frac{1}{F}\left(\mu^{\circ}_{VO_2^+} - \mu^{\circ}_{VO^{2+}} - \mu^{\circ}_{OH^-}\right). \tag{4.39}$$

Note that $E^{P,\circ}$ is independent of composition, since it is measured in the limit of zero molality, see for example [5].

Using standard chemical potentials from [97], the standard electrode potential of the positive half-cell becomes

$$E^{P,\circ} = 0.17V \tag{4.40}$$

where the following values were used that

$$\Delta_f G^{\circ}_{VO_2^+} = -587kJ/mol \text{ and } \Delta_f G^{\circ}_{VO^{2+}} = -446.4kJ/mol. \tag{4.41}$$

Standard chemical potential of hydroxyl anions is given in formula (B.17).

The value of standard electrode potential (4.40) differs from the standard electrode potential for the positive electrode given for example in [17]. The reason is that chemical potential of water is replaced by chemical potential of protons and hydroxyl anions according to formula (4.35). Indeed, if we do not make this replacement, we obtain by the same procedure as above a different but equivalent form of the Nernst relation

$$E^{P,H}_{H_2O} = E^{P,\circ}_{H_2O} + \frac{RT}{F}\ln\frac{a^{P}_{VO_2^+}a^{P}_{H^+}}{a^{P}_{VO^{2+}}a^{P}_{H_2O}} \tag{4.42}$$

with standard electrode potential

$$E^{P,\circ}_{H_2O} = \frac{1}{F}\left(\mu^{\circ}_{VO_2^+} - \mu^{\circ}_{VO^{2+}} - \mu^{\circ}_{H_2O}\right) = 1.000V. \tag{4.43}$$

This value is calculated from the corresponding Gibbs energies of formation and it is equal to the commonly used standard electrode potential of the positive electrode from [17], see for example [51, 26, 39]. Note that it is important to realize from which standard chemical potentials standard electrode potentials are constructed before using them. The form (4.38) has the advantage to (4.42) that it contains less activities and so less activity coefficients have to be determined. Nevertheless, both forms (4.38) with (4.40) and (4.42) with (4.43) are equivalent and consistent.

Negative half-cell with reference electrode

Consider now the negative half-cell connected with a reference hydrogen electrode. The calculation is analogical to the preceding section. OCV can be expressed as

$$E^{N,H} = \Phi^N - \Phi^H = E^{N,\circ} + \frac{RT}{F} \ln \frac{a^N_{V^{3+}}}{a^H_{H^+} a^N_{V^{2+}}} \tag{4.44}$$

with standard electrode potential equal to

$$E^{N,\circ} = \frac{1}{F} \left(\mu^\circ_{V^{3+}} - \mu^\circ_{V^{2+}} \right) = -0.256V \tag{4.45}$$

because

$$\Delta_f G_{V^{3+}} = -242kJ/mol \text{ and } \Delta_f G_{V^{2+}} = -218kJ/mol \tag{4.46}$$

according to [40]. This value of standard electrode potential is compatible with the commonly used standard electrode potential of the negative electrode from [17]. Note that activity of protons in the negative half-cell is present in the formula (4.44) instead of activity in the positive half-cell because the condition

$$\tilde{\mu}^N_{H^+} = \tilde{\mu}^H_{H^+} \tag{4.47}$$

was used in order to get rid of the Maxwell potential difference, see 3.1.1.

Final form of Nernst relation

Now we are in a position to write down the final form of Nernst relation for the whole VRFB

$$E = \Phi^P - \Phi^N = E^{P,H} - E^{N,H} = E^{P,\circ} - E^{N,\circ} + \frac{RT}{F} \ln \frac{a^P_{VO^+_2} a^N_{V^{2+}} a^N_{H^+}}{a^P_{VO^{2+}} a^N_{V^{3+}} a^P_{OH^-}}. \tag{4.48}$$

Assuming all activity coefficients equal to 1, this formula becomes

$$E = E^{P,\circ} - E^{N,\circ} + \frac{RT}{F} \ln \frac{b^P_{VO^+_2} b^N_{V^{2+}} b^N_{H^+}}{b^P_{VO^{2+}} b^N_{V^{3+}} b^P_{OH^-}} \tag{4.49}$$

where b_α is molality of species α, see formula (3.9). Formula (4.49) can be easily plotted against SOC and compared with experimental data.

Using equation (4.42) instead of equation (4.38), the formula for OCV becomes

$$E = E^\circ_{H_2O} + \frac{RT}{F} \ln \frac{a^P_{VO^+_2} a^N_{V^{2+}} a^P_{H^+} a^N_{H^+}}{a^P_{VO^{2+}} a^N_{V^{3+}} a^P_{H_2O}} \tag{4.50}$$

where the reference electrode potential is defined as

$$E^\circ_{H_2O} = E^{P,\circ}_{H_2O} - E^{N,\circ}. \tag{4.51}$$

Formula (4.50) is close to the commonly used Nernst relations, e.g. [51], but it still differs. Firstly, it contains activity of water in the positive half-cell, which has not been considered to best of author's knowledge in the literature so far. However, the activity does not vary much during charging the battery as can

be easily calculated (when approximating the activity coefficients by unity), and this term does not affect the resulting dependence of OCV on SOC appreciably. Secondly, instead of square of proton activity in the positive half-cell, see [51], the Nernst relation contains activity of protons in the positive half-cell and negative half-cell, which already makes appreciable difference as shown in Section 4.2.2. Finally, assuming all activity coefficients equal to one, formula (4.50) becomes

$$E = E^{\circ}_{H_2O} + \frac{RT}{F} \ln \frac{b^P_{VO_2^+} b^N_{V^{2+}} b^P_{H^+} b^N_{H^+}}{b^P_{VO^{2+}} b^N_{V^{3+}} b^P_{H_2O} b^{\circ}}. \tag{4.52}$$

Both equations (4.48) and (4.50) are precise in the sense that they hold exactly for steady state VRFB with disconnected external circuit. In particular, there is no way how to incorporate any other activities into the equations because otherwise the formulas would not be consistent with thermodynamics. The only thing that can and has to be tuned now are expressions for the activity coefficients. In other words, all discrepancies between plots of formulas (4.48) or (4.50) and experimental data should be caused only by using imperfect expressions for the activity coefficients or inaccurate experimental measurements. Note also that both formulas (4.48) and (4.50) are equivalent. Note also that formula (4.50) can be derived straightforwardly by setting affinities of reactions (4.21) and (4.22) equal to zero and by using condition (B.15). This more direct approach is followed in Section 4.2.3.

What makes the difference?

In this section the differences between the usual Nernst relation (4.20) and the relation implied by thermodynamics (4.50) are discussed and Eq. (4.50) is derived in a shorter way than in the preceding sections.

Let us start with the shorter derivation. Eq. (4.28) simply expresses that the steady state where no reactions take place has been reached. At first glance it may seem that there should be a term with $\left(a^P_{H^+}\right)^2$ in the final form of the Nernst relation because that is what comes from the term $2\tilde{\mu}^P_{H^+}$ after expansion (3.9). But let us expand the other terms in the equation as well. After expanding all terms in Eq. (4.28) according to (3.9), the equation becomes

$$E = E^{\circ}_{H_2O} + \frac{RT}{F} \ln \left(\frac{a^P_{VO_2^+} a^N_{V^{2+}}}{a^P_{VO^{2+}} a^N_{V^{3+}}} \frac{\left(a^P_{H^+}\right)^2}{a^P_{H_2O}} \right) + \varphi^P - \varphi^N. \tag{4.53}$$

Except for the last term this equation provides a relation between OCV and activities of the species in the electrolytes. Let us, therefore, have a look at the last term. Using the condition of equilibrium (4.29), one obtains that

$$\varphi^P - \varphi^N = \frac{RT}{F} \ln \frac{a^N_{H^+}}{a^P_{H^+}}, \tag{4.54}$$

and thus Eq. (4.53) transforms to Eq. (4.50).

In summary, the final form of the Nernst relation (4.48) or (4.50) can be derived directly from the steady state condition (4.28), and the difference between the usual Nernst relation and the relation implied by thermodynamics stems from taking into account the Maxwell potentials in both electrolytes properly.

Debye-Hückel

In Eq. (4.52) all activity coefficients were neglected. One can ask the question whether this assumption is correct or not. Let us, for simplicity, assess the influence of the assumption by approximating activity of protons in the positive electrolyte by Debye-Hückel theory with ionic strength calculated from molalities of protons, hydroxyl anions and bisulphates in the positive half-cell. Following [70], the OCV is equal to

$$E_{D.-H.} = E + E_{corr} \tag{4.55}$$

where E is the ideal OCV, given by (4.48), and the correction term is equal to

$$E_{corr} = \frac{RT}{F} A\sqrt{I} \tag{4.56}$$

where $A = 1.17$ for aqueous solutions and ionic strength I is calculated as

$$I = \frac{1}{2}\left(\left(\frac{b^P_{OH^-}}{b^\circ}\right)^2 + \left(\frac{b^P_{H+}}{b^\circ}\right)^2 + \left(\frac{b^P_{HSO_4^-}}{b^\circ}\right)^2\right). \tag{4.57}$$

Formula (4.55) is compared with formula (4.49) in figure 4.4. Note that this correction only picks a part of the correction predicted by the Debye-Hückel theory. The problem is that it is assumed in the theory that neutral molecules dissociate to one cation and one anion, which is not true for example for $V_2(SO_4)_3$. Therefore, only a piece of the theory was used in order to show that corrections to the activity coefficients may indeed improve the agreement with experimental data considerably.

Comparison with experimental data

In this section formula (4.52) is compared with our experimental results, see figure 4.3. In order to accomplish this, molalities present in the formula have to be expressed as function of SOC as indicated in Section B.1.1. Deviations of

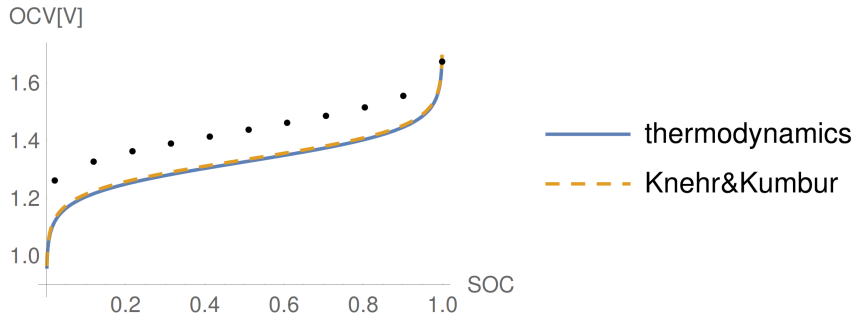

Figure 4.3: Comparison of the thermodynamic formula (4.52) (the curve *thermodynamics*), the usual formula (4.20) from [51] (with concentrations replaced by molalities) and our experimental data. Both the formulas clearly coincide while underestimating the OCV.

the theoretical curve from the experimental results are caused by neglecting the

activity coefficients. Indeed, including activity coefficients obtained by Debye-Hückel theory significantly improves agreement between formula (4.48) and the experimental data as shown in figure 4.4 below. It should be borne in mind that formula (4.50) is completely equivalent to formula (4.48). Since the latter formula contains less activity coefficients, we prefer to include the activity coefficients into the latter formula.

OCV with the Debye-Hückel correction, Eq. (4.55), is compared with the original formula (4.49) and experimental data in figure 4.4.

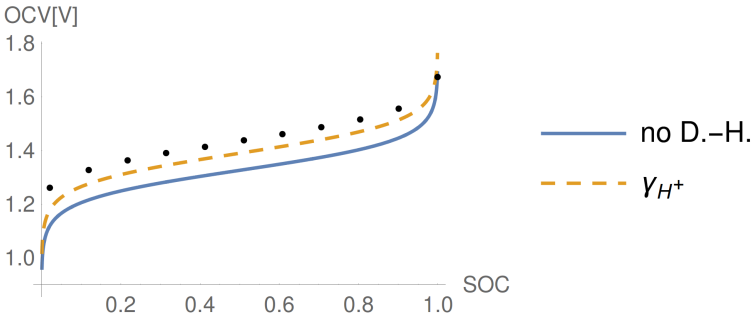

Figure 4.4: Comparison of formula (4.49), where all activity coefficients are neglected (lower curve) and formula (4.55), where activity coefficient of protons in the positive electrolyte was estimated by the Debye-Hückel theory.

Correction (4.55) obviously improves agreement with the experiment. Knehr and Kumbur [51] suggest improving the formula for OCV by adding a term referred to as the Donnan potential. This term, however, provides only a rather minute correction to the OCV in our case since it affects the final OCV by less than $0.02V$.

In summary, the thermodynamic formula for OCV without activity coefficients, Eq. (4.49) or Eq. (4.52), describes the experimental data as well as for example the formula proposed in [51] (either with the Donnan potential or without). It is shown, however, that activity coefficients can improve agreement with experiments considerably which emphasizes the importance of evaluation of the activity coefficients for more precise quantification of OCV as a function of SOC. In fact, the activity coefficients may be calculated by fitting formula (4.50) to the experimental OCV curves. The advantage of formula (4.49) is that the deviation between OCV predicted by this formula and experimental data can only be caused by neglecting the activity coefficients, which should be included according to formula (4.48) or (4.50).

4.2.3 Anex membranes

Nernst relation

In this section we calculate OCV of a VRFB with an anex membrane. The difference between the analysis for catex membranes is that instead of condition (4.29), one has

$$\tilde{\mu}^P_{HSO_4^-} = \tilde{\mu}^N_{HSO_4^-}, \tag{4.58}$$

which can be rewritten, using (3.9), as

$$\varphi^P - \varphi^N = \frac{RT}{F} \ln \frac{a^P_{HSO_4^-}}{a^N_{HSO_4^-}}. \tag{4.59}$$

OCV from formula (4.28) then becomes

$$E = E^\circ_{H_2O} + \frac{RT}{F} \ln \frac{a^P_{VO_2^+}(a^P_{H^+})^2 a^N_{V^{2+}} a^P_{HSO_4^-}}{a^P_{VO^{2+}} a^P_{H_2O} a^N_{V^{3+}} a^N_{HSO_4^-}}, \tag{4.60}$$

which is different from formula (4.50) for catex membranes in general.

Comparison with catex membranes

Let us now compare formula (4.60) with formula (4.50), which gives OCV for a battery with a catex membrane. To do so, one has to find composition of electrolytes as a function of SOC. This function will be different than in the case of catex membrane because bisulphates pass through the membrane instead of protons, see Sec. B.1.1. Assuming activity coefficients equal to unity, the two formulas for OCV can now be compared quantitatively, see figure 4.5. In order to validate the comparison, we have conducted our own experimental measurement of OCV of a VRFB with an anex membrane [99] (dots on figure 4.5), see Appendix B.1.1 for details. The experimental results are represented by dots in figure 4.5.

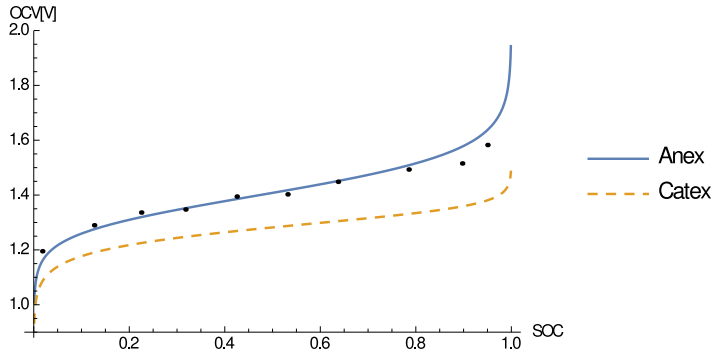

Figure 4.5: Comparison of OCV during charging VRFB with an anex membrane and with an catex membrane, formulas (4.50) and (4.60) and our experimental results. Both batteries start with the same composition specified above. Both curves are clearly different. Formula (4.60) clearly desribes the experimental data (dots) better.

In summary, VRFBs with anex membranes exhibit neither the same dependence of OCV on SOC nor the same composition of electrolytes during the charging process as VRFBs with catex membranes, and the formula for anex membranes (4.60) describes experiments with anex membranes better than the corresponding formula for batteries with catex membranes (4.50). It is, therefore, important to distinguish between the formulas for OCV for anex membranes and catex membranes.

4.2.4 Discussion

OCV of VRFBs as a function of SOC has been calculated many times any many different Nernst relations have been proposed. To our best knowledge, none of the forms of Nernst relation is compatible with formulas (4.48), (4.50) and (4.60) and so none of the preceding Nernst relations known from the literature can be considered compatible with thermodynamics.

Knehr and Kumbur [51] propose a formula, which differs from (4.50) in the terms expressing molalities of protons, and thus is not consistent with thermodynamics. Moreover, they did not take into account activity of water (which is, however, near to unity for experimental setup from [39]). To obtain better agreement with experimental data they also proposed that sulphuric acid almost completely dissociates into protons and SO_4^{2-} ions, which is unlikely since gradients of electric potential in VRFB are not high enough. Indeed, intensity of electric field has to be of order of $10^6 V/m$ in order to alter dissociation appreciately, see [74]. Moreover, neither the Donnan potential suggested therein makes the Nernst relation compatible with thermodynamics.

Corcuera and Skyllas-Kazacos [26] also presented a Nernst relation, where as well as in the previous case concentrations of hydrogen were not treated properly. Indeed, the relation should contain a product of concentration of protons in the positive half-cell and concentration of protons in the negative half-cell instead of just square of concentration of protons in the positive half-cell. The same is true for [90, 42, 23].

4.2.5 Conclusion

Open circuit voltage in VRFB was calculated as a function of states-of-charge by means of equilibrium thermodynamics. The result was compared with our experiments showing good agreement between the theory and experimental data. The advantage of this thermodynamic calculation is that there is no uncertainty in formula for OCV (4.48), which is written in terms of activities, and all deviations from experimental data are then caused by imperfect expressions of activity coefficients. An approximation of activity coefficients by Debye-Hückel theory is shown to provide better agreement with experimental data.

Moreover, it is shown that batteries with catex membranes follow different Nernst relation than batteries with anex membranes. This difference is caused by different conditions for equilibrium of the species transported through the membranes (protons or bisulphates). These two forms of Nernst relation are compared, and it is showed that indeed the anex form describes experiments with anex membranes better than the corresponding formula for catex membranes.

Conclusion

Let us now recall the problems stated in the introduction and how the thesis contributes to solving the problems.

- *Which processes are reversible and which irreversible? And how does non-equilibrium thermodynamics describe these two kinds of processes?*

  A method for splitting evolution equations into reversible and irreversible parts is developed in Chap. 1. The splitting is based on behavior of the evolution equations with respect to the time-reversal transformation (TRT). Reversible evolution is such that it is not altered by TRT while direction of the irreversible evolution is reversed.

  Dissipation potential is shown to generate only irreversible evolution, see Lemma 3, while a hierarchy of Poisson brackets is identified in Sec. A.2, which generates only reversible evolution. However, an open problem remains whether any Poisson bracket describing a real system is part of the hierarchy.

- *Can Onsager-Casimir reciprocal relations (OCRR) be derived from non-equilibrium thermodynamics?*

  OCRR are shown to be a near-global equilibrium implication of GENERIC, see Sec. 1.1.4, and GENERIC itself can be then considered as the far from equilibrium generalization of OCRR.

- *Once reversible dynamics on a more detailed level of description is known, is it possible to derive reversible dynamics on a lower level?*

  The hierarchy of Poisson brackets identified in Sec. A.2 provides a means how to derive the reversible evolution on the lower level of description.

- *How to describe processes in electrochemistry within thermodynamics efficiently?*

  Electrochemical reactions and diffusion processes can be described on the level of mechanical equilibrium. Sec. 3.1 contains a thermodynamic formulation of transport processes in porous media, and Sec. 3.2 contains a thermodynamic formulation of electrochemical reactions. The level of mechanical equilibrium provides a unifying framework where all these processes are incorporated within non-equilibrium thermodynamics.

- *Absorption of water into Nafion membranes is much slower than desorption from the membranes. What is the reason?*

  This asymmetry is explained in Sec. 3.4, where experimental sorption results are predicted quantitatively. The reason for the asymmetry is the nonlinear dependence of water uptake on water activity as elucidated in Sec. 3.4.9. It is worth noting that the only physics involved in the sorption model is balance of mass of water accompanied with experimental dependencies of equilibrium water uptake and swelling strain on water activity.

- *How does the coupling between water and proton transport in fuel cells affect the resulting I/V curve?*

  As shown in Fig. 3.5, the coupling affects the slope of the I/V curve while it does not affect the limiting current.

- *Consider a device producing electricity, e.g. a fuel cell. When having a continuous thermodynamic model of the device, is it possible to show where and how much of efficiency is being lost?*

  Although the standard exergy analysis, which identifies the losses of useful work with entropy production rate, might seem to be answering that question, it is shown in Sec. 3.6 that there is an assumption inherently incorporated into the standard exergy analysis, which restricts validity of the theory if boundary of the device is not isothermal. Subsequently, in Sec. 3.7 a generalization of exergy analysis is proposed within non-equilibrium thermodynamics on the level of mechanical equilibrium. The generalized theory is equivalent with the standard exergy analysis when boundary of the device is isothermal. If not, however, the difference between the generalized theory and the standard theory is demonstrated on a toy model of non-isothermal solid oxide fuel cells in Sec. 3.7.2. Moreover, various losses of useful work are demonstrated in isothermal polymer-electrolyte membrane fuel cells in Sec. 3.7.1. Finally, it is shown in our paper [79] that both theories are equivalent when describing heat engines while the generalized theory provides new insight into efficiency analysis of saline power plants.

  The outcome of the generalized theory is a map of losses indicating where exactly and how much useful work is lost. This method could has the potential to become crucial in optimization of power generating devices.

- *What is the open circuit voltage (OCV) of a vanadium redox flow battery (VRFB) at different states of charge?*

  The formulation of electrochemical processes within non-equilibrium thermodynamics in Sec. 3.1 provides theoretical background for derivation of the open circuit voltage in Sec. 4.2. Although the dependence of OCV on the state of charge has been published many times in various non-equivalent forms, our result seems to be the first thermodynamically consistent derivation.

- *What is the meaning of partial pressures in a mixture of non-ideal fluids?*

  In our paper [81], which is reviewed in Sec. A.3 briefly, a formula for partial pressure is derived, which is equivalent to a formula suggested by Samohýl et al. [87].

In summary, the non-equilibrium thermodynamic framework used and partially developed in this thesis provides means of efficient description of processes in electricity producing devices. The generalization of exergy analysis may become a very useful method in optimization of such devices. It is our future goal to apply the theory to real fuel cells and to compare results of the theory with experiments. To this end it is necessary to develop precise enough thermodynamic models of the devices, and that is the reason why effort is spent on the general

theory of non-equilibrium thermodynamics. The theory of non-equilibrium thermodynamics thus stands side by side with optimization of industrial electricity producing devices this way.

Bibliography

[1] Nafion® membranes, extrusion-cast. `http://www2.dupont.com/FuelCells/en_US/assets/downloads/dfc101.pdf`. Accessed: 2015-01-27.

[2] Abraham, R., and Marsden, J. E. *Foundations of Mechanics*. AMS Chelsea publishing. AMS Chelsea Pub./American Mathematical Society, 1978.

[3] Andersson, M., Yuan, J., and Sunden, B. Review on modeling development for multiscale chemical reactions coupled transport phenomena in solid oxide fuel cells. *Applied Energy 87*, 5 (MAY 2010), 1461–1476.

[4] Angrist, S. W., and Helper, L. G. *Order and Chaos - Laws of Energy and Entropy*. New York: Basic Books, 1967.

[5] Atkins, P., and De Paula, J. *Atkins' Physical Chemistry*. Oxford University Press, 2002.

[6] Balmer, R. *Modern Engineering Thermodynamics*. Elsevier Science, 2011.

[7] Barbir, F. *Pem Fuel Cells: Theory And Practice*. Academic Press Sustainable World Series. Elsevier Acad. Press, 2005.

[8] Bard, A., and Faulkner, L. *Electrochemical Methods: Fundamentals and Applications*. Wiley, 2000.

[9] Bearman, R. On Molecular Basis of Some Current Theories of Diffusion. *Journal of Physical Chemistry 65*, 11 (1961), 1961–1968.

[10] Bejan, A. Entropy generation minimization: The new thermodynamics of finite size devices and finite time processes. *Journal of Applied Physics 79*, 3 (1996), 1191–1218.

[11] Bejan, A. Fundamentals of exergy analysis, entropy generation minimization, and the generation of flow architecture. *International Journal of Energy Research 26*, 7, SI (JUN 10 2002), 545–565.

[12] Bejan, A., Tsatsaronis, G., and Moran, M. *Thermal Design and Optimization*. Wiley-Interscience publication. Wiley, 1996.

[13] Benziger, J., Bocarsly, A., Cheah, M. J., Majsztrik, P., Satterfield, B., and Zhao, Q. Mechanical and transport properties of nafion: Effects of temperature and water activity. *Struct Bond 141* (2011), 85–113.

[14] Benziger, J., Kimball, E., Mejia-Ariza, R., and Kevrekidis, I. Oxygen Mass Transport Limitations at the Cathode of Polymer Electrolyte Membrane Fuel Cells. *AIChE Journal 57*, 9 (SEP 2011), 2505–2517.

[15] Biesheuvel, P. M., van Soestbergen, M., and Bazant, M. Z. Imposed currents in galvanic cells. *Electrochimica Acta 54*, 21 (AUG 30 2009), 4857–4871.

[16] Bothe, D., and Dreyer, W. Continuum thermodynamics of chemically reacting fluid mixtures. *ArXiv e-prints* (2014).

[17] Bratsch, S. Standard electrode-potentials and temperature coefficients in water at 298.15-K. *Journal of Physical and Chemical Reference Data 18*, 1 (1989), 1–21.

[18] Butler, J. A. V. Studies in heterogeneous equilibria. part ii. the kinetic interpretation of the nernst theory of electromotive force. *Trans. Faraday Society 19* (1924), 729–733.

[19] Callen, H. *Thermodynamics: an introduction to the physical theories of equilibrium thermostatics and irreversible thermodynamics*. Wiley, 1960.

[20] Casimir, H. B. G. On Onsager's principle of microscopic reversibility. *Rev. Mod. Phys. 17* (Apr 1945), 343–350.

[21] Chase, W. *NIST-JANAF Thermochemical Tables*. Journal of physical and chemical reference data: Monograph. American Chemical Society, 1998.

[22] Cheah, M. J., Kevrekidis, I. G., and Benziger, J. Effect of Interfacial Water Transport Resistance on Coupled Proton and Water Transport Across Nafion. *Journal of Physical Chemistry B 115*, 34 (SEP 1 2011), 10239–10250.

[23] Chen, C. L., Yeoh, H. K., and Chakrabarti, M. H. An enhancement to Vynnycky's model for the all-vanadium redox flow battery. *Electrochimica Acta 120* (FEB 20 2014), 167–179.

[24] Chen, F. *Introduction to plasma physics*. Plenum Press, 1974.

[25] Choi, P., Jalani, N. H., and Datta, R. Thermodynamics and proton transport in Nafion: Ii. proton diffusion mechanisms and conductivity. *Journal of The Electrochemical Society 152*, 3 (2005), E123–E130.

[26] Corcuera, S., and Skyllas-Kazacos, M. State-of-charge monitoring and electrolyte rebalancing methods for the vanadium redox flow battery. *European Chemical Bulletin 1*, 12 (2012).

[27] Crank, J. *The Mathematics of Diffusion*. Oxford science publications. Clarendon Press, 1979.

[28] de Groot, S. R., and Mazur, P. *Non-equilibrium Thermodynamics*. Dover Publications, New York, 1984.

[29] Elfring, G. J., and Struchtrup, H. Thermodynamic considerations on the stability of water in Nafion. *Journal of Membrane Science 297*, 1–2 (2007), 190 – 198.

[30] Erdey-Gruz, T., and Volmer, M. Zur theorie der wasserstoffüberspannung. *Z. Phys. Chem. 150 (A)* (1930), 203–213.

[31] Evans, L. *Partial Differential Equations*. Graduate studies in mathematics. American Mathematical Society, 1998.

[32] Fecko, M. *Differential Geometry and Lie Groups for Physicists*. Cambridge University Press, 2006.

[33] Fletcher, S. Tafel slopes from first principles. *Journal of Solid State Electrochemistry 13*, 4 (APR 2009), 537–549.

[34] Freger, V. Hydration of ionomers and Schroeder's paradox in Nafion. *The Journal of Physical Chemistry B 113*, 1 (2009), 24–36.

[35] Grmela, M. Reciprocity relations in thermodynamics. *Physica A: Statistical Mechanics and its Applications 309*, 3 (2002), 304–328.

[36] Grmela, M. Fluctuations in extended mass-action-law dynamics. *Physica D Nonlinear Phenomena 241* (May 2012), 976–986.

[37] Grmela, M. Contact Geometry of Mesoscopic Thermodynamics and Dynamics. *Entropy 16*, 3 (MAR 2014), 1652–1686.

[38] Grmela, M., and Öttinger, H. C. Dynamics and thermodynamics of complex fluids. i. development of a general formalism. *Phys. Rev. E 56* (Dec 1997), 6620–6632.

[39] Heintz, A., and Illenberger, C. Thermodynamics of Vanadium redox flow batteries electrochemical and calorimetric investigations. *Berichte der Bunsen-Gesellschaft-Physical Chemistry Chemical Physics 102*, 10 (OCT 1998), 1401–1409.

[40] Hill, J., Worsley, I., and Hepler, L. Thermochemistry and oxidation potentials of vanadium, niobium, and tantalum. *Chemical Reviews 71*, 1 (1971), 127–&.

[41] Hirschfelder, J., Curtiss, C., Bird, R., and of Wisconsin. Theoretical Chemistry Laboratory, U. *Molecular theory of gases and liquids*. Structure of matter series. Wiley, 1954.

[42] Hudak, N. S. Practical thermodynamic quantities for aqueous vanadium- and iron-based flow batteries. *Journal of Power Sources 269* (DEC 10 2014), 962–974.

[43] Hurley, J., and Garrod, C. Generalization of the Onsager reciprocity theorem. *Physical Review Letters 48*, 23 (1982), 1575.

[44] ISHIDA, M., ZHENG, D., and AKEHATA, T. Evaluation of a chemical-looping-combustion power-generation system by graphic exergy analysis. *Energy 12*, 2 (FEB 1987), 147–154.

[45] Jeck, S., Scharfer, P., and Kind, M. Absence of Schroeder's paradox: Experimental evidence for water-swollen Nafion®membranes. *Journal of Membrane Science 373*, 1-2 (2011), 74–79.

[46] Jou, D., Casas-Vázquez, J., and Lebon, G. *Extended Irreversible Thermodynamics*, 4th ed. Springer-Verlag, New York, 2010.

[47] Kampen, N. V. Quantum statistics of irreversible processes. *Physica 20*, 1–6 (1954), 603 – 622.

[48] Kjelstrup, S., and Bedeaux, D. *Non-Equilibrium Thermodynamics of Heterogeneous Systems*. Series on Advances in Statistical Mechanics. World Scientific, 2008.

[49] Kjelstrup, S., Bedeaux, D., and Johannessen, E. *Non-Equilibrium Thermodynamics for Engineers*. Science and culture series (Singapore).: Physics. World Scientific, 2010.

[50] Kjelstrup, S., and Røsjorde, A. Local and total entropy production and heat and water fluxes in a one-dimensional polymer electrolyte fuel cell. *The Journal of Physical Chemistry B 109*, 18 (2005), 9020–9033. PMID: 16852075.

[51] Knehr, K. W., and Kumbur, E. C. Open circuit voltage of vanadium redox flow batteries: Discrepancy between models and experiments. *Electrochemistry Communications 13*, 4 (APR 2011), 342–345.

[52] Krishna, R., and Wesselingh, J. Review article number 50 - The Maxwell-Stefan approach to mass transfer. *Chemical Engineering Science 52*, 6 (MAR 1997), 861–911.

[53] Landau, L., and Lifschitz, E. *Statistical physics*. No. pt. 1 in Course of theoretical physics. Pergamon Press, 1969.

[54] Landau, L., and Lifshitz, E. *Mechanics*. Butterworth Heinemann. Butterworth-Heinemann, 1976.

[55] Lebon, G., Jou, D., and Vázquez, J. *Understanding Non-Equilibrium Thermodynamics: Foundations, Applications, Frontiers*. SpringerLink: Springer e-Books. Springer London, Limited, 2008.

[56] Logg, A., Mardal, K.-A., Wells, G. N., et al. *Automated Solution of Differential Equations by the Finite Element Method*. Springer, 2012.

[57] Maes, C., and Netočný, K. Time-reversal and entropy. *eprint arXiv:cond-mat/0202501* (2002).

[58] Maginn, E., Bell, A., and Theodorou, D. Transport Diffusivity of Methane in Silicalite from Equilibrium and Nonequilibrium Simulations. *Journal of Physical Chemistry 97*, 16 (APR 22 1993), 4173–4181.

[59] Majsztrik, P. W., Satterfield, M. B., Bocarsly, A. B., and Benziger, J. B. Water sorption, desorption and transport in Nafion membranes. *Journal of Membrane Science 301*, 1-2 (SEP 1 2007), 93–106.

[60] Marsden, J., and Weinstein, A. The Hamiltonian-Structure of the Maxwell-Vlasov Equations. *Physica D 4*, 3 (1982), 394–406.

[61] Maršík, F., and Dvořák, I. *Biotermodynamika*. Academia, 1998. In Czech.

[62] Mason, E., and Malinauskas, A. *Gas transport in porous media: the dusty-gas model*. No. v. 17 in Chemical engineering monographs. Elsevier, 1983.

[63] Mauritz, K. A., and Moore, R. B. State of understanding of Nafion. *Chemical Reviews 104*, 10 (2004), 4535–4586.

[64] Meixner, J. Zur Thermodynamik der irreversiblen Prozesse in Gasen mit chemisch reagierenden, dissoziierenden und anregbaren Komponenten. *Annalen der Physik 43*, 5 (1943), 244–270.

[65] Meixner, J., and Reik, H. *Thermodynamik der Irreversible Prozesse, in Handbuch der Physik*, vol. 3/II. Springer, Berlin Heidelberg New York, 1959.

[66] Mielke, A. Formulation of thermoelastic dissipative material behavior using GENERIC. *Continuum Mechanics and Thermodynamics 23*, 3 (MAY 2011), 233–256.

[67] Monroe, C. W., Romero, T., Merida, W., and Eikerling, M. *J. Membr. Sci. 324*, 1 (2008).

[68] Müller, I., and Ruggeri, T. *Rational extended thermodynamics*. Springer tracts in natural philosophy. Springer, 1998.

[69] Muschik, W. A phenomenological foundation of non-linear OC-reciprocal relations (irreversible thermodynamics approach). *Periodica polytechnica. Chemical engineering 42*, 2 (1998), 85–96.

[70] Newman, J., and Thomas-Alyea, K. *Electrochemical Systems*. Electrochemical Society series. Wiley, 2004.

[71] Ni, M., Leung, M. K. H., and Leung, D. Y. C. Mathematical modeling of the coupled transport and electrochemical reactions in solid oxide steam electrolyzer for hydrogen production. *Electrochimica Acta 52*, 24 (AUG 1 2007), 6707–6718.

[72] Onsager, L. Reciprocal relations in irreversible processes. I. *Phys. Rev. 37* (Feb 1931), 405–426.

[73] Onsager, L. Reciprocal relations in irreversible processes. ii. *Phys. Rev. 38* (Dec 1931), 2265–2279.

[74] Onsager, L. Deviations from Ohm's law in weak electrolytes. *The Journal of Chemical Physics 2*, 9 (1934), 599–615.

[75] Öttinger, H. *Beyond Equilibrium Thermodynamics*. Wiley, 2005.

[76] Öttinger, H. C. Constraints in nonequilibrium thermodynamics: General framework and application to multicomponent diffusion. *Journal of chemical physics 130*, 11 (MAR 21 2009).

[77] Öttinger, H. C., and Grmela, M. Dynamics and thermodynamics of complex fluids. ii. illustrations of a general formalism. *Phys. Rev. E 56* (Dec 1997), 6633–6655.

[78] Pavelka, M., Klika, V., and Grmela, M. Time reversal in nonequilibrium thermodynamics. *Phys. Rev. E 90* (Dec 2014), 062131.

[79] Pavelka, M., Klika, V., Vágner, P., and Maršík, F. Generalization of exergy analysis. *Applied Energy 137*, 0 (2015), 158 – 172.

[80] Pavelka, M., and Maršík, F. Detailed thermodynamic analysis of polymer electrolyte membrane fuel cell efficiency. *International Journal of Hydrogen Energy 38*, 17 (2013), 7102–7113.

[81] Pavelka, M., Maršík, F., and Klika, V. Consistent theory of mixtures on different levels of description. *International Journal of Engineering Science 78*, 0 (2014), 192 – 217.

[82] Pavelka, M., Mazur, P., and Wandschneider, F. Thermodynamic derivation of open circuit voltage in vanadium redox flow batteries. *Journal of Power Sources* (2015). Submitted.

[83] Prigogine, I. *Thermodynamics of Irreversible Processes*. Thomas, 1955.

[84] Renardy, M., and Rogers, R. *An Introduction to Partial Differential Equations*. Texts in Applied Mathematics. Springer, 2004.

[85] Rubi, J. M., and Kjelstrup, S. Mesoscopic nonequilibrium thermodynamics gives the same thermodynamic basis to Butler-Volmer and nernst equations. *The Journal of Physical Chemistry B 107*, 48 (2003), 13471–13477.

[86] Sadeghi, E., Putz, A., and Eikerling, M. Hierarchical model of reaction rate distributions and effectiveness factors in catalyst layers of polymer electrolyte fuel cells. *Journal of the Electrochemical Society 160*, 10 (2013), F1159–F1169.

[87] Samohýl, V., Samohýl, I., and Voňka, P. Partial pressures in thermodynamics of classical fluid mixtures. *Acta Chimica Slovaca 5*, 1 (2012), 29–36.

[88] Satterfield, M. B., and Benziger, J. B. Non-fickian water vapor sorption dynamics by Nafion membranes. *The Journal of Physical Chemistry B 112*, 12 (2008), 3693–3704. PMID: 18314970.

[89] Springer, T., Zawodzinski, T., and Gottesfeld, S. Polymer Electrolyte Fuel-Cell Model. *Journal of the Electrochemical Society 138*, 8 (AUG 1991), 2334–2342.

[90] Sukkar, T., and Skyllas-Kazacos, M. Water transfer behaviour across cation exchange membranes in the vanadium redox battery. *Journal of Membrane Science 222*, 1-2 (SEP 1 2003), 235–247.

[91] Sum, E., Rychcik, M., and Skyllas-Kazacos, M. Investigation of the V(V)/V(IV) system for use in the positive half-cell of a redox battery. *Journal of Power Sources 16*, 2 (OCT 1985), 85–95.

[92] Sum, E., and Skyllas-Kazacos, M. A study of the V(II)/V(III) redox couple for redox flow cell applications. *Journal of Power Sources 15*, 2-3 (1985), 179–190.

[93] Sun, C., Chen, J., Zhang, H., Han, X., and Luo, Q. Investigations on transfer of water and vanadium ions across Nafion membrane in an operating vanadium redox flow battery. *Journal of Power Sources 195*, 3 (FEB 1 2010), 890–897.

[94] Vágner, P. Physical analysis of the main processes in the solid oxide fuel cells and their mathematical description. Master's thesis, Faculty of Mathematics and Physics, Charles University in Prague, Czech Republic, 2014.

[95] Vrentas, J., and Duda, J. Diffusion in Polymer - Solvent Systems .1. Re-Examination of Free-Volume Theory. *Journal of Polymer Science Part B-Polymer Physics 15*, 3 (1977), 403–416.

[96] Vrentas, J., and Duda, J. Diffusion in Polymer-Solvent Systems .2. Predictive Theory for Dependence of Diffusion-Coefficients on Temperature, Concentration, and Molecular-Weight. *Journal of Polymer Science Part B-Polymer Physics 15*, 3 (1977), 417–439.

[97] Wagman, D., Evans, W., Parker, V., Schumm, R., Halow, I., Bailey, S., Churney, K., and Nuttall, R. The NBS tables of chemical thermodynamic properties - selected values for inorganic and C-1 and C-2 organic-substances in si units. *Journal of Physical and Chemical Reference Data 11*, 2 (1982), 1–&.

[98] Waldram, J. *The Theory of Thermodynamics*. Cambridge University Press, 1985.

[99] Wandschneider, F. T., Finke, D., Grosjean, S., Fischer, P., Pinkwart, K., Tuebke, J., and Nirschl, H. Model of a vanadium redox flow battery with an anion exchange membrane and a Larminie-correction. *Journal of Power Sources 272* (DEC 25 2014), 436–447.

[100] Weber, A. Z., and Newman, J. *J. Electrochem. Soc. 150*, 7 (2003), A1008–A1015.

[101] Zhang, J. *PEM Fuel Cell Electrocatalysts and Catalyst Layers: Fundamentals and Applications*. Springer-Verlag, 2008.

[102] Zhao, Q., Majsztrik, P., and Benziger, J. Diffusion and interfacial transport of water in Nafion. *The Journal of Physical Chemistry B 115*, 12 (2011), 2717–2727.

[103] Zwanzig, R. *Nonequilibrium Statistical Mechanics*. Oxford University Press, USA, 2001.

List of Tables

List of Abbreviations

GENERIC	...	General equation for the nonequilibrium reversible-irreversible coupling
CIT	...	Classical Irreversible Thermodynamics
EIT	...	Extended Irreversible Thermodynamics
TRT	...	time-reversal transformation
OCRR	...	Onsager-Casimir reciprocity relations
STR	...	stirred tank reactor
PEM	...	polymer-electrolyte membrane
FC	...	fuel cell
ACL	...	anode catalyst layer
CCL	...	cathode catalyst layer
AC	...	anode channel
CC	...	cathode channel
MoL	...	map of losses
SOFC	...	solid oxide fuel cell
OCV	...	open-circuit voltage
VRFB	...	vanadium redox flow battery
SOC	...	state of charge

Attachments

A. Another levels of description

A.1 Boltzmann equation

Boltzmann equation, which describes evolution of dilute gases, can be regarded as a prototype of an evolution equation combining both reversible and irreversible processes. Therefore, it is illustrative to formulate it within non-equilibrium thermodynamics. The purpose of this section is to demonstrate the notion of reversibility and irreversibility on the Boltzmann equation and to elucidate how the irreversible part may be formulated by means of a dissipation potential.

Boltzmann equation is an evolution equation for the field of probability density $f(\mathbf{r}, \mathbf{v})$, and the field constitutes the state variables on the Boltzmann level of description. In accordance with [38], Boltzmann equation can be written as

$$\frac{\partial f(\mathbf{r}, \mathbf{v})}{\partial t} = \int \mathrm{d}\mathbf{r}' \, \mathrm{d}\mathbf{v}' L(\mathbf{r}, \mathbf{v}, \mathbf{r}', \mathbf{v}') \frac{\delta E}{\delta f(\mathbf{r}', \mathbf{v}')} + \frac{\delta \Xi}{\delta \frac{\delta S}{\delta f(\mathbf{r}, \mathbf{v})}} \tag{A.1}$$

within the GENERIC framework. The Poisson bivector, the dissipation potential, energy and entropy are specified in the two following sections.

A.1.1 Reversible evolution

In accordance with [38], the Poisson bivector field is given by

$$L(\mathbf{r}, \mathbf{v}, \mathbf{r}', \mathbf{v}') = \frac{1}{m} \left(\frac{\partial \delta_{\mathbf{v}}}{\partial v'_\gamma} \frac{\partial \delta_{\mathbf{r}} f(\mathbf{r}', \mathbf{v}')}{\partial r'_\gamma} - \frac{\partial \delta_{\mathbf{r}} f(\mathbf{r}, \mathbf{v})}{\partial r_\gamma} \frac{\partial \delta_{\mathbf{v}}}{\partial v_\gamma} \right) \tag{A.2}$$

where $\delta_{\mathbf{v}} = \delta(\mathbf{v} - \mathbf{v}')$, $\delta_{\mathbf{r}} = \delta(\mathbf{r} - \mathbf{r}')$ and m is mass of a particle of the gass. The corresponding Poisson bracket then reads

$$\begin{aligned} \{A, B\} &= \int \mathrm{d}\mathbf{r} \int \mathrm{d}\mathbf{v} \int \mathrm{d}\mathbf{r}' \int \mathrm{d}\mathbf{v}' \frac{\delta A}{\delta f(\mathbf{r}, \mathbf{v})} L(\mathbf{r}, \mathbf{v}, \mathbf{r}', \mathbf{v}') \frac{\delta B}{\delta f(\mathbf{r}', \mathbf{v}')} = \\ &= \int \mathrm{d}\mathbf{r} \int \mathrm{d}\mathbf{v} \frac{f}{m} \left(\frac{\partial A_f}{\partial r_\gamma} \frac{\partial B_f}{\partial v_\gamma} - \frac{\partial B_f}{\partial r_\gamma} \frac{\partial A_f}{\partial v_\gamma} \right). \end{aligned} \tag{A.3}$$

This Poisson bivector field can be derived from Liouville equation as shown later in Sec. A.2.3.

Energy on the Boltzmann level is given by

$$E = \int \mathrm{d}\mathbf{r} \int \mathrm{d}\mathbf{v} \left(\frac{1}{2} m \mathbf{v}^2 + \varphi(\mathbf{r}) \right) f(\mathbf{r}, \mathbf{v}) \tag{A.4}$$

where φ is an external force field potential. Note also that instead of velocity, all the expressions can be expressed in terms of momentum $\mathbf{p} = m\mathbf{v}$ equivalently, and we often switch between these two options without notice.

A.1.2 Irreversible evolution

Entropy on the Boltzmann level is given by

$$S = -k_B \int \mathrm{d}\mathbf{r} \int \mathrm{d}\mathbf{p} f(\mathbf{r}, \mathbf{p}) \ln f(\mathbf{r}, \mathbf{p}). \tag{A.5}$$

The irreversible evolution of the Boltzmann equation is prescribed by considering the following dissipation potential

$$\Xi(X(f^\star)) = \int \mathrm{d}\mathbf{1} \int \mathrm{d}\mathbf{1}' \int \mathrm{d}\mathbf{2} \int \mathrm{d}\mathbf{2}' W(f, \mathbf{1}, \mathbf{1}', \mathbf{2}, \mathbf{2}') \left(e^{\frac{X(\mathbf{1},\mathbf{2},\mathbf{1}',\mathbf{2}')}{2}} + e^{-\frac{X(\mathbf{1},\mathbf{2},\mathbf{1}',\mathbf{2}')}{2}} - 2 \right) \tag{A.6}$$

where thermodynamic force[1] X is defined as

$$X(\mathbf{1}, \mathbf{2}, \mathbf{1}', \mathbf{2}') = \frac{1}{k_B} \left(f^\star(\mathbf{1}) + f^\star(\mathbf{2}) - f^\star(\mathbf{1}') - f^\star(\mathbf{2}') \right). \tag{A.7}$$

Note that for example $\mathbf{1}$ stands for position and momentum $(\mathbf{r}_1, \mathbf{p}_1)$. The conjugate variable to the distribution function f was denoted by $f^\star$. What is the physical motivation for such expression? The irreversible part of the Boltzmann equation is associated with collisions of particles, see e.g. [28], and a collision can be regarded as a chemical reaction. Since derivative of entropy with respect to the distribution function is to be substituted for the conjugate variable, the conjugate variable represents chemical potential on the Boltzmann level. Therefore, the thermodynamic force (A.7) can be regarded as a chemical affinity similarly to Sec. 3.2, where the same form of dissipation potential was proposed to describe the Butler-Volmer equation. W stands for a function of the distribution function evaluated at the indicated points.

Let us denote the thermodynamic force (A.7) also by $X(f^\star)$. The force has the following symmetries

$$X(\mathbf{1}, \mathbf{2}, \mathbf{1}', \mathbf{2}') = X(\mathbf{2}, \mathbf{1}, \mathbf{1}', \mathbf{2}') = X(\mathbf{1}, \mathbf{2}, \mathbf{2}', \mathbf{1}') = -X(\mathbf{1}', \mathbf{2}', \mathbf{1}, \mathbf{2}). \tag{A.8}$$

From these symmetries and the definition of the disipation potential (A.6), it follows that the following symmetries can be required without loss of generality.

$$W(\mathbf{1}, \mathbf{2}, \mathbf{1}', \mathbf{2}') = W(\mathbf{2}, \mathbf{1}, \mathbf{1}', \mathbf{2}') = W(\mathbf{1}, \mathbf{2}, \mathbf{2}', \mathbf{1}') = W(\mathbf{1}', \mathbf{2}', \mathbf{1}, \mathbf{2}). \tag{A.9}$$

Let us now calculate the irreversible part of the Boltzmann equation generated

[1] The association of the quantity X with a thermodynamic force serves only for the purpose of interpretation, and has no physical consequences.

by dissipation potential (A.6) explicitly.

$$
\begin{aligned}
& \frac{\mathrm{d}}{\mathrm{d}\lambda}\Big|_{\lambda=0} \Xi(f^\star + \lambda\delta f^\star) = \\
= \; & \frac{\mathrm{d}}{\mathrm{d}\lambda}\Big|_{\lambda=0} \int \mathrm{d}\mathbf{1} \int \mathrm{d}\mathbf{1}' \int \mathrm{d}\mathbf{2} \int \mathrm{d}\mathbf{2}' W(f, \mathbf{1}, \mathbf{1}', \mathbf{2}, \mathbf{2}') \\
& \left(e^{\frac{X(f^\star+\lambda\delta f^\star)}{2}} + e^{-\frac{X(f^\star+\lambda\delta f^\star)}{2}} - 2 \right) \\
= \; & \int \mathrm{d}\mathbf{1} \int \mathrm{d}\mathbf{1}' \int \mathrm{d}\mathbf{2} \int \mathrm{d}\mathbf{2}' \frac{W(f, \mathbf{1}, \mathbf{1}', \mathbf{2}, \mathbf{2}')}{2k_B} \left(e^{\frac{X(f^\star)}{2}} - e^{-\frac{X(f^\star)}{2}} \right) \\
& (\delta f^\star(\mathbf{1}) + \delta f^\star(\mathbf{2}) - \delta f^\star(\mathbf{1}') - \delta f^\star(\mathbf{2}')) \\
= \; & \int \mathrm{d}\mathbf{3} \int \mathrm{d}\mathbf{1} \int \mathrm{d}\mathbf{1}' \int \mathrm{d}\mathbf{2} \int \mathrm{d}\mathbf{2}' \frac{W}{k_B} sh\left(\frac{X(f^\star)}{2} \right) \\
& (\delta(\mathbf{3}-\mathbf{1}) + \delta(\mathbf{3}-\mathbf{2}) - \delta(\mathbf{3}-\mathbf{1}') - \delta(\mathbf{3}-\mathbf{2}'))\, \delta f^\star(\mathbf{3}) \\
= \; & \int \mathrm{d}\mathbf{3} \Bigg(\\
& \int \mathrm{d}\mathbf{2} \int \mathrm{d}\mathbf{1}' \int \mathrm{d}\mathbf{2}' \frac{W(\mathbf{3}, \mathbf{2}, \mathbf{1}', \mathbf{2}')}{k_B} sh \frac{X(\mathbf{3}, \mathbf{2}, \mathbf{1}', \mathbf{2}')}{2} + \\
& + \int \mathrm{d}\mathbf{1} \int \mathrm{d}\mathbf{1}' \int \mathrm{d}\mathbf{2}' \frac{W(\mathbf{1}, \mathbf{3}, \mathbf{1}', \mathbf{2}')}{k_B} sh \frac{X(\mathbf{1}, \mathbf{3}, \mathbf{1}', \mathbf{2}')}{2} - \\
& - \int \mathrm{d}\mathbf{1} \int \mathrm{d}\mathbf{2} \int \mathrm{d}\mathbf{2}' \frac{W(\mathbf{1}, \mathbf{2}, \mathbf{3}, \mathbf{2}')}{k_B} sh \frac{X(\mathbf{1}, \mathbf{2}, \mathbf{3}, \mathbf{2}')}{2} - \\
& - \int \mathrm{d}\mathbf{1} \int \mathrm{d}\mathbf{2} \int \mathrm{d}\mathbf{1}' \frac{W(\mathbf{1}, \mathbf{2}, \mathbf{1}', \mathbf{3})}{k_B} sh \frac{X(\mathbf{1}, \mathbf{2}, \mathbf{1}', \mathbf{3})}{2} \\
& \Bigg) \delta f^\star(\mathbf{3}).
\end{aligned}
\tag{A.10}
$$

Now by considering the symmetries (A.8) and (A.9) and by relabeling $\mathbf{1}$ to $\mathbf{2}$ in the second summand and $\mathbf{1}'$ to $\mathbf{2}'$ in the fourth summand, the first summand becomes equal to the second and the third summand becomes equal the fourth. Finally, swapping the first two arguments in all the forces with two last two arguments of the forces and using the antisymmetry of X with respect to such swapping, all the summands become equal and the derivative of the dissipation potential becomes

$$
\begin{aligned}
& \frac{\mathrm{d}}{\mathrm{d}\lambda}\Big|_{\lambda=0} \Xi(f^\star + \lambda\delta f^\star) = \\
& \quad = \int \mathrm{d}\mathbf{3} \underbrace{\int \mathrm{d}\mathbf{2} \int \mathrm{d}\mathbf{1}' \int \mathrm{d}\mathbf{2}' \frac{4W(\mathbf{3}, \mathbf{2}, \mathbf{1}', \mathbf{2}')}{k_B} sh\left(\frac{X(\mathbf{3}, \mathbf{2}, \mathbf{1}', \mathbf{2}')}{2} \right)}_{\frac{\partial \Xi}{\partial f^\star(\mathbf{3})}} \delta f^\star(\mathbf{3}).
\end{aligned}
\tag{A.11}
$$

Now the explicit expression for $f^\star$ (1.13) has to be employed, and

$$
f^\star(\mathbf{3}) = \frac{\partial S}{\partial f(\mathbf{3})} = -k_B \ln f(\mathbf{3}) - k_B \tag{A.12}
$$

in accordance with Eq. (A.5). It follows that

$$\begin{aligned} sh\left(\frac{X(\mathbf{1},\mathbf{2},\mathbf{1}',\mathbf{2}')}{2}\right) = \\ = sh\left(\frac{1}{2}\left(-\ln f(\mathbf{1}) - 1 - \ln f(\mathbf{2}) - 1 + \ln f(\mathbf{1}') + 1 + \ln f(\mathbf{2}') + 1\right)\right) = \\ = sh\left(\frac{\sqrt{f(\mathbf{1}')f(\mathbf{2}')}}{\sqrt{f\mathbf{1}f(\mathbf{2})}}\right) = \frac{1}{2}\left(\frac{\sqrt{f(\mathbf{1}')f(\mathbf{2}')}}{\sqrt{f\mathbf{1}f(\mathbf{2})}} - \frac{\sqrt{f(\mathbf{1})f(\mathbf{2})}}{\sqrt{f\mathbf{1}'f(\mathbf{2}')}}\right) = \\ = \frac{1}{2\sqrt{f(\mathbf{1})f(\mathbf{2})f(\mathbf{1}')f(\mathbf{2}')}}\left(f(\mathbf{1}')f(\mathbf{2}') - f(\mathbf{1})f(\mathbf{2})\right). \end{aligned} \tag{A.13}$$

Therefore, the irreversible part of the Boltzmann equation can be writen down as

$$\frac{\partial\Xi}{\partial\frac{\partial S}{\partial f(\mathbf{1})}} = \int \mathrm{d}\mathbf{2}\int \mathrm{d}\mathbf{1}'\int \mathrm{d}\mathbf{2}'\frac{2W(\mathbf{1},\mathbf{2},\mathbf{1}',\mathbf{2}')}{k_B\sqrt{f(\mathbf{1})f(\mathbf{2})f(\mathbf{1}')f(\mathbf{2}')}}\left(f(\mathbf{1}')f(\mathbf{2}') - f(\mathbf{1})f(\mathbf{2})\right). \tag{A.14}$$

Finally, for concrete calculations, the function W has to be supplied, see e.g. [28] or [41].

Note also that the thermodynamic potential (1.18) is equal to

$$\Phi = -S + \frac{1}{T_0}\int \mathrm{d}\mathbf{r}\int \mathrm{d}\mathbf{p}\frac{\mathbf{p}^2}{2m}f(\mathbf{r},\mathbf{p}) - \frac{\mu_0}{T_0}\int \mathrm{d}\mathbf{r}\int \mathrm{d}\mathbf{p}mf(\mathbf{r},\mathbf{p}), \tag{A.15}$$

and that the function $W(\mathbf{1},\mathbf{2},\mathbf{1}\,\mathbf{2}')$, which represents differential cross-section of a collision, is zero if $\mathbf{p}_1^2 + \mathbf{p}_2^2 \neq \mathbf{p}_{1'}^2 + \mathbf{p}_{2'}^2$. Therefore, Eq. (A.13) gives the same result with $f^\star = \frac{\partial\Phi}{\partial f}$.

The dissipation potential (A.6) is clearly symmetric with respect to TRT since after replacing $\mathbf{p}$ with $-\mathbf{p}$ the change of variables from $\mathbf{p}$ to $-\mathbf{p}$ yields the original dissipation potential.

In summary, the Boltzmann equation with a general differential cross-section has been specifiec within GENERIC completely.

A.1.3 Time-reversal transformation

Does the Poisson bivector really generate only reversible evolution and does the dissipation potential only generate irreversible evolution? This is indeed so as it has already been shown that any even dissipation potential generates only irreversible evolution in Lemma 3. Moreover, in Sec. A.2.4 it is shown that the Poisson bivector generates reversible evolution. But let us check these properties explicitly at first.

TRT applied on probability distribution inverts velocities, i.e.

$$\mathbf{I}f(\mathbf{r},\mathbf{v}) = f(\mathbf{r},-\mathbf{v}). \tag{A.16}$$

Let us now formulate the notion of reversibility/irreversibility geometrically. The manifold of state variables is given by probability density at each place of phase

space $f(\mathbf{r},\mathbf{v})$. TRT is given by (A.16) and Jacobi matrix of the transformation is thus given by

$$\frac{\partial \mathbf{I}(f(\mathbf{r},\mathbf{v}))}{\partial f(\mathbf{r}',\mathbf{v}')} = \frac{\partial \int \mathrm{d}\mathbf{r} \int \mathrm{d}\mathbf{v}\delta(\mathbf{v}+\mathbf{v}')\delta(\mathbf{r}-\mathbf{r}')f(\mathbf{r}',\mathbf{v}')}{\partial f(\mathbf{r}',\mathbf{v}')} = \delta(\mathbf{r}-\mathbf{r}')\delta(\mathbf{v}+\mathbf{v}'). \quad \text{(A.17)}$$

The vector field generating reversible evolution in Boltzmann equation is equal to

$$\mathcal{V} = \int \mathrm{d}\mathbf{r} \int \mathrm{d}\mathbf{v} \int \mathrm{d}\mathbf{r}' \int \mathrm{d}\mathbf{v}' L(\mathbf{r},\mathbf{v},\mathbf{r}',\mathbf{v}') \frac{\delta E}{\delta f(\mathbf{r}',\mathbf{v}')} \frac{\partial}{\partial f(\mathbf{r},\mathbf{v})} \quad \text{(A.18)}$$

where $L(\mathbf{r},\mathbf{v},\mathbf{r}',\mathbf{v}')$ is specified by formula (A.2). After some algebra, the push-forward induced by TRT transforms the field to

$$\begin{aligned}\mathbf{I}_\star\mathcal{V} = -\int \mathrm{d}\mathbf{r} \int \mathrm{d}\mathbf{v} \frac{1}{m} \Bigg(& \frac{\partial\delta(\mathbf{v}'-\mathbf{v})}{\partial v'_\gamma} \frac{\partial\delta(\mathbf{r}'-\mathbf{r}) f(\mathbf{r}',-\mathbf{v}')}{\partial r'_\gamma} \\ & - \frac{\partial\delta(\mathbf{v}'-\mathbf{v})}{\partial v_\gamma} \frac{\partial\delta(\mathbf{r}'-\mathbf{r}) f(\mathbf{r},-\mathbf{v})}{\partial r_\gamma} \Bigg) \cdot \\ & \cdot \frac{\delta E}{\delta f(\mathbf{r}',-\mathbf{v}')} \frac{\partial}{\partial f(\mathbf{r},-\mathbf{v})},\end{aligned}$$

which indeed has only different sign compared with the original field, and thus the Poisson bracket indeed generates reversible evolution.

Applying TRT on dissipation potential means applying the push-forward $\mathbf{I}_\star$ as

$$\mathbf{I}_\star\Xi = \Xi(\mathbf{I}(f)) = \Xi(f), \quad \text{(A.19)}$$

where the last equality follows from simple substitution $-\mathbf{v} \to \mathbf{v}$, etc., in the expression for $\Xi(\mathbf{I}(f))$. The dissipation potential is thus even with respect to TRT and according to Lemma 3 it only generates irreversible evolution. In summary, we have shown that the Poisson bracket generates reversible evolution while the dissipation potential generates irreversible evolution.

Although the distribution function has no parity and so Theorem 2 can not be applied directly, new state variables which already have definite parities can be introduced. For example the distribution function $f(\mathbf{r},\mathbf{v})$ is fully characterized by its moments with respect to velocity, and the moments have clear physical interpretation. The zeroth moment,

$$\rho(\mathbf{r}) = m \int f(\mathbf{r},\mathbf{v})\,\mathrm{d}\mathbf{r}, \quad \text{(A.20)}$$

is just density, which is even under TRT. The first moment,

$$\mathbf{u}(\mathbf{r}) = m \int f(\mathbf{r},\mathbf{v})\mathbf{v}\,\mathrm{d}\mathbf{r}, \quad \text{(A.21)}$$

is momentum of the fluid (an odd variable), and higher moments may be constructed. Evolution equations for the moments follow from the Boltzmann equation straightforwardly. In particular, for the two first moments we obtain evolution equations of classical hydrodynamics from Section 2.2, where it already has

been shown that Theorem 2 applies. Hence, OCRR appear when parity can be assigned to the state variables.

In summary, Theorem 2 does not apply to the Boltzmann equation directly since distribution function itself has no parity. OCRR can be revealed, however, when considering moments of the distribution function, which already have parities, as state variables instead of the distribution function itself. The assumption that relations (1.27) are valid is fulfilled since the Poisson bivector from Boltzmann equation has already been shown to generate only reversible evolution and the dissipation potential is even with respect to TRT. Theorem 2 then applies to these new variables, and the statement that variables of the same parity are coupled through the dissipative bracket while variables with opposite parities are coupled through the Poisson bracket near equilibrium is valid for Boltzmann equation as well.

A.2 A hierarchy of Poisson brackets

A.2.1 Introduction

Is it possible to construct Poisson bracket on a level of description if dynamics on a more detailed level is known? The answer is positive and it is the goal of this chapter to show the construction of various Poisson brackets in detail.

One can start on the level where state variables are N-particle distribution functions, the Liouville level. Evolution on this level is given by Liouville equation, see e.g. [103], which is completely reversible[2]. Then by simply defining projection from the N-particle distributions to a lower (less detailed) level of description, Poisson bracket on the lower level can be calculated straightforwardly. For example, Poisson bracket from the Boltzmann equation follows by projection from the Liouville Poisson bracket, and the hydrodynamic Poisson bracket follows from the Boltzmann Poisson bracket (the Poisson bracket generating the reversible part of the Boltzmann equation). One can also consider mixtures of fluids easily, obtaining Boltzmann Poisson bracket for a binary mixture and, consequently, hydrodynamic Poisson brackets of mixtures on various levels of description (EIT, CIT, mechanical equilibrium).

The projection, moreover, ensures that the constructed Poisson bracket generates only reversible evolution and that it really is a Poisson bracket, i.e. it fulfills the Jacobi identity.

A.2.2 Liouville equation

Consider an isolated system containing N interacting particles. The corresponding phase space consists of positions and momenta of all particles. Position and momentum of the first particle is denoted by $\mathbf{r}_1$ and $\mathbf{p}^1$, respectively, etc. The couple $(\mathbf{r}_1, \mathbf{p}^1)$ is denoted by $\mathbf{1}$ for convenience and analogically for the other particles. Evolution equation for the N-particle phase space density $f_N(\mathbf{1}, \ldots, \mathbf{N}, t)$, or distribution function, is the standard Liouville equation, see e.g. [103],

$$\frac{\partial f_N}{\partial t} = -\frac{\partial E^N}{\partial p_i^j}\frac{\partial f_N}{\partial r_j^i} + \frac{\partial E^N}{\partial r_j^i}\frac{\partial f_N}{\partial p_i^j} \tag{A.22}$$

where $E^N(\mathbf{1}, \ldots, \mathbf{N})$ is energy of the system which depends on positions and momenta of the particles. Liouville equation is usually derived within non-equilibrium statistical physics, e.g. [103], from the requirement that probability density behaves as an incompressible fluid. Note, however, that it is possible to derive Liouville equation by geometric means. Indeed, following [60] step by step in the N-particle phase space instead of the one-particle phase space leads to the equation. Introducing energy in terms of the distribution function

$$E = \int \mathrm{d}\mathbf{1} \ldots \int \mathbf{N} E^N, \tag{A.23}$$

derivative of which with respect to f_N is clearly

$$\frac{\partial E}{\partial f_N} = E^N, \tag{A.24}$$

[2]The reversibility can be checked the same way as for the reversible part of Boltzmann equation in Sec. A.1.

Eq. (A.22) implies that an arbitrary functional of the distribution function $A(f_N)$ evolves as

$$\frac{\mathrm{d}A}{\mathrm{d}t} = \int \mathrm{d}\mathbf{1} \ldots \int \mathrm{d}\mathbf{N} \frac{\partial A}{\partial f_N} \frac{\partial f_N}{\partial t} = \{A, E\}^{(L)} \tag{A.25}$$

where the Poisson bracket on the Liouville level (or the Liouville Poisson bracket) is equal to

$$\{A, B\}^{(L)} = \int \mathrm{d}\mathbf{1} \ldots \int \mathrm{d}\mathbf{N} f_N \left(\frac{\partial A_{f_N}}{\partial r^i_j} \frac{\partial B_{f_N}}{\partial p^j_i} - \frac{\partial B_{f_N}}{\partial r^i_j} \frac{\partial A_{f_N}}{\partial p^j_i} \right). \tag{A.26}$$

Integration with respect to for example $\mathrm{d}\mathbf{1}$ stands for $\int \mathrm{d}\mathbf{r}_1 \int \mathrm{d}\mathbf{p}^1$, etc. This Poisson bracket can be also rewritten in terms of the Poisson bracket of classical mechanics as

$$\{A, B\}^{(L)} = \int \mathrm{d}\mathbf{1} \ldots \int \mathrm{d}\mathbf{N} f_N \{A_{f_N}, B_{f_N}\}^{(CM)} \tag{A.27}$$

where the Poisson bracket of classical mechanics is the standard canonical Poisson bracket, see e.g. [32],

$$\{C, D\}^{(CM)} = \frac{\partial C}{\partial r^i_j} \frac{\partial D}{\partial p^j_i} - \frac{\partial D}{\partial r^i_j} \frac{\partial C}{\partial p^j_i} \tag{A.28}$$

for any two functions $C(\mathbf{1}, \ldots, \mathbf{N})$ and $D(\mathbf{1}, \ldots, \mathbf{N})$. The derivative A_{f_N} stands for $\frac{\partial A}{\partial f_N}$.

Later in this chapter it is shown that Poisson bracket (A.26) can be used to derive Poisson brackets on lower levels of description. In particular, Poisson bracket for the Boltzmann equation, for classical hydrodynamics or for mixtures of fluids can be obtained by a straightforward geometric projection of the Liouville Poisson bracket, see Sec. A.2.4.

A.2.3 From Liouville to Boltzmann

Boltzmann equation, see Sec. A.1, consists of both reversible and irreversible dynamics. Let us now derive the reversible part from the Liouville Poisson bracket (A.26). One-particle distribution function (or one-particle phase space density) $f(\mathbf{r}, \mathbf{p})$, evolution of which is described by Boltzmann equation, can be defined as a projection of the N-particle distribution function. Indeed when denoting $(\mathbf{r}_a, \mathbf{p}^a)$ by $\mathbf{a}$, the one-particle distribution function can be introduced as

$$f(\mathbf{a}) = \int \mathrm{d}\mathbf{1} \ldots \int \mathrm{d}\mathbf{N} \sum_{i=1}^{N} \delta(\mathbf{a} - \mathbf{i}) \tag{A.29}$$

where $\mathbf{1}$ denotes position and momentum of the first particle, $(\mathbf{r}_1, \mathbf{p}_1)$, and $\mathbf{i}$ analogically for the i-th particle. Delta distribution $\delta(\mathbf{a} - \mathbf{i})$ stands for $\delta(\mathbf{r}_a - \mathbf{r}_i)\delta(\mathbf{p}^a - \mathbf{p}^i)$. Derivative of f with respect to f_N is

$$\frac{\partial f(\mathbf{a})}{\partial f_N(\mathbf{1}, \ldots, \mathbf{N})} = \sum_{i=1}^{N} \delta(\mathbf{a} - \mathbf{i}). \tag{A.30}$$

Consider now two arbitrary functionals of the one-particle distribution function, $A(f)$ and $B(f)$. Let us now evaluate the Liouville Poisson bracket, (A.26), of these two functionals.

$$\{A,B\}^{(L)} = \int \mathrm{d}\mathbf{1}\ldots\int \mathrm{d}\mathbf{N}\int \mathrm{d}\mathbf{a}\int \mathrm{d}\mathbf{b} f_N \frac{\partial A}{\partial f(\mathbf{a})}\left\{\frac{f(\mathbf{a})}{\partial f_N},\frac{\partial f(\mathbf{b})}{\partial f_N}\right\}^{(CM)}\frac{\partial B}{\partial f(\mathbf{b})} \tag{A.31}$$

Now using the definition (A.28) this last equation becomes

$$= \sum_{i_a}\sum_{i_b}\int \mathrm{d}\mathbf{1}\ldots\int \mathrm{d}\mathbf{N}\int \mathrm{d}\mathbf{a}\int \mathrm{d}\mathbf{b}\frac{\partial A}{\partial f(\mathbf{a})}\frac{\partial B}{\partial f(\mathbf{b})}\left(\frac{\partial \delta(\mathbf{a}-\mathbf{i_a})}{\partial r_i^\alpha}\frac{\partial \delta(\mathbf{b}-\mathbf{i_b})}{\partial p_\alpha^i}-\ldots\right) f_N \tag{A.32}$$

where $\ldots$ stand for the same term as already present in the bracket but with $\mathbf{a}$ swapped with $\mathbf{b}$. Since for example the delta distribution $\delta(\mathbf{r}_a-\mathbf{r}_{i_a})$ only depends on $\mathbf{r}_{i_a}$ among positions of all particles, the two sums over i_a and i_b disappear and the last equality can be rewritten as

$$= \int \mathrm{d}\mathbf{1}\ldots\int \mathrm{d}\mathbf{N}\int \mathrm{d}\mathbf{r}_a\int \mathrm{d}\mathbf{p}^b f_N\frac{\partial A}{\partial f(\mathbf{r}_a,\mathbf{p}^i)}\frac{\partial B}{\partial f(\mathbf{r}_i,\mathbf{p}^b)}\frac{\partial\delta(\mathbf{r}_a-\mathbf{r}_i)}{\partial r_i^\alpha}\frac{\partial\delta(\mathbf{p}^b-\mathbf{p}^i)}{\partial p_\alpha^i}-\ldots \tag{A.33}$$

Now by integrating by parts with respect to $\mathbf{r}_i$ and, subsequently, applying the $\delta(\mathbf{r}_a-\mathbf{r}_i)$ term, the last equality becomes

$$= -\int \mathrm{d}\mathbf{1}\ldots\int \mathrm{d}\mathbf{N}\int \mathrm{d}\mathbf{p}^b\frac{\partial A}{\partial f(\mathbf{r}_i,\mathbf{p}^i)}\frac{\partial}{\partial r_i^\alpha}\left(\frac{\partial B}{\partial f(\mathbf{r}_i,\mathbf{p}^b)}f_N\right)\frac{\partial\delta(\mathbf{p}^b-\mathbf{p}^i)}{\partial p_\alpha^i}. \tag{A.34}$$

Similarly, integrating by parts with respect to $\mathbf{p}^i$ and applying the corresponding delta-destribution yields

$$\begin{aligned} = & \int \mathrm{d}\mathbf{1}\ldots\int \mathrm{d}\mathbf{N}\frac{\partial}{\partial p_\alpha^i}\left(\frac{\partial A}{\partial f(\mathbf{r}_i,\mathbf{p}^i)}f_N\right)\frac{\partial}{\partial r_i^\alpha}\frac{\partial B}{\partial f(\mathbf{r}_i,\mathbf{p}^i)}+ \\ & +\frac{\partial}{\partial p_\alpha^i}\left(\frac{\partial A}{\partial f(\mathbf{r}_i,\mathbf{p}^i)}\frac{\partial f_N}{\partial r_i^\alpha}\right)\frac{\partial B}{\partial f(\mathbf{r}_i,\mathbf{p}^i)}-\ldots \end{aligned} \tag{A.35}$$

Now by using integration by parts so that derivatives of f_N disappear and expressing the $\ldots$ explicitly leads to the following equality

$$= \int \mathrm{d}\mathbf{1}\ldots\int \mathrm{d}\mathbf{N} f_N\left(\frac{\partial}{\partial r_i^\alpha}\frac{\partial A}{\partial f(\mathbf{i})}\frac{\partial}{\partial p_\alpha^i}\frac{\partial B}{\partial f(\mathbf{i})}-\frac{\partial}{\partial r_i^\alpha}\frac{\partial B}{\partial f(\mathbf{i})}\frac{\partial}{\partial p_\alpha^i}\frac{\partial A}{\partial f(\mathbf{i})}\right). \tag{A.36}$$

Adding the term $\int \mathrm{d}\mathbf{r}\int \mathrm{d}\mathbf{p}\delta(\mathbf{r}-\mathbf{r}_i)\delta(\mathbf{p}-\mathbf{p}^i)$ in front of this expression, which clearly does not alter the expression, and using the projection (A.29), this last equation becomes

$$= \int \mathrm{d}\mathbf{r}\int \mathrm{d}\mathbf{p} f(\mathbf{r},\mathbf{p})\left(\frac{\partial A_f}{\partial r^\alpha}\frac{\partial B_f}{\partial p_\alpha}-\frac{\partial B_f}{\partial r^\alpha}\frac{\partial A_f}{\partial p_\alpha}\right) \tag{A.37}$$

$$= \{A,B\}^{(B)} \tag{A.38}$$

where A_f stands for $\frac{\partial A}{\partial f(\mathbf{r},\mathbf{p})}$. This last equation is exactly the Poisson bracket that generates the reversible part of the Boltzmann equation, referred to as the Boltzmann Poisson bracket. We have thus obtained that

$$\{A,B\}^{(L)} = \{A,B\}^{(B)} \tag{A.39}$$

for functionals A, B dependent only[3] on the one-particle distribution function f.

In summary, starting with functionals dependent only on the one-particle distribution function, f, the Liouville Poisson bracket becomes the Boltzmann Poisson bracket. In other words, the reversible part of Boltzmann equation is just a "projection" of the reversible evolution governed by the Liouville equation. Let us make this statement more rigorous.

A.2.4 Geometric interpretation

In Appendix A.2.3 the Boltzmann Poisson bracket was derived by evaluating the Liouville Poisson bracket on functionals dependent only on the one-particle distribution function. Each Poisson bracket can be interpreted in terms of the corresponding Poisson bivector field, see [32]. What is the relation between the Poisson bivector on the Liouville level of description and the Poisson bivector on the Boltzmann level?

The Boltzmann Poisson bracket can be expressed in terms of its Poisson bivector as follows

$$\{A, B\}^{(B)} = \int \mathrm{d}\mathbf{a} \int \mathrm{d}\mathbf{b} \frac{\partial A}{\partial f(\mathbf{a})} L_B^{\mathbf{a},\mathbf{b}} \frac{\partial B}{\partial f(\mathbf{b})}, \tag{A.40}$$

and analogically the Poisson bivector generating the Liouville Poisson bracket is defined as

$$\begin{aligned} \{A, B\}^{(L)} \quad = \quad & \int \mathrm{d}\mathbf{1} \ldots \int \mathrm{d}\mathbf{N} \int \mathrm{d}\mathbf{1}' \ldots \int \mathrm{d}\mathbf{N}' \int \mathrm{d}\mathbf{a} \int \mathrm{d}\mathbf{b} \\ & \frac{\partial A}{\partial f(\mathbf{a})} \frac{\partial f(\mathbf{a})}{\partial f_N} L_L^{f_N, f_{N'}} \frac{\partial B}{\partial f(\mathbf{b})} \frac{\partial f(\mathbf{b})}{\partial f_{N'}} \end{aligned} \tag{A.41}$$

where ${f_N}' = f_N(\mathbf{1}', \ldots, \mathbf{N}')$ and $L_L^{f_N, f_{N'}}$ is the component of the Liouville Poisson bivector that provides coupling between $\mathbf{1}, \ldots, \mathbf{N}$ and $\mathbf{1}', \ldots, \mathbf{N}'$. Now from Eq. (A.39) it follows that

$$L_B^{\mathbf{a},\mathbf{b}} = \int \mathrm{d}\mathbf{1} \ldots \int \mathrm{d}\mathbf{N} \int \mathrm{d}\mathbf{1}' \ldots \int \mathrm{d}\mathbf{N}' \frac{\partial f(\mathbf{a})}{\partial f_N} L_L^{f_N, f_{N'}} \frac{\partial f(\mathbf{b})}{\partial {f_N}'}. \tag{A.42}$$

Let us now have a look at the relation (A.42) geometrically. Consider the manifold of state variables on a higher level of description (e.g. Liouville), and denote the state variables by x^i. On a lower level of description the state variables (denoted by y^a) are obtained by a projection

$$\pi : \mathbf{x} \to \mathbf{y}(\mathbf{x}). \tag{A.43}$$

Poisson bivectors are twice contravariant tensors and thus the projection transforms them as follows, see e.g. [32],

$$L_{lower}^{ab} = \frac{\partial \pi^a}{\partial x^i} L_{higher}^{ij} \frac{\partial \pi^b}{x^j} = \left\{ \pi^a, \pi^b \right\}^{(higher)}. \tag{A.44}$$

But this is exactly how formula (A.42) works. The only problem is that projection π is typically no diffeomorphism and thus it may not induce the mapping between the bivectors. Let us return to this problem later in this section.

[3]The functionals, of course, also depend on f_N but only through the function f.

In summary, obtaining the Poisson bracket on a lower level of description by evaluating the Poisson bracket on a higher level on functionals dependent only on state variables of the lower level is equivalent to projecting the Poisson bivector from the higher level of description to the lower level. Moreover, components of the Poisson bivector on the lower level of description are given by Poisson bracket on the higher level applied on components of the projector.

Consider now state variables with definite parities and suppose that a Poisson bracket on the higher level of description generates reversible evolution, which means that

$$L^{ij}_{higher}|_{\mathbf{I}(\mathbf{x})} = -P(x^i)P(x^j)L^{ij}_{higher}|_{\mathbf{x}} \tag{A.45}$$

in accordance with Eq. 1.42. The Poisson bivector at the lower level evaluated at inverted coordinates becomes

$$\begin{aligned} L^{ab}_{lower}|_{\mathbf{I}(\mathbf{y})} &= \sum_{i,j} \frac{\partial \mathbf{I} \circ \pi^a}{\partial x^i}|_{\mathbf{I}(\mathbf{x})} L^{ij}_{higher}|_{\mathbf{I}(\mathbf{x})} \frac{\partial \mathbf{I} \circ \pi^b}{x^j}|_{\mathbf{I}(\mathbf{x})} && \text{(A.46)} \\ &= \sum_{i,j} P(y^a)P(y^b)P(x^i)P(x^j) \frac{\partial \pi^a}{\partial x^i} L^{ij}_{higher}|_{\mathbf{I}(\mathbf{x})} \frac{\partial \pi^b}{x^j} && \text{(A.47)} \\ &= \sum_{i,j} -P(y^a)P(y^b) \frac{\partial \pi^a}{\partial x^i} L^{ij}_{higher} \frac{\partial \pi^b}{\partial x^j} && \text{(A.48)} \\ &= -P(y^a)P(y^b)L^{ab}_{lower}, && \text{(A.49)} \end{aligned}$$

which means that any Poisson bivector obtained as the projection of a Poisson bivector generating reversible evolution generates only reversible evolution as well. Since the Poisson bivector of classical mechanics or Liouville equation generates reversible evolution, all the Poisson bivectors (or Poisson brackets) derived by the projection from the Liouville Poisson bivector generate only reversible evolution.

Let us now return to the problem that the projector π is no diffeomorphism, and thus the push-forward mapping bivectors on the manifold of state variables on a higher level, M, to bivectors on the manifold on a lower level, N, does not exist in general, see [32], and without providing any additional knowledge about the system under consideration there is no a priori guarantee that the result of the projection is well defined. An example of the additional knowledge that ensures possibility of the projection is a symmetry permitting a symplectic or Poisson reduction, see [32] or [2]. If, on the other hand, the result of the projection given by Eq. (A.44) only depends on state variables of the lower level, x, the projection is well defined, and one may use the result as the Poisson bivector on the lower level.

But is the Jacobi identity guaranteed for the result of the projection? Firstly, consider smooth functions on M, $\mathcal{F}(M)$, which are also referred to as the algebra of observables on M. Functions from $\mathcal{F}(M)$ indeed form an (associative) algebra since they form a linear space and the standard pointwise multiplication is the bilinear operation necessary for $\mathcal{F}(M)$ being an algebra. Moreover, Poisson bracket of two functions from $\mathcal{F}(M)$ stays in $\mathcal{F}(M)$ and so $\mathcal{F}(M)$ is even a Lie algebra, referred to as an algebra of observables.

Secondly, consider functions on M that are projectable onto N, i.e.

$$\mathcal{F}_\pi(M) = \{A \in \mathcal{F}(M) : \pi(x_1) = \pi(x_2) \Rightarrow A(x_1) = A(x_2)\}. \tag{A.50}$$

Functions $\mathcal{F}_\pi(M)$ form an algebra isomorphic to the algebra of functions on N, $\mathcal{F}(N)$. Indeed, there is a bijective mapping between $\mathcal{F}_\pi(M)$ and $\mathcal{F}(N)$ which respects the bilinear operation (pointwise multiplication) given by $A^H \sim A^L \circ \pi$, where $A^H \in \mathcal{F}_\pi(M)$ and $A^L \in \mathcal{F}(N)$.

So far we have shown that $\mathcal{F}_\pi(M)$ is an algebra isomorphic with $\mathcal{F}(N)$. Let us now introduce a Poisson structure inherited from the algebra of observables $\mathcal{F}(M)$ so that $\mathcal{F}_\pi(M)$ also becomes an algebra of observables. Consider two functions A^L and B^L from $\mathcal{F}_\pi(M)$ and define their Poisson bracket as

$$\begin{aligned}\{A^L, B^L\}^L &\stackrel{def}{=} \{A^L, B^L\}^H = L_H^{ij}\frac{\partial A^L}{\partial x^i}\frac{\partial B^L}{\partial x^j} = \\ &= \underbrace{L_H^{ij}\frac{\partial \pi^a}{\partial x^i}\frac{\partial \pi^b}{\partial x^j}}_{L_L^{ab}}\frac{\partial A^L}{\partial y^a}\frac{\partial B^L}{\partial y^b}. \end{aligned} \tag{A.51}$$

Does this expression give a function from $\mathcal{F}_\pi(M)$? Not in general since one has to check that the Poisson bivector on the lower level of description L_L^{ab} does not depend on x but only on y. Note, however, that such calculation has to be carried out anyway when one wishes to express the tensor explicitly.

But when the resulting bivector field depends only on state variables $\mathbf{y}$, the expression $\{A^L, B^L\}^L$ indeed is in $\mathcal{F}_\pi(M)$, and due to the properties of the Poisson bracket $\{\bullet, \bullet\}^H$ (antisymmetry, Jacobi identity) the $\{\bullet, \bullet\}^L$ is indeed a Poisson bracket. Since $\mathcal{F}_\pi(M)$ and $\mathcal{F}(N)$ are isomorphic, the Poisson bracket works on $\mathcal{F}(N)$ as well, and we have thus obtained an algebra of observables $\mathcal{F}(N)$ with the Poisson bracket $\{\bullet, \bullet\}^L$ inherited from $\mathcal{F}(M)$. The expression for the Poisson bracket on the lower level of description and the expression for the new Poisson bivector are exactly the same as in the illustrations demonstrated in this chapter, and so one does not need to check whether the in this chapter derived Poisson brackets really are Poisson brackets (antisymmetry, Jacobi identity) since that is satisfied automatically.

In summary, it has been shown that when starting with a Poisson bracket generating reversible evolution on a higher level of description, there is a natural way to construct a Poisson bracket on a lower level of description. The new Poisson bracket indeed satisfies all the properties of Poisson brackets and it generates only reversible evolution. The passage to the lower level is generated by defining a projection from state variables on the higher level to state variables on the lower level. During the passage one has to check whether the constructed Poisson bivector depends only on the state variables of the lower level of description. If this is true, the passage is complete and the dynamics on the lower level of description has been derived from the reversible dynamics on the higher level, it is reversible and the Poisson bracket indeed fulfills all the necessary properties (antisymmetry, Jacobi identity).

A.2.5 From Boltzmann to classical hydrodynamics

Having derived the Boltzmann Poisson bracket, we are able to derive the hydrodynamic Poisson bracket in a convenient way. One could, of course, start with the Liouville Poisson bracket and go directly to hydrodynamics, but the calculation would be longer than when starting from the Boltzmann Poisson bracket. Let

us, therefore, introduce the projection from the Boltzmann level of description to the level of classical hydrodynamics. The hydrodynamic state variables are

$$\rho(\mathbf{r}_a) = \int \mathrm{d}\mathbf{r} \int \mathrm{d}\mathbf{p} m f(\mathbf{r},\mathbf{p}) \delta(\mathbf{r}-\mathbf{r}_a) \tag{A.52}$$

$$u_i(\mathbf{r}_a) = \int \mathrm{d}\mathbf{r} \int \mathrm{d}\mathbf{p} p_i f(\mathbf{r},\mathbf{p}) \delta(\mathbf{r}-\mathbf{r}_a) \tag{A.53}$$

$$s(\mathbf{r}_a) = \int \mathrm{d}\mathbf{r} \int \mathrm{d}\mathbf{p} s_f(f(\mathbf{r},\mathbf{p})) \delta(\mathbf{r}-\mathbf{r}_a) \tag{A.54}$$

where m is mass of one particle and s_f is a real-valued function. Therefore, derivatives of the hydrodynamic state variables with respect to $f(\mathbf{r},\mathbf{p})$ are

$$\frac{\partial \rho(\mathbf{r}_a)}{\partial f(\mathbf{r},\mathbf{p})} = m\delta(\mathbf{r}-\mathbf{r}_a) \tag{A.55a}$$

$$\frac{\partial u_i(\mathbf{r}_a)}{\partial f(\mathbf{r},\mathbf{p})} = p_i\delta(\mathbf{r}-\mathbf{r}_a) \tag{A.55b}$$

$$\frac{\partial s(\mathbf{r}_a)}{\partial f(\mathbf{r},\mathbf{p})} = s'_f(f(\mathbf{r},\mathbf{p}))\delta(\mathbf{r}-\mathbf{r}_a). \tag{A.55c}$$

To obtain the hydrodynamic Poisson bracket, it is advantageous, in contrast to the Section A.2.3, to construct the Poisson bivector directly. Therefore, one has to calculate how the Boltzmann Poisson bracket acts on some arbitrary functionals of the hydrodynamic state variables, A and B, in accordance with formula (A.44).

$$L_{CH}^{\rho(\mathbf{r}_a),\rho(\mathbf{r}_b)} = \{\rho(\mathbf{r}_a),\rho(\mathbf{r}_b)\}^{(B)} = \tag{A.56a}$$

$$= \int \mathrm{d}\mathbf{r} \int \mathrm{d}\mathbf{p} f(\mathbf{r},\mathbf{p}) \left(\frac{\partial}{\partial r^k} \frac{\partial \rho(\mathbf{r}_a)}{\partial f(\mathbf{r},\mathbf{p})} \frac{\partial}{\partial p_k} \frac{\partial \rho(\mathbf{r}_b)}{\partial f(\mathbf{r},\mathbf{p})} - \dots \right) \tag{A.56b}$$

where $\dots$ stand for the same term as already present in the bracket but with a and b swapped. Using relations (A.55), this last equality becomes

$$= \int \mathrm{d}\mathbf{r} \int \mathrm{d}\mathbf{p} f(\mathbf{r},\mathbf{p}) \left(\frac{\partial m\delta(\mathbf{r}_a-\mathbf{r})}{\partial r^k} \underbrace{\frac{\partial m\delta(\mathbf{r}_b-r)}{\partial p_k}}_{=0} - \dots \right) = 0. \tag{A.56c}$$

Therefore, this component of the hydrodynamic Poisson bivector, coupling density with density, disappears. The component coupling density with momentum can be obtained analogically.

$$L_{CH}^{\rho(\mathbf{r}_a),u_j(\mathbf{r}_b)} = \{\rho(\mathbf{r}_a),u_j(\mathbf{r}_b)\}^{(B)} = \tag{A.57a}$$

$$= \int \mathrm{d}\mathbf{r} \int \mathrm{d}\mathbf{p} f(\mathbf{r},\mathbf{p}) \left(\frac{\partial m\delta(\mathbf{r}_a-\mathbf{r})}{\partial r^k} \frac{\partial p_j\delta(\mathbf{r}_b-\mathbf{r})}{\partial p_k} - 0 \right) \tag{A.57b}$$

$$= \rho(\mathbf{r}_b) \frac{\partial \delta(\mathbf{r}_a-\mathbf{r}_b)}{\partial r_b^j}. \tag{A.57c}$$

Coupling between density and entropy is given by

$$\begin{aligned}
\{\rho(\mathbf{r}_a), s(\mathbf{r}_b)\}^{(B)} &= \int \mathrm{d}\mathbf{r} \int \mathrm{d}\mathbf{p} f(\mathbf{r},\mathbf{p}) \\
&\quad \left(\frac{\partial m\delta(\mathbf{r}_a - \mathbf{r})}{\partial r^k} \frac{\partial s'_f(f(\mathbf{r},\mathbf{p}))\delta(\mathbf{r}_b - \mathbf{r})}{\partial p_k} \right) && \text{(A.58a)} \\
&= -m\frac{\partial}{\partial r_a^k} \int \mathrm{d}\mathbf{p} f(\mathbf{r}_a,\mathbf{p}) \frac{\partial s'_f(f(\mathbf{r}_b,\mathbf{p}))}{\partial p_k} \delta(\mathbf{r}_b - \mathbf{r}_a) && \text{(A.58b)} \\
&= m\frac{\partial}{\partial r_a^k} \left(\delta(\mathbf{r}_b - \mathbf{r}_a) \underbrace{\int \mathrm{d}\mathbf{p} \frac{\partial s_f(f(\mathbf{r}_a,\mathbf{p}))}{\partial p_k}}_{=0} \right) && \text{(A.58c)} \\
&= 0. && \text{(A.58d)}
\end{aligned}$$

Note that it was used in the last equality that all boundary terms simply disappear. This equation means that

$$L_{CH}^{\rho(\mathbf{r}_a), s(\mathbf{r}_b)} = 0. \tag{A.59}$$

Coupling between momenta is given by

$$L_{CH}^{u_i(\mathbf{r}_a), u_j(\mathbf{r}_b)} = \{u_i(\mathbf{r}_a), u_j(\mathbf{r}_b)\}^{(B)}. \tag{A.60a}$$

Plugging relation (A.55b) into this expression, the expression becomes

$$\begin{aligned}
= \int \mathrm{d}\mathbf{r} \int \mathrm{d}\mathbf{p} f(\mathbf{r},\mathbf{p}) \Bigg(& \frac{\partial p_i \delta(\mathbf{r}_a - \mathbf{r})}{\partial r^k} \frac{\partial p_j \delta(\mathbf{r}_b - \mathbf{r})}{\partial p_k} \\
& - \frac{\partial p_i \delta(\mathbf{r}_a - \mathbf{r})}{\partial p_k} \frac{\partial p_j \delta(\mathbf{r}_b - \mathbf{r})}{\partial r^k} \Bigg). \qquad \text{(A.60b)}
\end{aligned}$$

Applying the delta-distributions then leads to

$$= u_i(\mathbf{r}_b) \frac{\partial \delta(\mathbf{r}_b - \mathbf{r}_a)}{\partial r_b^j} - u_j(\mathbf{r}_a) \frac{\partial \delta(\mathbf{r}_b - \mathbf{r}_a)}{\partial r_a^i}. \tag{A.60c}$$

Coupling between momentum and entropy is given by

$$\begin{aligned}
L_{CH}^{u_i(\mathbf{r}_a), s(\mathbf{r}_b)} = \{u_i(\mathbf{r}_a), s(\mathbf{r}_b)\}^{(B)} &= \int \mathrm{d}\mathbf{r} \int \mathrm{d}\mathbf{p} f(\mathbf{r},\mathbf{p}) \cdot \\
& \cdot \Bigg(\frac{\partial p_i \delta(\mathbf{r}_a - \mathbf{r})}{\partial r^k} \frac{\partial s'_f(f(\mathbf{r},\mathbf{p}))\delta(\mathbf{r}_b - \mathbf{r})}{\partial p_k} \\
& \quad - \frac{\partial s'_f(f(\mathbf{r},\mathbf{p}))\delta(\mathbf{r}_b - \mathbf{r})}{\partial r^k} \frac{\partial p_k \delta(\mathbf{r}_a - \mathbf{r})}{\partial p_k} \Bigg). \qquad \text{(A.61a)}
\end{aligned}$$

Integrating by parts with respect to $\mathbf{r}$ and applying the delta-distributions $\delta(\mathbf{r}_a - \mathbf{r})$, this last expression becomes

$$\begin{aligned}
= & \int \mathrm{d}\mathbf{p} - p_i \frac{\partial}{\partial r_a^k} \left(f(\mathbf{r}_a,\mathbf{p}) \frac{\partial s'_f(f(\mathbf{r}_a,\mathbf{p}))}{\partial p_k} \delta(\mathbf{r}_b - \mathbf{r}_a) \right) \\
& - \int \mathrm{d}\mathbf{p} f(\mathbf{r}_a,\mathbf{p}) \delta_i^k \frac{\partial s'_f(f(\mathbf{r}_a,\mathbf{p}))\delta(\mathbf{r}_b - \mathbf{r}_a)}{\partial r_a^k}. \qquad \text{(A.61b)}
\end{aligned}$$

Integrating by parts in the first term leads to

$$= \frac{\partial}{\partial r_a^k}\left(\int \mathrm{d}\mathbf{p}\delta(\mathbf{r}_b-\mathbf{r}_a)\left(\delta_i^k f(\mathbf{r}_a,\mathbf{p})+p_i\frac{\partial f(\mathbf{r}_a,\mathbf{p})}{\partial p_k}\right)s_f'(f(\mathbf{r}_a,\mathbf{p}))\right) - \int \mathrm{d}\mathbf{p} f(\mathbf{r}_a,\mathbf{p})\delta_i^k\frac{\partial s_f'(f(\mathbf{r}_a,\mathbf{p}))\delta(\mathbf{r}_b-\mathbf{r}_a)}{\partial r_a^k}. \tag{A.61c}$$

Part of the first term cancels with the last term, and what remains can be rewritten as

$$= \int \mathrm{d}\mathbf{p}\delta(\mathbf{r}_b-\mathbf{r}_a)\frac{\partial s_f(f(\mathbf{r}_a,\mathbf{p}))}{\partial r_a^i}+\frac{\partial}{\partial r_a^k}\int \mathrm{d}\mathbf{p}\delta(\mathbf{r}_b-\mathbf{r}_a)p_i\frac{\partial s_f(f(\mathbf{r}_a,\mathbf{p})}{\partial p_k}. \tag{A.61d}$$

Using the definition (A.54), this last equality becomes

$$= \delta(\mathbf{r}_b-\mathbf{r}_a)\frac{\partial s(\mathbf{r}_a)}{\partial r_a^i}+\frac{\partial}{\partial r_a^k}\left(\delta(\mathbf{r}_b-\mathbf{r}_a)\int \mathrm{d}\mathbf{p}-\delta_i^k s_f(f(\mathbf{r}_a,\mathbf{p}))\right). \tag{A.61e}$$

Finally, using the projection (A.54) again, one obtains

$$\begin{aligned} &= \delta(\mathbf{r}_b-\mathbf{r}_a)\frac{\partial s(\mathbf{r}_a)}{\partial r_a^i}+ \\ &\quad +\frac{\partial\delta(\mathbf{r}_b-\mathbf{r}_a)}{\partial r_a^k}\left(-\delta_i^k s(\mathbf{r}_a)\right)+\delta(\mathbf{r}_b-\mathbf{r}_a)\frac{\partial(-s(\mathbf{r}_a))}{\partial r_a^i} \\ &= -s(\mathbf{r}_a)\frac{\partial\delta(\mathbf{r}_b-\mathbf{r}_a)}{\partial r_a^i}. \end{aligned} \tag{A.61f}$$

The last part of the hydrodynamic Poisson bivector that remains to be calculated is component providing coupling between entropy and entropy.

$$\{s(\mathbf{r}_a),s(\mathbf{r}_b)\}^{(B)} = \int \mathrm{d}\mathbf{r}\int \mathrm{d}\mathbf{p} f(\mathbf{r},\mathbf{p})\cdot \tag{A.62a}$$
$$\cdot\left(\frac{\partial s_f'(f(\mathbf{r},\mathbf{p}))\delta(\mathbf{r}_a-\mathbf{r})}{\partial r^k}\frac{\partial s_f'(f(\mathbf{r},\mathbf{p}))\delta(\mathbf{r}_b-\mathbf{r})}{\partial p_k}-\dots\right)$$

where $\dots$ stand for the same term as already present in the bracket but with a and b swapped. Integrating by parts in the terms containing $\delta(\mathbf{r}_a-\mathbf{r})$ yields

$$\begin{aligned} &= \int \mathrm{d}\mathbf{r}\int \mathrm{d}\mathbf{p} -\frac{\partial s_f(f(\mathbf{r},\mathbf{p}))}{\partial r^k}\delta(\mathbf{r}_a-\mathbf{r})\frac{\partial s_f'(f(\mathbf{r},\mathbf{p}))\delta(\mathbf{r}_b-\mathbf{r})}{\partial p_k}+ \\ &\quad +\int \mathrm{d}\mathbf{r}\int \mathrm{d}\mathbf{p} -s_f'(f(\mathbf{r},\mathbf{p}))\delta(\mathbf{r}_a-\mathbf{r})f(\mathbf{r},\mathbf{p})\frac{\partial^2 s_f'(f(\mathbf{r},\mathbf{p}))\delta(\mathbf{r}_b-\mathbf{r})}{\partial r^k\partial p_k}+ \\ &\quad +\int \mathrm{d}\mathbf{r}\int \mathrm{d}\mathbf{p}\frac{\partial s_f(f(\mathbf{r},\mathbf{p}))}{\partial p_k}\delta(\mathbf{r}_a-\mathbf{r})\frac{\partial s_f'(f(\mathbf{r},\mathbf{p}))\delta(\mathbf{r}_b-\mathbf{r})}{\partial r^k}+ \\ &\quad +\int \mathrm{d}\mathbf{r}\int \mathrm{d}\mathbf{p} f(\mathbf{r},\mathbf{p})s_f'(f(\mathbf{r},\mathbf{p}))\delta(\mathbf{r}_a-\mathbf{r})\frac{\partial^2 s_f'(f(\mathbf{r},\mathbf{p}))\delta(\mathbf{r}_b-\mathbf{r})}{\partial r^k\partial p_k}. \end{aligned} \tag{A.62b}$$

The second term cancels with the last term and thus the equality becomes, after aplying the $\delta(\mathbf{r}_a-\mathbf{r})$ distribution,

$$\begin{aligned} &= \int \mathrm{d}\mathbf{p}\frac{\partial s_f(f(\mathbf{r}_a,\mathbf{p}))}{\partial p_k}\frac{\partial s_f'(f(\mathbf{r}_a,\mathbf{p}))\delta(\mathbf{r}_b-\mathbf{r}_a)}{\partial r_a^k}- \\ &\quad -\int \mathrm{d}\mathbf{p}\frac{\partial s_f(f(\mathbf{r}_a,\mathbf{p}))}{\partial r_a^k}\frac{\partial s_f'(f(\mathbf{r}_a,\mathbf{p}))\delta(\mathbf{r}_b-\mathbf{r}_a)}{\partial p_k}. \end{aligned} \tag{A.62c}$$

Integrating by parts in the first term and differentiating with respect to parameter in the second term then leads to

$$
\begin{aligned}
= & \int \mathrm{d}\mathbf{p} - s_f(f(\mathbf{r}_a,\mathbf{p}))\left(\frac{\partial^2 s'_f(f(\mathbf{r}_a,\mathbf{p}))}{\partial p_k \partial r_a^k}\delta(\mathbf{r}_b-\mathbf{r}_a)+\frac{\partial s'_f(f(\mathbf{r}_a,\mathbf{p}))}{\partial p_k}\frac{\partial\delta(\mathbf{r}_b-\mathbf{r}_a)}{\partial r_a^k}\right)+ \\
& + \int \mathrm{d}\mathbf{p} s_f(f(\mathbf{r}_a,\mathbf{p}))\left(\frac{\partial^2 s'_f(f(\mathbf{r}_a,\mathbf{p}))}{\partial p_k \partial r_a^k}\delta(\mathbf{r}_b-\mathbf{r}_a)+\frac{\partial s'_f(f(\mathbf{r}_a,\mathbf{p}))}{\partial p_k}\frac{\partial\delta(\mathbf{r}_b-\mathbf{r}_a)}{\partial r_a^k}\right)- \\
& - \frac{\partial}{\partial r_a^k}\left(\delta(\mathbf{r}_b-\mathbf{r}_a)\int \mathrm{d}\mathbf{p}\underbrace{s_f(f(\mathbf{r}_a,\mathbf{p}))s''_f(f(\mathbf{r}_a,\mathbf{p}))}_{\alpha'(f(\mathbf{r}_a,\mathbf{p}))}\frac{\partial f(\mathbf{r}_a,\mathbf{p})}{\partial p_k}\right). \qquad \text{(A.62d)}
\end{aligned}
$$

The first two terms clearly cancel out with each other. Let a primitive function of function α' be denoted by α. The last term can be then rewritten as

$$
= -\frac{\partial}{\partial r_a^k}\left(\delta(\mathbf{r}_b-\mathbf{r}_a)\int \mathrm{d}\mathbf{p}\frac{\partial\alpha(f(\mathbf{r}_a,\mathbf{p}))}{\partial p_k}\right). \qquad \text{(A.62e)}
$$

But integral of divergence of a function is zero as boundary terms vanish and so we have obtained that

$$
L_{CH}^{s(\mathbf{r}_a),s(\mathbf{r}_b)} = 0. \qquad \text{(A.62f)}
$$

Comparing the components of the $\mathbf{L}_{CH}$ tensor with the hydrodynamic Poisson bivector[4] (2.26), we can conclude that the projection indeed gives exactly the Poisson bracket of classical hydrodynamics.

A.2.6 From Liouville to binary Boltzmann

Consider now that there are particles of two different species in the isolated system. Their positions and momenta are denoted by $\mathbf{1},\ldots,\mathbf{N}$ and $\tilde{\mathbf{1}},\ldots,\tilde{\mathbf{N}}$. The overall $2N$-particle distribution function, which evolves according to Liouville equation, is denoted by $f_{N\tilde{N}}$. One-particle distribution functions of the two species are then defined by the following projections.

$$
f(\mathbf{a}) = \int \mathrm{d}\mathbf{1}\ldots\int \mathrm{d}\mathbf{N} f_{N\tilde{N}}\sum_{i=1}^{N}\delta(\mathbf{i}-\mathbf{a}) \Rightarrow \frac{\partial f(\mathbf{a})}{\partial f_{N\tilde{N}}} = \sum_{i=1}^{N}\delta(\mathbf{i}-\mathbf{a}) \qquad \text{(A.63)}
$$

$$
\tilde{f}(\mathbf{a}) = \int \mathrm{d}\mathbf{1}\ldots\int \mathrm{d}\mathbf{N} f_{N\tilde{N}}\sum_{\tilde{i}=1}^{N}\delta(\tilde{\mathbf{i}}-\mathbf{a}) \Rightarrow \frac{\partial \tilde{f}(\mathbf{a})}{\partial f_{N\tilde{N}}} = \sum_{\tilde{i}=1}^{N}\delta(\tilde{\mathbf{i}}-\mathbf{a}). \qquad \text{(A.64)}
$$

Let us now calculate the Liouville Poisson bracket applied to functionals de-

[4] after transforming it to the $(\rho,\mathbf{u},s)$ variables, see [75]

pendent only on f and $\tilde{f}$.

$$\begin{aligned}\{A,B\}^{(L)} &= \int \mathrm{d}\mathbf{1}\ldots\int \mathrm{d}\mathbf{N}\int \mathrm{d}\tilde{\mathbf{1}}\ldots\int \mathrm{d}\tilde{\mathbf{N}} f_{N\tilde{N}}\int \mathrm{d}\mathbf{a}\int \mathrm{d}\tilde{\mathbf{a}}\int \mathrm{d}\mathbf{b}\int \mathrm{d}\tilde{\mathbf{b}}\Bigg(\\ &\frac{\partial A}{\partial f(\mathbf{a})}\left\{\frac{\partial f(\mathbf{a})}{\partial f_{N\tilde{N}}},\frac{\partial f(\mathbf{b})}{\partial f_{N\tilde{N}}}\right\}^{(CM)}\frac{\partial B}{\partial f(\mathbf{b})}+ \\ &+\frac{\partial A}{\partial \tilde{f}(\tilde{\mathbf{a}})}\left\{\frac{\partial \tilde{f}(\tilde{\mathbf{a}})}{\partial f_{N\tilde{N}}},\frac{\partial f(\mathbf{b})}{\partial f_{N\tilde{N}}}\right\}^{(CM)}\frac{\partial B}{\partial f(\mathbf{b})}+ \\ &+\frac{\partial A}{\partial f(\mathbf{a})}\left\{\frac{\partial f(\mathbf{a})}{\partial f_{N\tilde{N}}},\frac{\partial \tilde{f}(\tilde{\mathbf{b}})}{\partial f_{N\tilde{N}}}\right\}^{(CM)}\frac{\partial B}{\partial \tilde{f}(\tilde{\mathbf{b}})}+ \\ &+\frac{\partial A}{\partial \tilde{f}(\tilde{\mathbf{a}})}\left\{\frac{\partial \tilde{f}(\tilde{\mathbf{a}})}{\partial f_{N\tilde{N}}},\frac{\partial \tilde{f}(\tilde{\mathbf{b}})}{\partial f_{N\tilde{N}}}\right\}^{(CM)}\frac{\partial B}{\partial \tilde{f}(\tilde{\mathbf{b}})}\Bigg). \end{aligned} \tag{A.65a}$$

Since the Poisson bracket of classical mechanics only couples positions and momenta of the same particles, the terms that contain derivatives with respect to both f and $\tilde{f}$, i.e. the second and the third line, disappear. Introducing N-particle distribution functions

$$f_N(\mathbf{1},\ldots,\mathbf{N}) = \int \mathrm{d}\tilde{\mathbf{1}}\ldots\int \mathrm{d}\tilde{\mathbf{N}} f_{N\tilde{N}} \tag{A.66}$$

$$\tilde{f_N}(\tilde{\mathbf{1}},\ldots,\tilde{\mathbf{N}}) = \int \mathrm{d}\mathbf{1}\ldots\int \mathrm{d}\mathbf{N} f_{N\tilde{N}}. \tag{A.67}$$

Poisson bracket (A.65a) can be rewritten as

$$\{A,B\}^{(L)} = \{A,B\}^{(L(N))} + \{A,B\}^{(L(\tilde{N}))} \tag{A.68}$$

where $\{A,B\}^{(L(N))}$ is the Liouville Poisson bracket of the two functionals constructed from the N-particle distribution function f_N, and $\{A,B\}^{(L(\tilde{N}))}$ the Liouville Poisson bracket constructed from $\tilde{f_N}$. But as we have already seen in Section A.2.3, these two Poisson brackets are equal to the Boltzmann Poisson brackets constructed from f_N and $\tilde{f_N}$, respectively.

In summary, the Poisson bracket governing reversible evolution of two one-particle distribution functions is

$$\{A,B\}^{(B\times\tilde{B})} = \{A,B\}^{(B)} + \{A,B\}^{(\tilde{B})} \tag{A.69}$$

where the latter bracket is the Boltzmann Poisson bracket with $\tilde{f}$ instead of f inside.

A.2.7 From binary Boltzmann to binary hydrodynamics

Poisson bracket of binary hydrodynamics, where each of the fluids is described by its density, momentum density and entropy density, can be obtained from the

binary Boltzmann Poisson bracket straightforwardly. The projection follows:

$$\rho(\rho_\alpha) = \int \mathrm{d}\mathbf{r} \int \mathrm{d}\mathbf{p} f(\mathbf{r},\mathbf{p}) m\delta(\mathbf{r}_a - \mathbf{r}) \tag{A.70a}$$

$$u_i(\rho_\alpha) = \int \mathrm{d}\mathbf{r} \int \mathrm{d}\mathbf{p} f(\mathbf{r},\mathbf{p}) p_i\delta(\mathbf{r}_a - \mathbf{r}) \tag{A.70b}$$

$$s(\rho_\alpha) = \int \mathrm{d}\mathbf{r} \int \mathrm{d}\mathbf{p} s_f(f(\mathbf{r},\mathbf{p}))\delta(\mathbf{r}_a - \mathbf{r}) \tag{A.70c}$$

$$\tilde{\rho}(\rho_\alpha) = \int \mathrm{d}\tilde{\mathbf{r}} \int \mathrm{d}\tilde{\mathbf{p}} \tilde{f}(\tilde{\mathbf{r}},\mathbf{p}) m\delta(\mathbf{r}_a - \tilde{\mathbf{r}}) \tag{A.70d}$$

$$\tilde{u}_i(\rho_\alpha) = \int \mathrm{d}\tilde{\mathbf{r}} \int \mathrm{d}\tilde{\mathbf{p}} \tilde{f}(\tilde{\mathbf{r}},\tilde{\mathbf{p}}) \tilde{p}_i\delta(\mathbf{r}_a - \tilde{\mathbf{r}}) \tag{A.70e}$$

$$\tilde{s}(\rho_\alpha) = \int \mathrm{d}\tilde{\mathbf{r}} \int \mathrm{d}\tilde{\mathbf{p}} \tilde{s_f}(\tilde{f}(\tilde{\mathbf{r}},\tilde{\mathbf{p}}))\delta(\mathbf{r}_a - \tilde{\mathbf{r}}). \tag{A.70f}$$

Consider now two functionals dependent only on these state variables. Poisson bracket (A.69) does not provide coupling between the two different species. Therefore, the bracket applied to the two functionals consists of two parts, each of which is obtained in the same way as the hydrodynamic Poisson bracket was obtained from the Boltzmann Poisson bracket. Therefore, the Poisson bracket describing evolution of state variables (A.70) is

$$\{A,B\}^{(CH\times\widetilde{CH})} = \{A,B\}^{(CH)} + \{A,B\}^{(\widetilde{CH})} \tag{A.71}$$

where the latter Poisson bracket is the standard hydrodynamic Poisson bracket constructed from state variables (A.70d)-(A.70f).

In summary, a binary mixture with state variables (A.70) evolves according to Poisson bracket (A.71), which is simply the sum of hydrodynamic Poisson brackets for each species. Note that this description of binary mixtures typically represents mixtures with multiple temperatures (like in cold plasma, where electrons have different temperature than ions, see [24]). Indeed, as there are two entropies, there are also two temperatures (derivatives of the entropies with respect to energy).

A.2.8 From binary hydrodynamics to mixtures with total entropy

What if one does not wish to handle multi-temperature mixtures? A lower level of description can be introduced where densities and momentum densities of both species are still among the state variables, but where only the total entropy

$$s^T(\mathbf{r}) = s^T(\rho(\mathbf{r}),\tilde{\rho}(\mathbf{r}),\mathbf{u}(\mathbf{r}),\tilde{\mathbf{u}}(\mathbf{r}),s(\mathbf{r}),\tilde{s}(\mathbf{r})) \tag{A.72}$$

remains among the state variables instead of the two entropies.

The Poisson bivector on this level of description can be obtained from the Poisson bracket (A.71) by the projection introduced in the preceding paragraph.

For example, for coupling between ρ and u_i one obtains

$$L^{\rho(\mathbf{r}_a),u_i(\mathbf{r}_b)}_{CH\times\widetilde{CH}(s^T)} = \{\rho(\mathbf{r}_a),u_i(\mathbf{r}_b)\}^{(CH\times\widetilde{CH})} \tag{A.73}$$

$$= \int \mathrm{d}\mathbf{r}\int \mathrm{d}\mathbf{r}'\frac{\partial\rho(\mathbf{r}_a)}{\partial\rho(\mathbf{r})}L^{\rho(\mathbf{r}),u_j(\mathbf{r}')}_{CH\times\widetilde{CH}}\frac{\partial u_i(\mathbf{r}_b)}{\partial u_j(\mathbf{r}')} \tag{A.74}$$

$$= L^{\rho(\mathbf{r}_a),u_i(\mathbf{r}_b)}_{CH\times\widetilde{CH}}. \tag{A.75}$$

Similar calculations for ρ, $\tilde{\rho}$, $\mathbf{u}$ and $\tilde{\mathbf{u}}$ imply that the part of the Poisson bivector that provides coupling between these state variables is the same as on the higher level of description.

But how does the total entropy (A.72) evolve? A proper projection to s^T has to be defined at first so that the resulting Poisson bivector only depends on s^T instead of entropies s and $\tilde{s}$. We conjecture that the way how entropy is introduced in our paper [81] is such projection, but the calculation has not been carried out yet as the theory from the paper has been reformulated within GENERIC only in the isothermal case.

A.2.9 From binary hydrodynamics to CIT

Let us approach an even lower level of description, where only densities, total momentum, and total entropy density constitute the state variables. The projection is then given by

$$\rho(\mathbf{r}) = \rho(\mathbf{r}) \tag{A.76}$$

$$\tilde{\rho}(\mathbf{r}) = \tilde{\rho}(\mathbf{r}) \tag{A.77}$$

$$u^T_i(\mathbf{r}) = u_i(\mathbf{r}) + \tilde{u}_i(\mathbf{r}) \tag{A.78}$$

$$s^T(\mathbf{r}) = s(\mathbf{r}) + \tilde{s}(\mathbf{r}). \tag{A.79}$$

This level of description is quite important since it is the level where CIT takes place. Indeed, the state variables are the same as within CIT.

Components of the Poisson bivector on this level of description that are coupling the total momentum with the densities are clearly the same as Sec. A.2.8. What about the component coupling the total momentum with itself?

$$\left\{u^T_i(\mathbf{r}_a),u^T_j(\mathbf{r}_b)\right\}^{(CH\times\widetilde{CH})} = \left\{u^T_i(\mathbf{r}_a),u^T_j(\mathbf{r}_b)\right\}^{(CH)} + \left\{u^T_i(\mathbf{r}_a),u^T_j(\mathbf{r}_b)\right\}^{(\tilde{CH})} \tag{A.80}$$

$$= u_i(\mathbf{r}_b)\frac{\partial\delta(\mathbf{r}_b-\mathbf{r}_a)}{\partial r^j_b} - u_j(\mathbf{r}_a)\frac{\partial\delta(\mathbf{r}_b-\mathbf{r}_a)}{\partial r^i_a} + $$

$$+\tilde{u}_i(\mathbf{r}_b)\frac{\partial\delta(\mathbf{r}_b-\mathbf{r}_a)}{\partial r^j_b} - \tilde{u}_j(\mathbf{r}_a)\frac{\partial\delta(\mathbf{r}_b-\mathbf{r}_a)}{\partial r^i_a} \tag{A.81}$$

$$= u^T_i(\mathbf{r}_b)\frac{\partial\delta(\mathbf{r}_b-\mathbf{r}_a)}{\partial r^j_b} - u^T_j(\mathbf{r}_a)\frac{\partial\delta(\mathbf{r}_b-\mathbf{r}_a)}{\partial r^i_a} \tag{A.82}$$

which is the component of the hydrodynamic Poisson bivector $L^{u_i(\mathbf{r}_a),u_j(\mathbf{r}_b)}_{CH}$ with $\mathbf{u}$ replaced by $\mathbf{u}^T$.

Coupling between momentum and entropy is given by

$$\left\{u^T_i(\mathbf{r}_a),s^T(\mathbf{r}_b)\right\}^{(CH\times\widetilde{CH})} = \{u_i(\mathbf{r}_a,s(\mathbf{r}_b)\}^{(CH)} + \{\tilde{u}_i(\mathbf{r}_a),\tilde{s}(\mathbf{r}_b)\}^{(\tilde{CH})} =$$

$$= -s^T(\mathbf{r}_a)\frac{\partial\delta(\mathbf{r}_b-\mathbf{r}_a)}{\partial r^i_a}. \tag{A.83}$$

Coupling between density and entropy and between entropy and entropy vanishes since it vanishes in classical hydrodynamics in Sec. A.2.5.

In summary, a mixture where densities, total momentum and total entropy constitute the state variables has the following Poisson bivector

$$L_{CIT}^{\rho(\mathbf{r}_a),u_j^T(\mathbf{r}_b)} = \rho(\mathbf{r}_b)\frac{\partial\delta(\mathbf{r}_b-\mathbf{r}_a)}{\partial r_b^j} \tag{A.84a}$$

$$L_{CIT}^{\tilde{\rho}(\mathbf{r}_a),u_j^T(\mathbf{r}_b)} = \tilde{\rho}(\mathbf{r}_b)\frac{\partial\delta(\mathbf{r}_b-\mathbf{r}_a)}{\partial r_b^j} \tag{A.84b}$$

$$L_{CIT}^{u_i^T(\mathbf{r}_a),u_j^T(\mathbf{r}_b)} = u_i^T(\mathbf{r}_b)\frac{\partial\delta(\mathbf{r}_b-\mathbf{r}_a)}{\partial r_b^j} - u_j^T(\mathbf{r}_a)\frac{\partial\delta(\mathbf{r}_b-\mathbf{r}_a)}{\partial r_a^i} \tag{A.84c}$$

$$L_{CIT}^{s^T(\mathbf{r}_a),u_j^T(\mathbf{r}_b)} = s^T(\mathbf{r}_b)\frac{\partial\delta(\mathbf{r}_b-\mathbf{r}_a)}{\partial r_b^j} \tag{A.84d}$$

where all other components are zero, and it has been thus shown how the reversible part of evolution within CIT can be derived by projection from the Liouville equation without the necessity to introduce Dirac structures as in [76].

One could also continue in the reduction to a lower level, where only the total density

$$\rho^T = \rho + \tilde{\rho}, \tag{A.85}$$

total momentum $\mathbf{u}^T$ and total entropy s^T are present. This is an alternative (and longer) way to obtain the classical hydrodynamic Poisson bracket.

Furthermore, one could project the total momentum to a constant. This is the passage to the level of mechanical equilibrium. The Poisson bracket, however, completely disappears during the passage since the CIT Poisson bivector does not provide coupling between densities and total entropy, which are the only state variables that remain on the level of mechanical equilibrium, studied in Chap. 3.

A.3 Theory of mixtures within EIT

The theory of mixtures developed within CIT has certain physical drawbacks. For example, the Fourier's law of heat conduction, which is derived within the theory, implies the standard heat equation. But the heat equation is a parabolic partial differential equation predicting infinite propagation of signals, [31]. This problem is solved by replacing the Fourier's law and the resulting heat equation by the Maxwell-Cattaneo equation, which is already hyperbolic, see [46]. This equation can be derived within non-equilibrium thermodynamics easily. Indeed, the only new step in comparison with CIT is promoting the heat flux to state variable. The evolution equation of the heat flux, which follows from non-equilibrium thermodynamics, can be then plugged into balance of energy, yielding the Maxwell-Cattaneo equation [46]. The same problem appears when modeling diffusion processes, and an analogical solution to the problem can be found, as shown in our paper [81].

Besides the problem of infinite signal propagation, it is common knowledge that partial pressures can be assigned to species of a gas mixture, see e.g. [5]. But usually, the partial pressures are only prescribed for a mixture of ideal (i.e. non-interacting) gases. How to define the partial pressures for a mixture of real (i.e. interacting) gases or, in general, for a mixture of real fluids? As well as total pressure is the part of the total Cauchy stress tensor causing reversible evolution, partial pressure is also the part of a partial Cauchy stress tensor that causes reversible evolution, and this definition is sufficient to derive an explicit expression for partial pressures in a real mixture within EIT, see [81]. Interestingly, the expression is the same as suggested by Samohýl et al. [87], namely

$$p_\alpha = p\rho_\alpha v_\alpha \tag{A.86}$$

where p_α, p, ρ_α and v_α are partial pressure of species α in the mixture, total pressure of the mixture, density of the species and partial molar volume of the species, respectively.

Moreover, the question whether kinetic energy of diffusion should be part of the internal energy or not is clarified in the paper, and closed evolution equations of a mixture where state variables of CIT are enriched with diffusion fluxes are presented in the paper.

Can the new EIT theory of mixtures from paper [81] contribute to the understanding processes in fuel cells? Transport of gases through a porous medium is often described by the dusty-gas model, which has been compared to experiments extensively, see [62]. In [52] the dusty-gas model is derived from the Maxwell-Stefan diffusion equations, and these equations can be derived within the framework of CIT as shown in [48]. Therefore, the dusty-gas model can be derived within CIT. Nevertheless, when having a closer look at the resulting dusty-gas model, there is a term proportional to

$$\nabla p - \rho\mathbf{f} \tag{A.87}$$

missing in the model derived from CIT[5] when comparing with the model from [62]. Recent (yet unpublished) calculations indicate that this term appears when

[5] $\mathbf{f}$ is the total force exerted on the mixture.

starting from the EIT theory of mixtures [81] instead of CIT. Indeed, when plugging Eqs. (65) and (91) of the paper into force-flux relation (69) of the paper leads to appearance of the missing term in the final equation governing the diffusion.

In summary, the EIT theory of mixtures [81] provides a simple expression for partial pressures, which are identified as the reversible parts of partial Cauchy stress tensors. The theory explains whether kinetic energy of diffusion should be considered part of internal energy or not, and closed EIT evolution equations for mixtures are formulated. The theory could also serve as the starting point for the thermodynamic derivation of the complete dusty-gas model from [62]. Such thermodynamic derivation would be useful for calculating the efficiency losses by diffusion in fuel cells since once having the thermodynamic formulation of the model, the map of losses (see Section 3.7) can be plotted. The explicit derivation of the dusty-gas model from the EIT theory of mixtures is, however, out of scope of this work.

B. Additional calculations

B.1 Supporting calculations for Sec. 4.2

This section contains certain calculations that are used in Sec. 4.2. Terminology is also explained in that section.

B.1.1 Molalities as functions of SOC

Catex membranes

One liter of the positive electrolyte at SOC equal to 0 in the experiment[1] with catex membrane consists of $779g$ H_2O, $2mol$ $VOSO_4$ and $3mol$ H_2SO_4. One liter of the negative electrolyte consists of $806g$ H_2O, $1mol$ $V_2(SO_4)_3$ and $2mol$ H_2SO_4. Apart from these values molalities of hydroxyl anions in both half-cells are needed as well. These are calculated from the condition of equilibrium between water, protons and hydroxyl anions, see B.1.2, for any SOC. When calculating dissociation of water with added H^+ ions according to B.1.2, we use the approximation of ideal solution and, consequently, it is necessary to assume how sulphuric acid dissociates. We suppose that it dissociates into H^+ and HSO_4^- in accordance with [26].

The electrochemical reaction in the positive half-cell is assumed to have the following form

$$2VOSO_4 + 2H_2O \rightarrow (VO_2)_2SO_4 + H_2SO_4 + 2e^- + 2H^+ \tag{B.1}$$

in the direction of charging. Electrons leave the half-cell to the external circuit while the protons leave through the membrane, thus they do not remain part of the electrolyte. Assuming that sulphuric acid dissociates completely to protons and bisulphates and that salts of sulphuric acid are completely dissociated as well, this last equation may be rewritten as

$$2VO^{2+} + 2SO_4^{2-} + 2H_2O \rightarrow 2VO_2^+ + SO_4^{2-} + H^+ + HSO_4^- + 2e^- + 2H^+. \tag{B.2}$$

The two protons at the end of the right hand side of this equation are transported to the negative half-cell. This chemical reaction is compatible with reaction mechanisms proposed in [51].

The electrochemical reaction in the negative half-cell is assumed to have the following form

$$V_2(SO_4)_3 + 2e^- + 2H^+ \rightarrow 2VSO_4 + H_2SO_4, \tag{B.3}$$

where the two protons on the left hand side come from the positive half-cell through the membrane. Using the same assumptions as in the case of the positive half-cell, the electrochemical reaction in the negative half-cell can be rewritten as

$$2V^{3+} + 3SO_4^{2-} + 2e^- + 2H^+ \rightarrow 2V^{2+} + 2SO_4^{2-} + H^+ + HSO_4^-. \tag{B.4}$$

State-of-charge (SOC) is defined as

$$SOC = \frac{b^P_{VO_2^+}}{b^P_{VO_2^+} + b^P_{VO^{2+}}}. \tag{B.5}$$

[1] Carried out by Petr Mazur, co-author of the submitted paper.

It follows that at SOC equal to zero, the electrolyte in the positive half-cell contains only VO^{2+} ions. Since the number of vanadium ions is conserved in the electrochemical reactions, the denominator of formula (B.5) is constant and equal to $b^{P,0}_{VO^{2+}}$, i.e. molality of VO^{2+} ions in the positive half-cell at SOC equal to zero. Therefore, if q moles of electrons pass through the circuit, the state of charge is equal to

$$SOC = \frac{q}{n^{P,0}_{VO^{2+}}} \tag{B.6}$$

where $n^{P,0}_{VO^{2+}}$ is number of moles of VO^{2+} in the positive half-cell at $SOC = 0$.

The amount of water in the positive half-cell changes when charging, and it can be expressed as

$$m^{P}_{H_2O} = m^{P,0}_{H_2O} - M_{H_2O} q = m^{P,0}_{H_2O} \left(1 - M_{H_2O} b^{P,0}_{VO^{2+}} SOC\right) \tag{B.7}$$

where M_{H_2O} is molar mass of water and $m^{P,0}_{H_2O}$ is mass of water in the positive half-cell at $SOC = 0$. Indeed, one molecule of water disappears in the positive half-cell when one proton passes through the membrane, according to formula (B.2). Transport of water through the membrane is neglected in accordance with [93]. No water is created or consumed by reaction (B.4), and so the amount of water in the negative half-cell is constant during charging. The ratio of weight of water in the positive-half cell at $SOC = 0$ and weight of water in the negative half-cell is denoted by k.

Consequently, molalities of all the other species can be expressed as

$$b^{P}_{VO^{2+}} = \frac{n^{P,0}_{VO^{2+}} - q}{m^{P}_{H_2O}} = \frac{b^{P,0}_{VO^{2+}}(1 - SOC)}{1 - M_{H_2O} b^{P,0}_{VO^{2+}} SOC} \tag{B.8a}$$

$$b^{P}_{VO_2^{+}} = \frac{q}{m^{P}_{H_2O}} = \frac{b^{P,0}_{VO^{2+}} SOC}{1 - M_{H_2O} b^{P,0}_{VO^{2+}} SOC} \tag{B.8b}$$

$$b^{N}_{V^{2+}} = \frac{q}{m^{N}_{H_2O}} = k \cdot SOC \cdot b^{P,0}_{VO^{2+}} \tag{B.8c}$$

$$b^{N}_{V^{3+}} = \frac{n^{N,0}_{V^{3+}} - q}{m^{N}_{H_2O}} = b^{N,0}_{V^{3+}} - k \cdot SOC \cdot b^{P,0}_{VO^{2+}} \tag{B.8d}$$

$$b^{P}_{HSO_4^{-}} = \frac{n^{P,0}_{H_2SO_4} + \frac{1}{2} q}{m^{P}_{H_2O}} = \frac{b^{P,0}_{H_2SO_4} + \frac{1}{2} b^{P,0}_{VO^{2+}} SOC}{1 - M_{H_2O} b^{P,0}_{VO^{2+}} SOC} \tag{B.8e}$$

$$b^{N}_{HSO_4^{-}} = \frac{n^{N,0}_{H_2SO_4} + \frac{1}{2} q}{m^{N}_{H_2O}} = b^{N,0}_{H_2SO_4} + \frac{1}{2} b^{P,0}_{VO^{2+}} kSOC \tag{B.8f}$$

$$b^{P}_{SO_4^{2-}} = b^{P}_{VO^{2+}} + \frac{1}{2} b^{P}_{VO_2^{+}} \tag{B.8g}$$

$$b^{N}_{SO_4^{2-}} = \frac{3}{2} b^{N}_{V^{3+}} + b^{N}_{V^{2+}} \tag{B.8h}$$

where $b^{P,0}_{VO^{2+}}$ is molality of VO^{2+} ions in the positive half-cell at $SOC = 0$, $b^{N,0}_{V^{3+}}$ is molality of V^{3+} ions in the negative half-cell at $SOC = 0$ and $b^{P,0}_{H_2SO_4}$ and $b^{N,0}_{H_2SO_4}$ are molality of sulphuric acid in the positive and negative half-cell, respectively, at $SOC = 0$.

Molalities of hydroxyl anions in the positive half-cell and in the negative half-cell can be determined by solving equation (B.24) when assuming that all protons in the electrolytes have been created by dissociation of sulphuric acid and water, i.e.

$$b_{H^+} = b_{OH^-} + b_{HSO_4^-}. \tag{B.9}$$

Values of b_{OH^-} obtained as solutions to equation (B.24) can be then plugged into this last equation to obtain molalities of protons in both electrolytes. Note that we assume that sulphuric acid dissociates completely into protons and bisulphates. Note also that denominators in equations (B.8a)-(B.8f) are caused by variation of the amount of water in the positive electrode.

Anex membranes

Charging of a VRFB with an anex membrane can be described by the same electrochemical reactions as in the previous section, i.e. (B.2) and (B.4). But since bisulphates are transferred through the membrane instead of protons, the two protons in reaction (B.4) are not supplied from the positive half-cell. Therefore, it is advantageous to rewrite the reaction in the following form

$$2V^{3+} + 3SO_4^{2-} + 2e^- + H^+ + HSO_4^- \rightarrow 2V^{2+} + 2SO_4^{2-} + 2HSO_4^-, \tag{B.10}$$

where the two bisulphates at the end of the right hand side are transferred into the positive half-cell through the membrane, where they form sulphuric acid with the two protons produced therein, see Eq. (B.2).

Formulas for molalities in terms of SOC and initial composition will be the same as in the case of catex membrane except for molalities of bisulphates, which become

$$b^P_{HSO_4^-} = \frac{b^{P,0}_{H_2SO_4} + 1.5 b^{P,0}_{VO^{2+}} SOC}{1 - M_{H_2O} b^{P,0}_{VO^{2+}} SOC} \tag{B.11a}$$

$$b^N_{HSO_4^-} = b^{N,0}_{H_2SO_4} - 0.5 b^{P,0}_{VO^{2+}} kSOC. \tag{B.11b}$$

Molalities $b^P_{H^+}$ and $b^N_{H^+}$ are then calculated from molalities of hydroxyl anions as in the case of catex membranes. Molalities of hydroxyl anions are calculated from Eq. (B.24) with molalities of added protons equal to molalities of bisulphates.

The electrolytes at $SOC = 0$ were prepared[2] from a basic solution one liter of which consists of $0.4mol\ V_2(SO_4)_3$, $0.8mol\ VOSO_4$, $2.0mol\ H_2SO_4$, $0.05mol\ H_3PO_4$ and water, see [99]. The phosphoric acid is neglected hereafter. Density of the solution was $1.34g\,cm^{-3}$. The amount of water can be calculated from the density. Initially, both half-cells were filled with the basic solution and, subsequently, the battery was charged to $SOC = 0$ by the following reactions:

$$2H_2SO_4 + 0.8VOSO_4 + 0.8e^- \rightarrow \tag{B.12}$$

$$\rightarrow 0.4V_2(SO_4)_3 + 0.8H_2O + 0.8H_2SO_4 + 0.8HSO_4^- \tag{B.13}$$

$$0.4V_2(SO_4)_3 + 1H_2O + 0.8HSO_4^- \rightarrow 0.8VOSO_4 + 1.2H_2SO_4 + 0.8e^-, \tag{B.14}$$

[2]by Frank Wandschneider, a co-author of the submitted paper [82]

where the former reaction takes place in the negative half-cell while the latter in the positive half-cell. Bisulphates created in the negative half-cell are transferred to the positive half-cell through the membrane. Similarly, electrons created in the positive half-cell are transferred through external circuit and participate in the reaction inside the negative half-cell. This way, one obtains electrolyte composed of $0.8mol\ V_2(SO_4)_3$, $0.8mol\ H_2SO_4$ and $48.2mol\ H_2O$ per liter in the negative half-cell and electrolyte composed of $1.6mol\ VOSO_4$, $3.2mol\ H_2SO_4$ and $46.4mol\ H_2O$ per liter in the positive half-cell at $SOC = 0$. Molalities of all the species at $SOC = 0$ can be then calculated from these two compositions.

B.1.2 Dissociation of water

In this section dissociation of pure water at standard conditions and dissociation of water with added H^+ ions at standard pressure and temperature are determined.

In thermodynamic equilibrium chemical potential of water is equal to sum of chemical potential of protons and chemical potential of hydroxyl anions, which is expressed in condition (4.35). Chemical potentials of both ions can be expressed, according to formula (3.9), as

$$\mu_{H^+} = \mu^\circ_{H^+} + RT \ln\left(\gamma_{H^+} \frac{b_{H^+}}{b^\circ}\right) \tag{B.15}$$

$$\mu_{OH^-} = \mu^\circ_{OH^-} + RT \ln\left(\gamma_{OH^-} \frac{b_{OH^-}}{b^\circ}\right) \tag{B.16}$$

where molalities express number of moles of ions per kilogram of the whole amount of water (mass of both dissociated and non-dissociated water molecules). Standard chemical potentials are, see [97],

$$\mu^\circ_{H^+} = 0 \qquad \text{and} \qquad \mu^\circ_{OH^-} = -157244 J/mol. \tag{B.17}$$

Chemical potential of water can be then determined from Gibbs-Duhem relation, see for example [5, 70, 81] or Eq. (2.14),

$$(d\mu_{H_2O})_{T,p} = -\sum_\alpha M_{H_2O} b_\alpha \, d(\mu_\alpha)_{T,P}, \qquad \alpha = H^+, OH^- \tag{B.18}$$

where $(d\bullet)_{T,p}$ means differentiation at constant temperature and pressure.

B.1.3 Pure water

For pure water at standard conditions chemical potential of water is equal to the standard Gibbs free energy of formation

$$\mu^\circ_{H_2O} = -237129 J/mol, \tag{B.19}$$

see [21]. Activity coefficients of protons and hydroxyl anions can be estimated by Debye-Hückel limiting law, very well presented for example in [70],

$$\ln \gamma_{H^+} = \ln \gamma_{OH^-} = -1.17 \sqrt{\frac{b_{H^+}}{b^\circ}}. \tag{B.20}$$

Plugging the last two equations into condition (4.35) yields the equilibrium molalities of protons and hydroxyl anions, which are equal to each other,

$$b^{\circ}_{H^+} = b^{\circ}_{OH^-} = 9.97 \cdot 10^{-8} mol/kg. \tag{B.21}$$

Water with additional H^+

What are the molalities of protons and hydroxyl anions in water at standard temperature and pressure if some amount $b^A_{H^+}$ of protons is added (e.g. by dissociation of sulphuric acid)? Assume that activity coefficients of protons and hydroxyl anions are equal to 1. Formula (B.18) can be then integrated to

$$\mu_{H_2O} = \mu^{\circ}_{H_2O} - M_{H_2O} RT (b_{H^+} - b^{\circ}_{H^+} + b_{OH^-} - b^{\circ}_{OH^-}). \tag{B.22}$$

Plugging this equation and equations (B.15) and (B.16) into condition (4.35) then gives, considering that

$$b_{H^+} = b_{OH^-} + b^A_{H^+}, \tag{B.23}$$

an equation for equilibrium concentration of hydroxyl anions in terms of molality of the added protons $b^A_{H^+}$

$$K_w = \frac{(b_{OH^-} + b^A_{H^+}) b_{OH^-}}{(b^{\circ})^2} e^{M_{H_2O}(2b_{OH^-} + b^A_{H^+} - 2b^{\circ}_{OH^-})} \tag{B.24}$$

where

$$K_w = \exp\left(\frac{\mu^{\circ}_{H_2O} - \mu^{\circ}_{H^+} - \mu^{\circ}_{OH^-}}{RT}\right) = 9.94 \cdot 10^{-15} \tag{B.25}$$

is the equilibrium constant of water. This equation can be easily solved for any $b^A_{H^+}$ to obtain the sought molality of hydroxyl anions b_{OH^-} and consequently also the molality of protons according to formula (B.23).